แบบจำลองการแทรกซึมของคลอไรด์เข้าสู่โครงสร้างคอนกรีตเสริมเหล็กภายใต้น้ำหนักกระทำ

และสภาวะแวดล้อมทางทะเล

นาย วูฮวาง ควอค

วิทยานิพนธ์นี้เป็นส่วนหนึ่งของการศึกษาตามหลักสูตรปริญญาวิศวกรรมศาสตรดุษฎีบัณฑิต
สาขาวิชาวิศวกรรมโยธา ภาควิชาวิศวกรรมโยธา
คณะวิศวกรรมศาสตร์ จุฬาลงกรณ์มหาวิทยาลัย
ปีการศึกษา 2554

MODEL FOR CHLORIDE INGRESS INTO REINFORCED CONCRETE STRUCTURE UNDER LOAD AND MARINE ENVIRONMENT

Mr. Quoc Vu Hoang

A Dissertation Submitted in Partial Fulfillment of the Requirements
for the Degree of Doctor of Philosophy Program in Civil Engineering
Department of Civil Engineering
Faculty of Engineering
Chulalongkorn University
Academic Year 2011

Thesis Title   MODEL FOR CHLORIDE INGRESS INTO REINFORCED CONCRETE STRUCTURE UNDER LOAD AND MARINE ENVIRONMENT
By   Mr. Quoc Vu Hoang
Field of Study   Civil Engineering
Thesis Advisor   Associate Professor Boonchai Stitmannaithum, D.Eng.
Thesis Co-advisor   Professor Sugiyama Takafumi, Ph.D.

        Accepted by the Faculty of Engineering, Chulalongkorn University in Partial Fulfillment of Requirements for the Doctoral Degree

…………………………………Dean of the Faculty of Engineering
(Associate Professor Boonsom Lerdhirunwong, D.Eng.)

THESIS COMMITTEE

………………………………………… Chairman
(Professor Teerapong Senjuntichai, Ph.D.)

…………………………………………. Thesis Advisor
(Associate Professor Boonchai Stitmannaithum, D.Eng.)

…………………………………………. Thesis Co-advisor
(Professor Sugiyama Takafumi, Ph.D.)

…………………………………………. Examiner
(Associate Professor Phoonsak Pheinsusom, D.Eng.)

…………………………………………. Examiner
(Assistant Professor Withit Pansuk, Ph.D.)

…………………………………………. External Examiner
(Assistant Professor Taweechai Sumranwanich, Ph.D.)

วูฮวาง ควอค : แบบจำลองการแทรกซึมของคลอไรด์เข้าสู่โครงสร้างคอนกรีตเสริมเหล็กภายใต้น้ำหนักกระทำและสภาวะแวดล้อมทางทะเล. (MODEL FOR CHLORIDE INGRESS INTO REINFORCED CONCRETE STRUCTURE UNDER LOAD AND MARINE ENVIRONMENT) อ. ที่ปรึกษาวิทยานิพนธ์หลัก : รศ. ดร.บุญไชย สถิตมั่นในธรรม, อ. ที่ปรึกษาวิทยานิพนธ์ร่วม : ศ. ดร.สึกิยามา ทาคาฟุมิ, 119 หน้า.

　　　　ความคงทนของโครงสร้างคอนกรีตเสริมเหล็กเป็นสิ่งสำคัญสำหรับงานก่อสร้าง และเป็นประเด็นปัญหาที่ถูกกล่าวถึงอย่างมากในปัจจุบัน มีปัจจัยหลายอย่างส่งผลต่อความคงทนของโครงสร้าง เช่น สัดส่วนผสมคอนกรีต น้ำหนักบรรทุก หรือสภาวะแวดล้อม โดยเฉพาะอย่างยิ่งในสภาวะแวดล้อมทางทะเลและบริเวณชายฝั่ง ที่ความคงทนของโครงสร้างคอนกรีตเสริมเหล็กลดลงอย่างรวดเร็ว ตลอดระยะเวลาที่ผ่านมา มีงานวิจัยจำนวนมากได้นำเสนอแบบจำลองการเคลื่อนที่ของคลอไรด์ในคอนกรีตและคอนกรีตเสริมเหล็ก แต่งานวิจัยส่วนใหญ่ได้ทำการศึกษาแบบจำลองด้วยคอนกรีตที่ไม่มีรอยร้าวเกิดขึ้น ซึ่งจะแตกต่างจากสภาพการใช้งานจริงของโครงสร้างที่มักพบรอยร้าวของคอนกรีตอยู่เสมอ รอยร้าวดังกล่าวส่งผลให้ความคงทนของโครงสร้างลดลงรวดเร็วกว่ากรณีที่ไม่มีรอยร้าวอย่างมีนัยสำคัญ

　　　　งานวิจัยนี้นำเสนอแบบจำลองสำหรับคาดการณ์การเคลื่อนที่ของคลอไรด์ผ่านรอยร้าวเข้าสู่คอนกรีตเสริมเหล็ก การแพร่ของคลอไรด์ผ่านรอยร้าวถูกจำลองทั้งในลักษณะมิติเดียวและสองมิติ โดยใช้การวิเคราะห์ทางทฤษฎีและใช้การทดสอบเพื่อหาสัมประสิทธิ์การแพร่ของคลอไรด์และลักษณะขอบของเส้นทางการแพร่ของคลอไรด์ (Chloride Profile) ส่วนรอยร้าวถูกสร้างขึ้นจากการให้แรงดัดกระทำต่อตัวอย่างคอนกรีตเสริมเหล็ก และสมมติให้รอยร้าวมีลักษณะเรียวเล็กเป็นรูปตัววี จากการศึกษาพบว่า นอกจากความกว้างของรอยร้าวแล้ว ความลึกของรอยร้าวเป็นอีกหนึ่งปัจจัยที่ส่งผลต่อระยะแทรกซึมของคลอไรด์ โดยระยะแทรกซึมของคลอไรด์จะเพิ่มขึ้นตามความลึกของรอยร้าว สัมประสิทธิ์การแพร่ของคลอไรด์ตามรอยร้าวจึงขึ้นอยู่กับความกว้าง ความลึก และรูปแบบของรอยร้าว สำหรับแบบจำลองสองมิตินั้น การแพร่ของคลอไรด์เข้าสู่เนื้อคอนกรีตจะขึ้นกับปริมาณคลอไรด์บนระนาบที่เกิดรอยร้าว และสัมประสิทธิ์การแพร่ของคลอไรด์ตามรอยร้าว การคาดการณ์ด้วยแบบจำลองได้ผลสอดคล้องกับผลการวิเคราะห์ทางเคมี และการตรวจวิเคราะห์ระดับจุลภาคด้วยสัญญาณประจุบอิเล็กตรอน (Electron Probe Microanalysis) เป็นอย่างดี

ภาควิชา　　วิศวกรรมโยธา　　　　　　　　　ลายมือชื่อนิสิต _____

สาขาวิชา　　วิศวกรรมโยธา　　　　　　　　　ลายมือชื่อ อ.ที่ปรึกษาวิทยานิพนธ์หลัก_____

ปีการศึกษา　2554　　　　　　　　　　　ลายมือชื่อ อ.ที่ปรึกษาวิทยานิพนธ์ร่วม_____

5271854921: MAJOR CIVIL ENGINEERING
KEYWORDS: MODEL / CHLORIDE INGRESS / CRACK / REINFORCED CONCRETE / MARINE ENVIRONMENT /

QUOC VU HOANG: MODEL FOR CHLORIDE INGRESS INTO REINFORCED CONCRETE STRUCTURE UNDER LOAD AND MARINE ENVIRONMENT. ADVISOR: ASSOC. PROF. BOONCHAI STITMANNAITUM, D.ENG., CO-ADVISOR: PROF. SUGIYAMA TAKAFUMI, Ph.D.,119 pp.

The durability of reinforced concrete structures is very important and becomes serious problems in construction technology nowadays. Many factors, such as concrete proportion, service load and environmental actions that effect on the durability of concrete structure. Particularly, the durability of reinforced concrete structure in marine environment has been reduced quickly. In the past, a large number of prior researchers have introduced the models for chloride penetration into plain concrete and reinforced concrete. However, they have had a disadvantage that almost of simulations are conducted with the pure concrete or uncracked concrete. In fact, in the real structure, most reinforced concrete structures are often exposed and accompanied with cracks that will reduce the durability of reinforced concrete faster than the uncracked concrete case.

In this research, the models were proposed to predict the chloride ingress through cracks into reinforced concrete. The chloride diffusivity into cracked reinforced were simulated following one and two dimensions. These models are based on the theoretical analysis and experiments of chloride diffusion coefficient and chloride profile. The cracks investigated were the tapered cracks or V-shaped cracks created by the flexural stress to reinforce concrete member. The research showed that in addition to the crack width, the crack depth must be considered as a factor effecting on the chloride penetration depth. The experiments indicated the chloride penetration depth would be increased in increase of the crack depth. The chloride diffusion coefficient was updated as a function of the crack characteristics, crack width and crack depth. The model for two dimensional chloride diffusivity was proposed based on an assumption of the surface chloride content on crack plane and the chloride diffusion coefficient of crack. The predicted results of models fit well with the experimental ones conducted by different methods, the chemical analysis and the electron probe microanalysis.

Department : Civil Engineering   Student's Signature

Field of Study : Civil Engineering   Advisor's Signature

Academic Year : 2011   Co-advisor's Signature

ACKNOWLEDGEMENTS

CONTENTS

LIST OF TABLES

LIST OF FIGURES

CHAPTER I

INTRODUCTION

1.1   Background

Up to now, reinforced concrete has become one of the most widely used construction materials in the world. Furthermore, it is predicted to be continually a material in 21st century and in the future due to its considerable strength and better resistance to the severe environment. Improvement of the living condition asks to recognize that the durability of reinforced concrete structures is very important and becomes serious problems in construction technology nowadays. Many factors, such as concrete proportion, service load and environmental conditions that influence on the durability of concrete structure. Specially, the durability of reinforced concrete structure in marine environment has been reduced quickly (Mehta, 2003).

In marine environment, there are many deterioration mechanisms of reinforced concrete structure by complexly physicochemical causes. However, corrosion of reinforced concrete is considered one of the major deterioration mechanisms where chloride attack is recognized as a main factor (Bermudez and Alaejos, 2010). In marine structure, chloride ions may attack in the pore structure by the transport of diffusion mechanism accompanying with chemical reactions (Sugiyama, Ritthichauy and Tsuji, 2003, 2008). They are able to penetrate through the concrete cover layer, destroy the protective oxide film on the steel surface and cause a corrosion of the steel reinforcements in concrete (Richardson, 2002). The corrosion results the increase in costs related to maintain and repair the damaged structure.

In the past, a large number of prior researchers have investigated the chloride penetration into reinforced concrete; in addition, numerous models to predict transport properties and service life have been introduced. The development of reliable models to predict chloride ingress into concrete is very important to prevent the deterioration of designed structures under exposed environment (Walraven, 2008). As these models have been experimented in laboratory condition, they often fail to predict service life of real structure accurately. It has a disadvantage that all the simulations are conducted with the pure concrete or uncracked concrete. In fact, in the real structure, most reinforced concrete structures are often exposed involving cracks that will reduce the durability of reinforced concrete faster than the uncracked concrete case.

The cracks due to a result of various physical and chemical interactions between concrete and environment can occur at any time, during all stages in the concrete structure life. Particularly, under loading it can rise and propagate quickly. Like a fast access slot, the cracks may take

chloride ions into concrete structure, that is why it becomes an important parameter strongly influencing on permeability of concrete and chloride ingress into concrete.

A lack of the previous models to predict service life of reinforced concrete is an influence of cracks to the reinforced concrete deterioration. Although, there are many models introduced to describe that the cracks are able to vary the transfer properties of concrete. However, a limitation is the previous researches have not yet satisfied an accurate quantification of crack effects. That results an insufficient knowledge about the influences of crack on the chloride penetration. One more reason, it is very complicate to analyze these models since the cracks are introduced, because they would become confusingly when many factors of crack were taken into account. These factors include the geometric characteristics of crack, such as crack width, crack depth, crack distribution and connectivity or the non-uniform of crack, and crack healing. These factors may cause a difficulty for simulation and prediction of concrete durability and give a new challenge for increasing the reliability of methods in concrete research field.

1.2 Statement of Problems

In the field, the concrete structure is affected by combine factors, such as loading and marine environment. Especially, the natural cracks maybe occur due to the service loads which are unexpected from accidental overload or collision etc. Although the service life prediction of reinforced concrete have been done with uncracked concrete in a durability design task, once a crack occurs in the concrete cover, chloride ions are accelerated to diffuse into concrete structure whose durability, as a result, will be reduced quickly. For this reason, a model should be proposed to predict again the chloride penetration through this crack into reinforced concrete; and this model may become an important solution to evaluate the remaining service life of concrete structure. Thus, it is very complicate to predict the chloride penetration in cracked reinforced concrete due to the unclear characteristics of crack. Conclusively, the highlight of this research is a prediction of chloride ingress into reinforced concrete under marine environment in case of cracks occurring on concrete member.

CHAPTER II

LITERATURE REVIEW

This chapter provides the basic knowledge and theory about the chloride ingress in cracked concrete and the influence of crack characteristics on the chloride penetration. The chloride ingress in cracked concrete was a main action causing corrosion of steel reinforcement embedded in concrete structure and numbers of researches were carried out to explore that problem before.

2.1 Chloride induced corrosion in cracked concrete

2.1.1 Corrosion mechanisms of steel reinforcement in concrete

Corrosion of a metal is a chemical reaction between the metal and surrounding environment. However, the steel reinforcement in concrete can be prevented the corrosion by a passive layer formed on the surface of steel (Bayliss and Deacon, 2004). The condition leads to form this passive layer is alkaline which is high concentrations of soluble calcium, sodium and potassium oxides accumulated in the microscopic pores of concrete (Mehta and Monteiro, 2006). The steel reinforcement is just corroded in acids, that is why it can be protected from corrosion by the alkalis being the opposite of acidity.

However, this passive layer is not always maintained. The chloride attack can destroy the passive layer on the surface of steel reinforcement in concrete prior attacking the concrete (Trejo and Pillai, 2003, 2004; Ha, Muralidharan, Bae et al., 2007). Once the passive layer acting as anodes breaks down, there is a potential difference along the steel in concrete by dissolution of corroded steel in the pore water and gives up electrons (Bertolini, Elsener, Pedeferri et al., 2004):

Anodic reaction: $Fe \rightarrow Fe^{2+} + 2e^-$ (2.1)
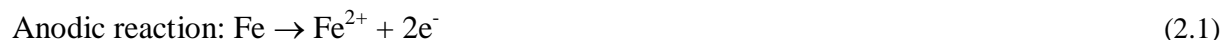
In addition, the rest of steel continues to remain passive and act as the cathode. In the cathode reaction, occurs the preservation of electrical neutrality, (Broomfield, 2007), the two electrons, which are created in the anodic reaction, have to react with the water and oxygen:

Cathodic reaction: $2e^- + 1/2O_2 + H_2O \rightarrow 2OH^-$ (2.2)

The cracking and spalling of the concrete would not be occurred if the iron were just to dissolve in the pore water, unless several more stages must occur for rust. There are several formations of rust depended on the oxygen supply and environmental conditions, such as ferric oxide Fe_2O_3 (red rust) or Fe_3O_4 (black rust):

$Fe^{+2} + 2(OH)^- \rightarrow Fe(OH)_2$

$$4Fe(OH)_2 + 2H_2O + O_2 \rightarrow 4Fe(OH)_3$$

$$2Fe(OH)_3 \rightarrow Fe_2O_3 + 3H_2O$$
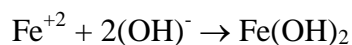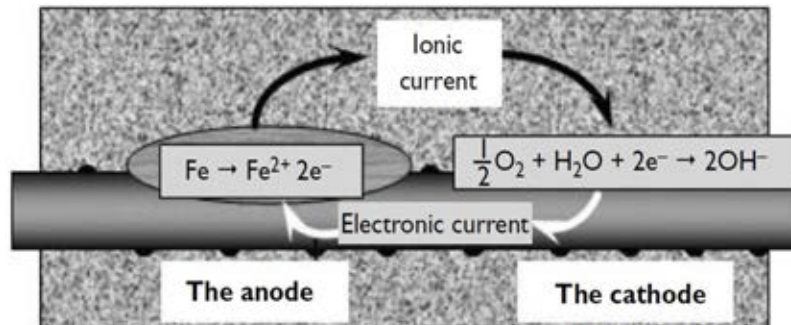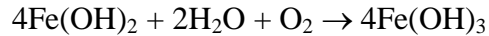
Figure 2.1. The anodic and cathodic reactions in the corrosion of steel bar in concrete (Broomfield, 2007)

The metallic iron transforms to rust causing an increase in volume on the steel surface. This volume depends on the state of oxidation and can be up to six time of the original metal, Figure 2.2. This volumetric increase creates expansive stresses within concrete and when the pressure stress exceeds the tensile strength of concrete cover, the concrete may crack. So, the increase in volume is considered to lead the principal cause to expanding and cracking of concrete cover. Since further development will leads to spalling and delamination and finally leading to falling of concrete cover (El-Reedy, 2008).
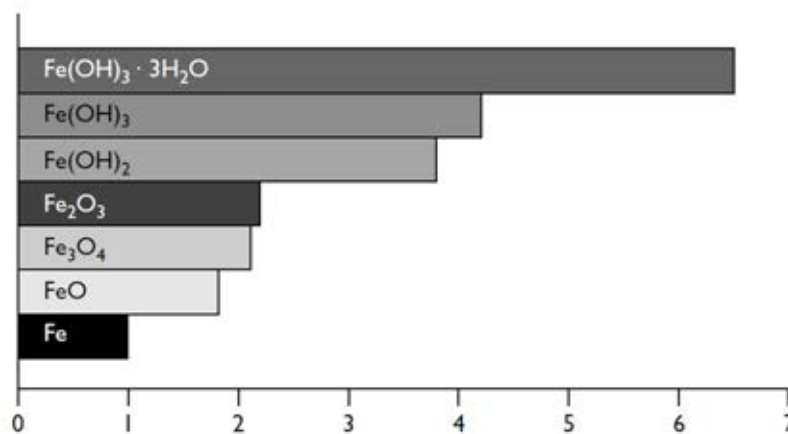
Figure 2.2. Volumetric expansion like a result of metallic iron (Broomfield, 2007)

2.1.2 The effect of crack on the steel reinforcement corrosion in concrete

In the field, cracks often occur in concrete structures due to the action of loads and other causes such as plastic shrinkage, thermal gradients, freezing and thawing, settlement cracking, chemical

reaction etc (ACI-224.1R, 1998). Comparing with uncracked concrete, cracks in concrete structures not only reduce the overall strength, bond strength of concrete structures and reinforcement but also accelerate the ingress of oxygen, water and other aggressive ions, which lead to other types of the corrosion and propagate much higher corrosion rate. Once a crack occurs in surface of reinforced concrete, it will provide an easy access for ingress agents, such as water, chloride and oxygen, to the steel surface. That is why the environment conditions play an important role for corrosion in cracked concrete more than in uncracked concrete (Boulfiza, Sakai, Banthia et al., 2000; Gjørv, 2009). The main transport mechanism for chloride ingress in cracked concrete is convection due to capillary suction where the crack walls act as the capillaries, while it is diffusion in uncracked concrete (Boulfiza, Sakai, Banthia et al., 2003). Therefore, chloride ions will destroy the passive layer of steel at the crack region and lead to corrosion much earlier than expected.

Schiessl (Schiessl and Raupach, 1997) proposed two different cases of corrosion mechanisms that a steel corrosion is theoretically possible to take place in the region of cracks:

- In case one, both the location of anodic and cathodic polarizations are close to each other in the crack zone (microcell corrosion). Required oxygen is principally through the crack to supply to the cathodic reaction acting surface zones.

- In case two, the anode polarization is the steel reinforcement in the crack regions, the passive steel surface between the cracks will form the cathode. Generally, the supplied oxygen transports to the cathode via the uncracked area of the concrete (macrocell corrosion). Because the steel surface involved in the cathodic reaction is much larger, so the corrosion rates are able much higher than in case 1.
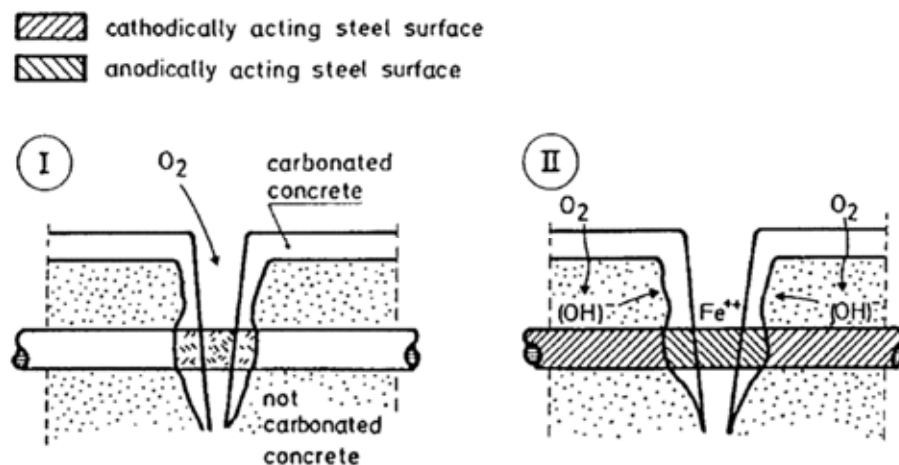
Figure 2.3. Schematic representation of two types for corrosion process in crack region (Schiessl and Raupach, 1997)

2.2 Transport mechanisms of chloride through cracked concrete

The fluids and ions can transport through concrete by four basic mechanisms (Soutsos, 2010):

- Capillary suction caused by capillary action inside capillaries,

- Permeation caused by pressure gradients,

- Diffusion caused by concentration gradients, and

- Migration caused by electrical potential gradients.

2.2.1 Capillary suction

The capillary suction is the transport of chloride containing liquids, sea water, into a porous material, concrete. Generally, when concrete touches water, which is absorbed rapidly by the surface tension acting in the pores of concrete. This absorption is a function of the surface tension, the viscosity and density of the liquid, the radius of the pore; in addition to the angle of contact between the liquid and the pore walls and the continuity of pore structures. Normally, a concrete containing more pore will absord more water and faster than denser concrete.

Especially, when concrete contains the cracks, the crack walls act as the capillaries like the straws to adsorb the chloride solution into concrete. Capillary action is stronger in decrease in the pore dimensions or crack width. However, the transport will be slower due to increasing friction if the pores become smaller or the influence of the tortuosity and constrictivity of crack (Vu, Hoang Quoc, Stitmannaithum, Boonchai and Takafumi, Sugiyma, 2011).

The velocity of the capilary rise is expressed by (Kropp and Hilsdorf, 1995):

$$\vartheta = \frac{1}{8\eta}\left(r\frac{2\sigma\cos\phi}{x} - g\rho r^2\right) \tag{2.3}$$

Where ϑ: velocity of capillary rise (m/s), η: the liquid viscosity (Ns/m^2), r: the capillary radius (m), σ: surface tension of the liquid (N/m), ϕ: wetting angle, g: gravity (m/s^2), ρ: density (kg/m^3), x: height (m).

2.2.2 Permeation of salt solution

Permeation is defined by a liquid penetrating into concrete that is saturated by a pressure head. The flow through the pores of conrete can be defined by Darcy's law:

$$\frac{Q}{t} = \frac{k.\Delta P.A}{L.\eta} \tag{2.4}$$

where Q: volume of liquid flowing (m^3), t: time (s), K: the permeability coefficient of concrete (m^2), η: the fluid viscosity (N.s/m^2), ΔP: the pressure difference (N/m^2), A: penetrated area (m^2) and L: the thickness of penetrated specimen (m).

The permeability of the concrete depends on the capillary porosity and pore conectivity. The permeability coefficient increases in increace on the W/C ratio and hydration proceeds. Wang (Wang, Jansen, Shah et al., 1997) and Aldea (Aldea, Shah and Karr, 1999b) employed the feedback controlled slitting test to create a crack and investigated the permeability of cracked concrete during 20 and 50 days (Figure 2.4). They concluded that the crack width had a relatioship to water peameabillty of cracked concrete. The permeability of water increased rapidly with increase on the crack width from 50 to 200 μm, and became steady when the crack width was larger than 200 μm (Wang et al., 1997). They also concluded that the water permeability was dependent on properties and performance of materials; typically, it decreased from paste, mortar, normal strength concrete and high strength concrete due to the increase in the density of concrete. Contrary to uncracked concrete, the permeability of cracked cocnrete was dependent on the morphology of the cracks and transtion zone effects (Aldea et al., 1999b).
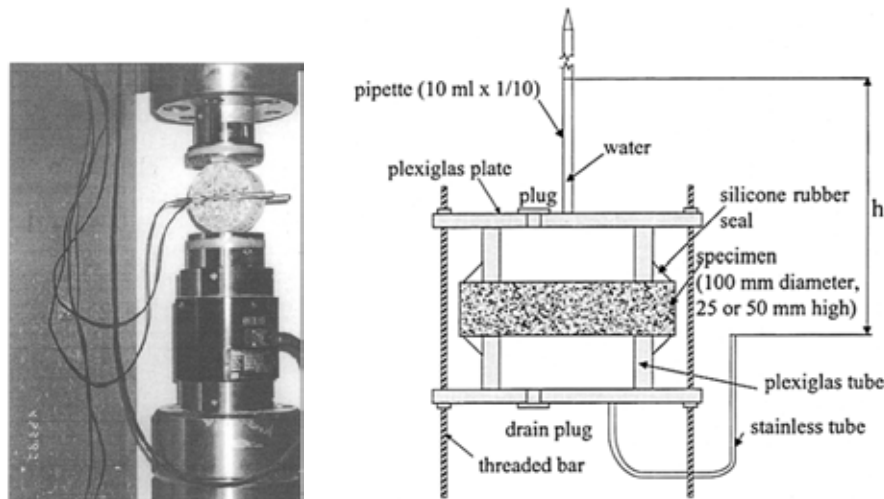
Figure 2.4. Feedback controlled slitting test and water permeability test setup (Aldea et al., 1999b)

Similar to Wang (Wang et al., 1997) and Aldea (Aldea et al., 1999b), Picandet (Picandet, Khelidj and Bellegou, 2009) used the controlled slitting test to investigate the water and gas permeability of cracked concrete. They also took into account the influence of the crack tortuosity and roughness on the permeability of cracked concrete. The water permeability of crack reduced when increase the crack tortuosity and the roughness of the crack plane.

2.2.3   Diffusion

Diffusion occurs by the effect of a concentration gradient in pores that are totally or partially water filled. Due to the difference of concentration on the surface of conrete and inner concrete, chloride ions can move through pores from the surface to internal zones. The concern is often characterised by a diffusion coefficient or effective diffusion coefficient.

- Fick's 1st Law

Fick's 1st Law describes the phenomenon of diffusion with the free concentration of dissolved chloride under conditions of stationary mass transfer, as the transport potential (Nilsson, 2005):

$$q_{Cl} = -D_{F1} \frac{\partial c}{\partial x}$$ (2.5)

where q_{Cl}: the flux of chloride (kg/m^2.s), c: the free concentration at distance x from the surface, D_{F1}: the diffusion coefficient (m^2/s),

The diffusion coefficient depends on the concrete characteristics, created by the pore structure which can be varied by hydration of the cement paste. In addition, this coefficient can vary as a function of the environmental conditions, such as humidity and temperature.

- Fick's 2nd Law

Since diffusion action rarely reaches stationary conditions in concrete structures, the flux gives the changes with time and is expressed by Fick's 2nd Law (Nilsson, 2005; Lindvall, 2007):

$$\frac{\partial C}{\partial x} = D_{F2} \frac{\partial^2 c}{\partial x^2}$$ (2.6)

The equations of both Fick's Law are equal, however different with the diffusion coefficient D_{F1} in Fick's First Law, the diffusion coefficient D_{F2} in Fick's Second Law is used for a porous material with binding.

This equation is always accompanied with the assumptions:

- The concrete is homogeneous, so the diffusion coefficient does not change through the concrete thickness.
- The concrete does not contain the initial chloride content (C = 0 for x > 0 and t = 0).
- The boundary condition: C = C_0 for x = 0 and t > 0.

A solution for equation (2.6) is given by the compliment to the error-function (Meijers, 2003):

$$C(x,t) = C_s \left(1 - erf \left(\frac{x}{2\sqrt{D_a.t}} \right) \right)$$ (2.7)

Where erf: error function, D_a: apparent chloride diffusion coefficient, t: exposed time.

However, in the field the chloride diffusion coeffcient and surface chloride content are time-dependent, typicaly, the chloride diffusion coeffcient will decrease in time and surface chloride content increase with time (Song, Lee and Ann, 2008).

2.2.4 Migration

The transport of ions in solution under the influence of an electrical potential gradient is called migration. The chloride migration tests have been used widespread to evaluate for ability to

chloride penetration and calculate chloride migration/diffusion coefficient. A type of migration test is non-steady-state migration, which is expressed as the chloride penetration depth into a specimen in an electrical potential gradient (Luping and Nilsson, 1993; Mien, 2008). The non-steady-state migration coefficient can be calculated by equation below (Northtest-NTBuild-492, 1999):

$$D_{nssm} = \frac{Rt}{zFE} \cdot \frac{x_d - \alpha\sqrt{x_d}}{t} \tag{2.8}$$

Where:

$$\alpha = 2\sqrt{\frac{RT}{zFE}} \cdot erf^{-1}\left(1 - \frac{2c_d}{c_0}\right); \quad E = \frac{U-2}{L}$$

z: absolute value of ion valence, for chloride, z = 1; F: Faraday constant, F = 9.648 ×104 J/(V.mol); U: absolute value of the applied voltage, V; R: gas constant, R = 8.314 J/(K.mol); T: average value of the initial and final temperatures in the anolyte solution, K; L: thickness of the specimen, m; t: test duration, seconds; erf^{-1}: inverse of error function; c_d: chloride concentration at which the color changes, $c_d \approx 0.07$ N for OPC concrete; c_0: chloride concentration in the catholyte solution, $c_0 \approx 2$ N.

Another method applies an electrical potential through a specimen until detecting the steady-state flow of chloride ions in the downstream cell. This method has been used widespread (Sugiyama, Bremner and Tsuji, 1996; Truc, Ollivier and Carcassès, 2000; Castellote, Alonso, Andrade et al., 2001; Sugiyama, Tsuji and Bremner, 2001; Yang and Cho, 2003; Yang and Cho, 2004; Yang and Wang, 2004; Yang and Cho, 2005; Sun, Sun, Zhang et al., 2012). The steady-state migration coefficient (effective diffusion coefficient) is expressed as follows (JSCE, 2003):

$$D_e = \frac{J_{Cl}RTL}{|Z_{Cl}|FC_{Cl}(\Delta E - \Delta E_c)} *100 \tag{2.9}$$

Where:

D_e: effective diffusion coefficient (cm^2/year); R: gas constant (=8.3 J/(mol.K)); T: absolute temperature; Z_{Cl}: charge of chloride ion (=-1); F: faraday constant (=96,500 C/mol); C_{Cl}: measured chloride ion concentration on cathode side (mol/l); $\Delta E - \Delta E_C$: electrical potential difference between specimen surface (V); L: length of specimen (mm). J_{Cl}: flux of chloride ion in steady state (mol/(cm^2.year))

$$J_{Cl} = \frac{V^{II}}{A}\frac{\Delta c_{Cl}^{II}}{\Delta t} \tag{2.10}$$

V^{II}: volume of anode solution (L); A: cross section of specimen (cm^2); $\Delta C_{Cl}^{II}/\Delta t$: rate of increase in chloride ion concentration on anode side ((mol/l)/year).

Moreover, the ions are able to transport only in water-filled and interconnected pores. That why, the volume, geometry and distribution of pore will effect on the rate of migration and diffusion into concrete. Consequently, magnitude of ion migration and diffusion into cement-based materials under saturate condition is lower of 2–3 times when compared to bulk solutions.

2.3 Background of correlations of crack to chloride ingress

2.3.1 Crack generation method

According to the previous researches, the crack studied on the influence of chloride penetration into concrete can be classified into two types, artificial cracks and natural cracks.

The artificial cracks have some disadvantages such as not reflected reality; the crack surface contains more cement paste, not tortuous, etc. However, the artificial cracks are easy to generate or model and they give the clear and unitive results in experiment. Normally, the artificial crack is generated by pressing the copper sheets having difference thickness on the fresh surface of concrete specimen (Marsavina, Audenaert, Schutter et al., 2009). This type of artificial crack also terms a notch.

Figure 2.5. The artificial crack (notch) by Marsavina (Marsavina et al., 2009)

Contrary to the artificial cracks, the natural cracks are very complicated to model and experiment. Moreover, it is very difficult to clearly identify the influences of the crack width and crack depth on the transportation of chloride ions (Kato, Kato and Uomoto, 2005). Up to now, there are different methods to create the real cracks. Regarding the prior researches, they can be divided into four groups:

- A crack can be created in the concrete core by the feedback controlled splitting test. The crack opening displacement was recorded by the linear variable displacement transducers (LVDT) attached on both crack sides (Wang et al., 1997; Aldea, Shah and Karr, 1999a; Rodriguez and Hooton, 2003; Djerbi, Bonnet, Khelidj et al., 2008a).

Figure 2.6. Controlled splitting test (Djerbi et al., 2008a)

- Apply the wedge splitting tests to generate a crack, this method were widely used in the fracture mechanic field and in the analytical description of the crack formation (Karihaloo, Abdalla and Xiao, 2006). Reinhardt (Reinhardt, Sosoro and Zhu, 1998) used the wedge splitting test to create a crack for conducting the penetration of organic fluid into the cracked concrete.
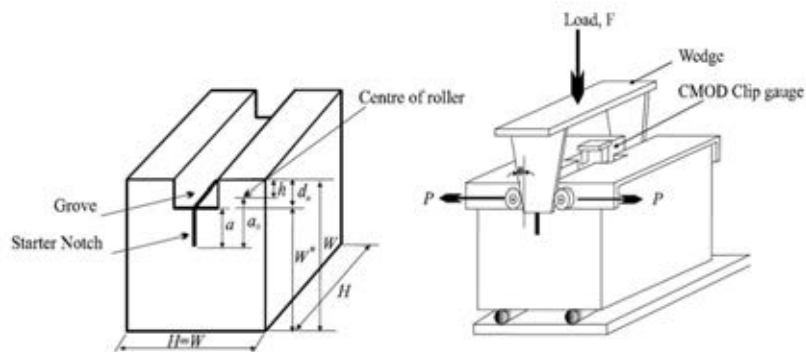
Figure 2.7. The wedge splitting test (Karihaloo et al., 2006)

- The cracks in the tensile stress were generated by the bending test (three or four-point) (Gowripalan, Sirivivatnanon and Lim, 2000; Li, Zheng and Shao, 2003; Win, Watanabe and Machida, 2004; Kato et al., 2005). The shape of this crack is nearly to the real crack appearing on reinforced concrete structure under loading in the field.
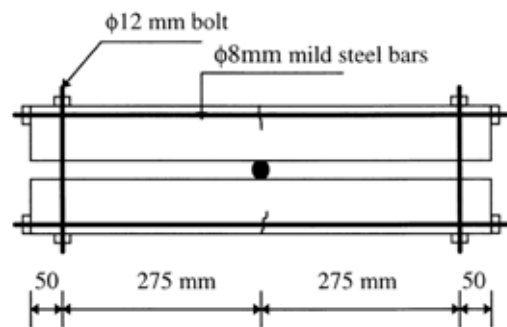
Figure 2.8. Crack crated by the bending test (Gowripalan et al., 2000)

- The tensile crack was generated by a mechanical expansive core and an external confinement steel ring (Ismail, Toumi, Francois et al., 2004; Ismail, Toumi, François et al., 2008).
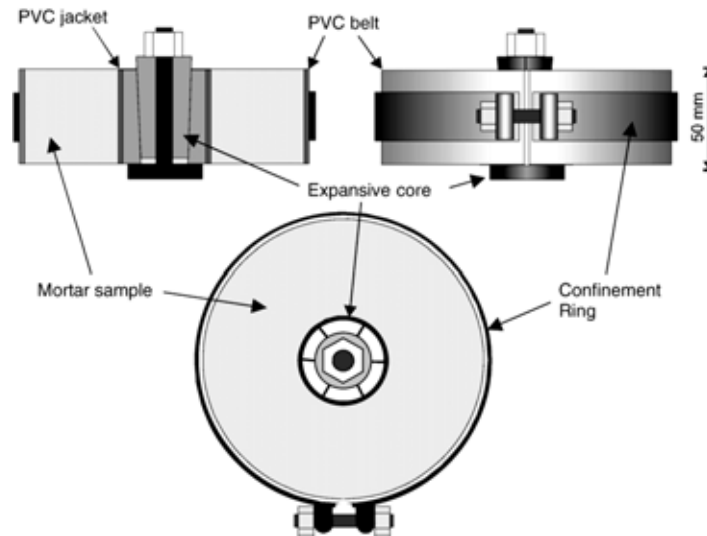
Figure 2.9. The sample and the expansive core (Ismail et al., 2008)

Conclusively, to model the real crack on concrete structure, the natural crack is still the preferably generated method more than the artificial crack to simulate, reach the conditions in the field and reflect the real results.

2.3.2 Influence of crack width and crack depth on chloride diffusion

2.3.2.1 Crack width

Table 2.1. Maximum permissible crack width (ACI-224-01, 2001)

Exposure condition	Permissible crack width (mm)
Dry air or protective membrane	0.4
Humidity, moist air, soil	0.3
Deicing chemicals	0.2
Seawater and seawater spray, wetting and drying	0.15
Water-retaining structures	0.1

Although the role of design task is to obtain the reinforced concrete structure without cracking, in the field during the service life, a crack may occur anywhere and anytime as an unexpected due to many reasons. In previous researches, there is an agreement that the maximum crack width and risk corrosion of steel reinforcement in concrete have had a relationship. That is why

there is a requirement in the reinforced concrete design for the limitation of maximum crack widths. ACI Committee (ACI-224-01, 2001) recommended the maximum permissible crack widths to prevent corrosion of reinforced concrete subjected under different exposure conditions.

Table 2.2. Permissible crack width and minimum concrete cover.

Code	Permissible crack width, W_{cr} (mm)	Minimum cover, C (mm)	W_{cr}/C
CEB/FIP Model Code (1990)	0.3	40	0.0075
ACI Manual (1994)	0.15	40-60	0.0025-0.003
ENV 1991 (1992)	0.3	40	0.0075
BS 8110 (1994)	0.3	50	0.006
AS 3600 (1997)	NA	40-50	-

Regarding Table 2.2, showed that many codes proposed different values for maximum permissible crack width; it is evidently because these values were suggested based on experiences, which are not the same for each country. Gowripalan (Gowripalan et al., 2000) surveyed the maximum permissible crack width and minimum concrete cover thickness proposed by various codes for reinforced concrete design under marine environment, Table 2.2, and also found that the lack in the AS 3600 code for the permissible crack width.
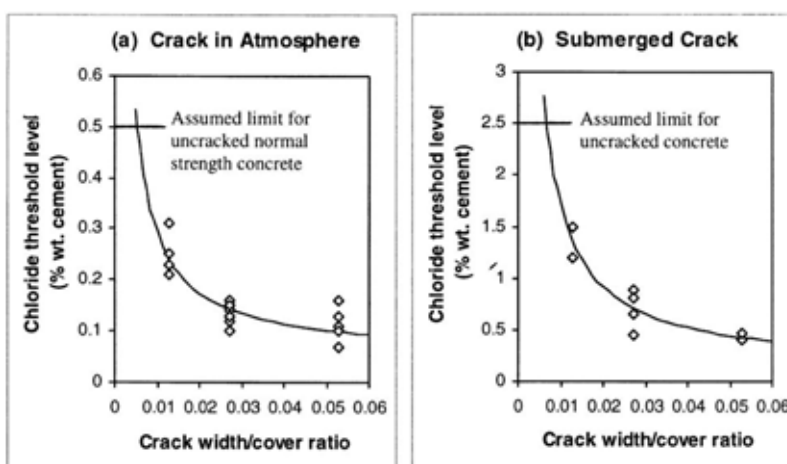
Figure 2.10. Correlation of chloride threshold level to Wcr /C (Gowripalan et al., 2000).

The initial corrosion is affected by the crack width; however, it is insufficient unless the combined influence of crack width and thickness of concrete cover is considered. The relationship of crack width to concrete cover thickness ratio and the value of chloride threshold

is investigated and illustrated in Figure 2.10 by Gowripalan (Gowripalan et al., 2000). Regarding these results, the value of chloride threshold would decrease with increase in the W_{cr}/C. Moreover, the critical chloride concentration for corrosion of a crack exposed in atmosphere is lower than that of a submerged crack.
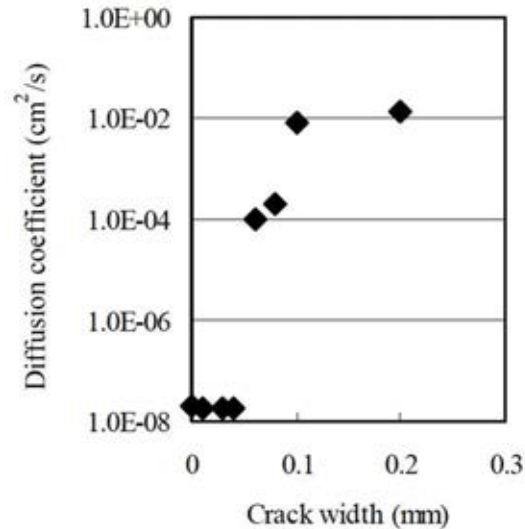
Figure 2.11. Diffusion coefficient and crack width tested with mortar specimens (Takewaka, Yamaguchi and Maeda, 2003)

Crack width is very important in corrosion of reinforced concrete due to a strong effect to the chloride permeability and the deterioration of concrete structures. Especially, the crack width opening can control the rate of chloride penetration through itself. To observe the influence of crack width on the diffusion property of chloride ions, Takewaka (Takewaka et al., 2003) used a sliced mortar specimen containing a crack put in a diffusion cell test apparatus. In their experiment results (Figure 2.11), they recognized that if the width of cracks is less than 0.05 mm, no influence diffusivity, and the diffusion effects of chloride ions became steady when the width of cracks exceed 0.1 mm.

Ismail also investigated the chloride diffusion into crack by the inert material (Ismail et al., 2004) and mortar (Ismail et al., 2008). In their research, cracks were generated by expansive cores and the chloride concentration profiles were collected at the exposed surface and perpendicular to crack wall (Figure 2.12). By comparing the chloride concentration profiles at the exposed surface and perpendicular to crack wall, they concluded that:

- With the inert material: the chloride profiles being perpendicular to crack wall were very similar to that on the exposed surface when crack width was 60 µm or wider. In case of crack widths of 53 µm or less, there was insignificant to chloride penetration perpendicular to crack wall.

- With the mortar specimens: similar to inert material, the mortar material also reflected the similar results, when crack width opening was lower than the critical value of 30 μm, chloride diffusion did not occur along the crack path. The curve of chloride profiles perpendicular to the crack wall was similar to that on the exposed surface when crack opening was larger 205 μm.
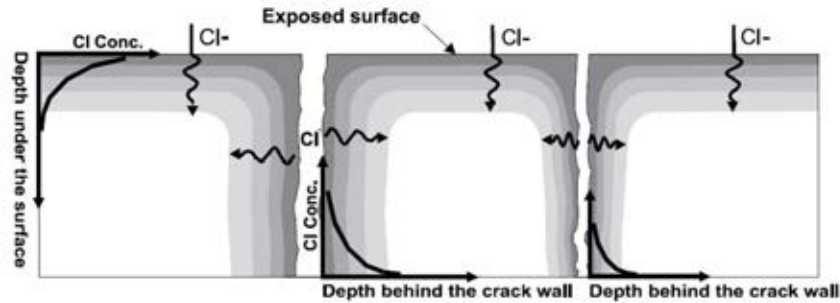
Figure 2.12. The chloride concentration profile collected at location of surface and perpendicular-to-crack wall (Ismail et al., 2004).

Besides creating cracks on the concrete specimens, cracks was introduced on the steel specimens as the slits by investigation of Kato (Kato et al., 2005), Figure 2.13. They experiment to find out a relationship between chloride diffusion coefficient and crack width on both concrete and steel specimens. Their experimental results indicated the apparent chloride diffusion coefficient through a crack increased with increases in crack width, but became steady when cracks in width larger than 75 μm; and formulated by Wang (Wang, Soda and Ueda, 2008) as follows:

$$\log D_{cr} = -2.277[1+1.311\exp(-20.6W_{cr})] \tag{2.11}$$
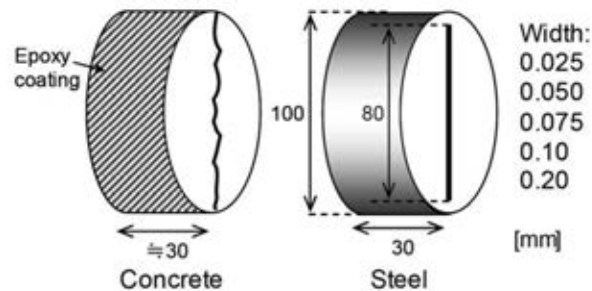
Figure 2.13. Study on chloride diffusion into cracks on concrete and steel specimens (Kato et al., 2005).

Similarly, Djerbi (Djerbi, Bonnet, Khelidj et al., 2008b) indicated that the chloride diffusion coefficient of crack correlated to crack width following equation (2.12). Moreover, the chloride diffusion through crack increased corresponding to increase in crack width. However, it became constant as crack width was larger than a threshold value of 80 μm. The experimental results also

indicated that the chloride diffusion coefficient of crack was not dependent on the material effects (Figure 2.14).

$$\begin{cases} D_{cr}(m^2/s) = (2x10^{-11})w - 4x10^{-12}, & \text{when } 30\mu m \leq w \leq 80\mu m \\ D_{cr}(m^2/s) \approx 14x10^{-10}, & \text{when } w > 80\mu m \end{cases}$$

(2.12)
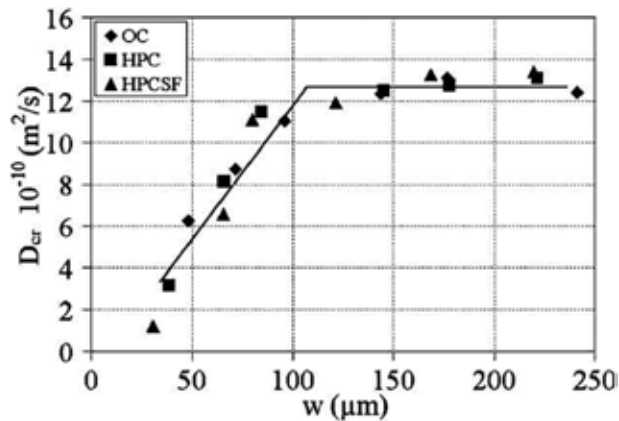
Figure 2.14. Correlation of crack width to diffusion coefficient of crack (Djerbi et al., 2008a).

According to Wang's research results (Wang and Ueda, 2010), this threshold value for crack width was 60 μm, because if it is larger than that the chloride diffusion coefficient (D_{cr}) is independent on crack width .

Conclusively, when surveying the chloride diffusion through a crack of concrete, previous studies took into account that there were lower and upper threshold values of crack width, (w_1, w_2 respectively) in which:

- When crack width (w) < w_1, the influence of crack on the chloride diffusion through this crack can be ignored. Chloride diffusion cannot occur along the crack path, because the crack would be blocked by self-healing due to deposition of cement hydration products in the crack path.

- When w1 ≤ w ≤ w2, the hydration products cannot block the crack completely, so chloride diffusion will happen in the unblocked parts. However, the chloride diffusion capacity reduces along the crack plane due the mechanical interactions between the fractured surfaces of crack plane when the crack width is reducing. In this region, the diffusion capacity of chloride ions will be depended on crack width.

- When w>w_2, the hydration products cannot block the crack, the environment between the crack planes can be considered as the environment on exposed surface. Alternatively, the chloride concentration in crack planes can be assumed to equal to that in the solution.

The surveying for lower (w_1) and upper (w_2) threshold values of crack width is shown in Table 2.3. The different threshold values of crack width varied in previous researches come from the different materials and methods for generating the cracks.

Table 2.3 The lower and upper threshold values of crack width influencing on chloride diffusion.

Sources	w1 (μm)	w2 (μm)	Material
Takewaka (2003)	50	100	Mortar
Ismail (2004)	53	60	Inert
Francois (2005)	30	-	Concrete
Kato (2005)	-	75	Concrete
Ismail (2008)	30	205	Mortar
Djerbi (2008)	30	80	Concrete
Wang (2010)	-	60	Concrete

2.3.2.2 Crack depth

On the other hand, the artificial crack depth, which was normally generated by the copper sheets put on the fresh concrete surface, strongly affected to the chloride penetration depth (Marsavina et al., 2009). A conclusion was given that the chloride concentration depth would be increased when the artificial crack depth increased.

Although number researches are studied crack width as only parameter influencing on the chloride diffusion, their results were not unity because of the difference between the generation methods of crack or the material of specimens in each researches. Hence, when concrete with natural cracks bears under cyclic loading and marine environment due to the continuous opening-closing crack width, the various magnitude of crack width and crack depth, chloride diffusion may be strongly varied.

2.3.3 Crack tortuosity and crack constrictivity

2.3.3.1 Crack tortuosity

Tortuosity (τ) was defined as the ratio of the actual pathways (Le) of a fluid particle to the corresponding straight transport path (L), (Figure 2.15) (Promentilla, Sugiyama, Hitomi et al., 2009; Sun, Zhang, Sun et al., 2011).
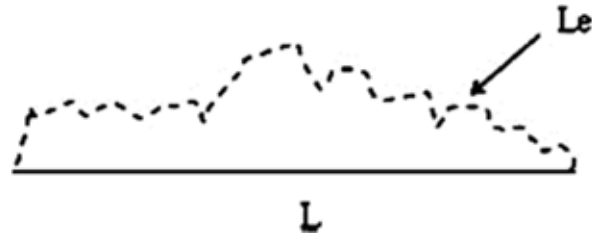
Figure 2.15. The definition of the tortuosity

By synchrotron-based microtomography and 3D pore micro-geometry analysis, Promentilla (Promentilla et al., 2009) proposed an equation to calculate the diffusion tortuosity (τ_{Dx}) of the pore space along the x-axis with random walk simulation of three simple capillary tube models (Figure 2.16):

$$\tau_{Dx} = \left[3\left\{ \lim_{t\to\infty} \frac{d(x^2(t))}{dt} \right\} \right]^{-1} \tag{2.13}$$
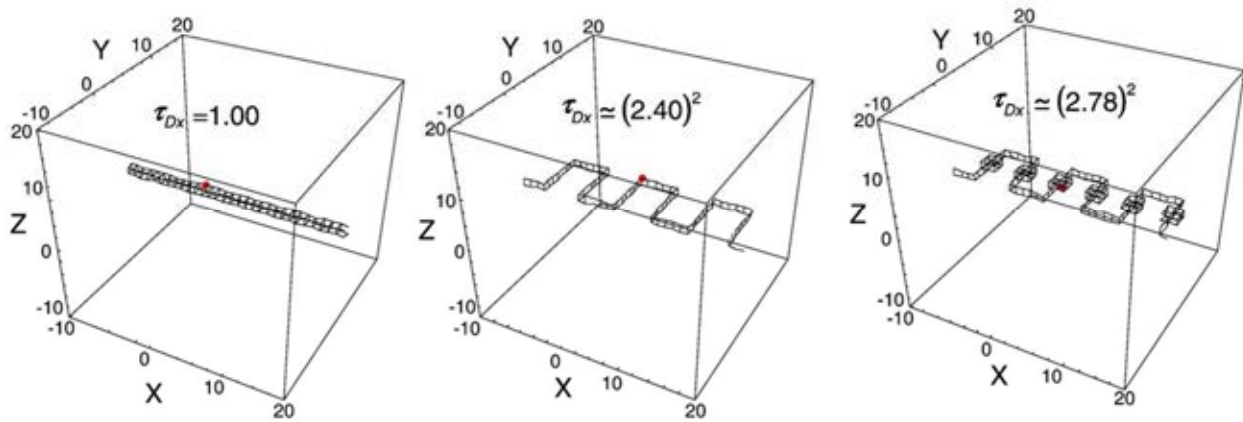
Figure 2.16. The directional diffusion tortuosity along the x-axis by three simple capillary tube models by (Promentilla et al., 2009)

In addition, the tortuosity of the matrix was calculated as a function of the paste porosity by the equation below (Nakarai, Ishida and Maekawa, 2006; Sun et al., 2011):

$$\tau = -1.5\tanh\{8.0(\phi_{paste} - 0.25)\} + 2.5 \tag{2.14}$$

Where: ϕ_{paste} is the total paste porosity (m^3/m^3)

For micro cracks, Mien (Mien, Stitmannaithum and Nawa, 2011) introduced a value of crack tortuosity (τ_{crack}) when studying the chloride penetration into invisible cracks in plain concrete:

$$\tau_{crack} = 1.65 \tag{2.15}$$

Furthermore, Ishida (Ishida, Iqbal and Anh, 2009) assumed the complexity of crack path will be less when comparing to the micro-pore structure of hardened cement based materials; and

proposed the tortuosity of crack was unity and introduced the tortuosity parameter of crack as follows:

$$\tau_{crack} = 1 \qquad (2.16)$$

In addition, regarding to the penetration profile collected from the simulated large cracks, Ismail (Ismail et al., 2008) also indicated that chloride diffusion into large cracks (crack width ≥ 225 μm) was not influenced by the crack tortuosity.

2.3.3.2 Crack constrictivity

Constrictivity (δ) was defined as a correlation of pore structure to ion transport. The constrictivity is unity when a segment of pore space is straight; otherwise it is less than unity if the segment is restricted (Figure 2.17), (Ishida et al., 2009).

(a) $\delta = 1$ (b) $\delta < 1$
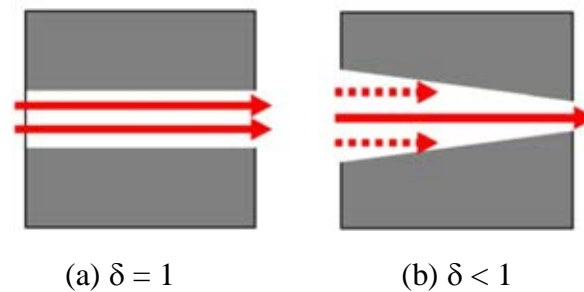
Figure 2.17. The concept for the constrictivity

A dependent relation of constrictivity of matrix on the peak radius of capillary pores was described and calculated as equation follows (Maekawa, Ishida and Kishi, 2003; Sun et al., 2011):

$$\delta = 0.395 \tanh\{8(\log(r_{cp}^{peak}) + 6.2)\} + 0.405 \qquad (2.17)$$

Where r_{cp}^{peak} : the peak radius of capillary pores (m).
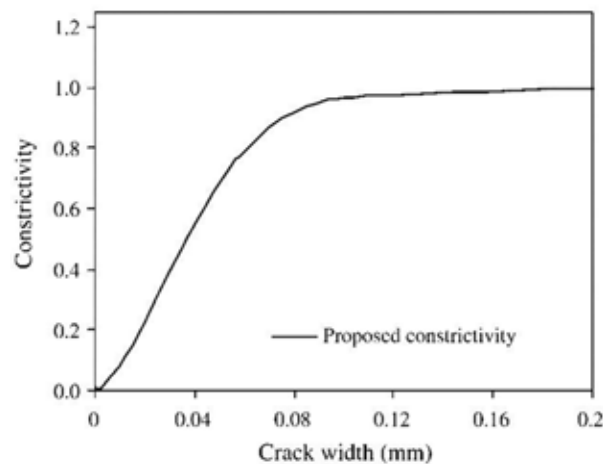
Figure 2.18. Effect of crack width on crack constrictivity parameter (Ishida et al., 2009)

For cracked concrete, Ishida (Ishida et al., 2009) also assumed that the influence of electrical interaction between chloride ions and the crack was ignored, so the relationship between the crack constrictivity (δ_{cr}) and crack width (W_x) was given as Figure 2.18 and equation below:

$$\delta_{cr} = 0.99\tanh\{3.8W_x(\log(W_x)+5.5)\}+0.01 \qquad (2.18)$$

2.4   The loading and marine environment

To survey the chloride permeation under loading, Lim (Lim, Gowripalan and Sirivivatnanon, 2000) used a rapid chloride permeability test to conducted the chloride permeability of plain concrete after bearing an uniaxial compressive load. They recognized that the chloride permeability of concrete began increasing when the stress-strength ratio was over 0.5 (Figure 2.19) and concluded that the characteristics of cracks were varied and influenced on the chloride permeability when a concrete member was subjected under a uniaxial compression load. When the stress-strength ratio was less than 0.5, the all micro-cracks of concrete close back after complete unloading. However, when the applied load was from 0.7-0.95 stress level, some residue specific crack areas are obtained immediately after complete unloading. This indicated only a partial of the micro-cracks was closed.
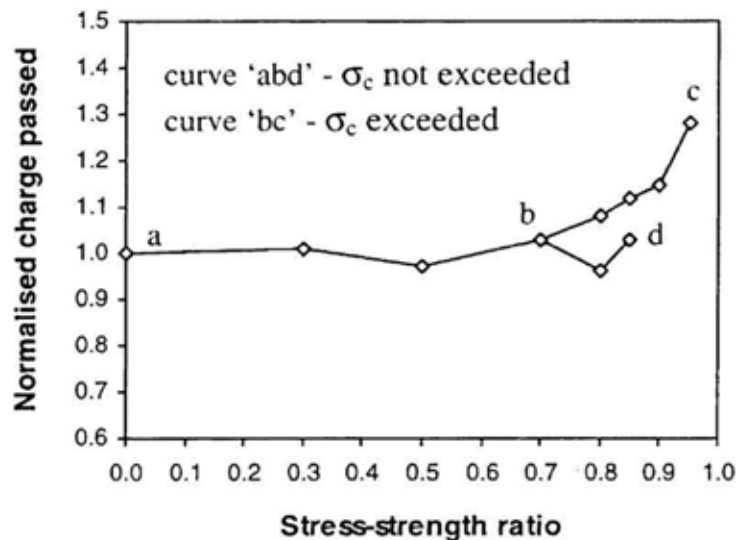
Figure 2.19. Rapid chloride permeability under different stress-strength ratio (Lim et al., 2000).

Wang (Wang et al., 2008) used Rigid Body Spring Model (RBSM) to predict the micro-cracks and the chloride penetration into concrete structure under meso-scale involving three-phase composite, such as coarse aggregate, mortar and interface transition zone (ITZ). Wang's results for the chloride diffusion coefficient of concrete after subjecting to the compressive loading were presented in Figure 2.20. The results showed the increased trends for chloride penetration in compressive zone and were similar with Lim's results, Figure 2.19.
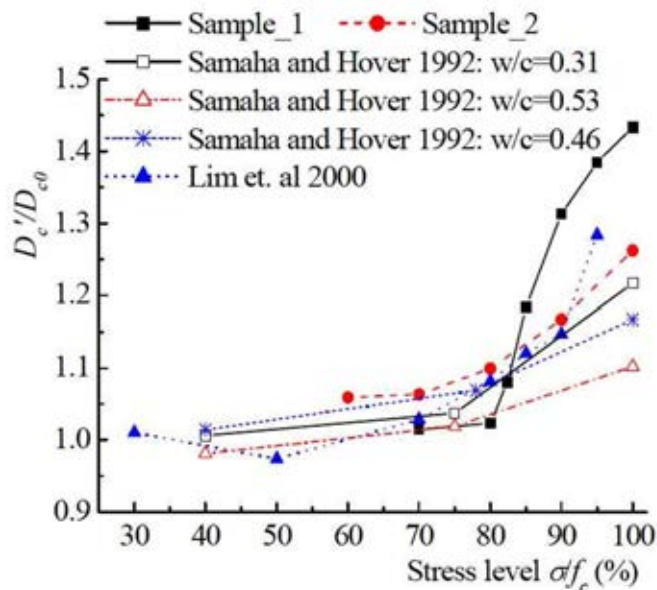
Figure 2.20. Chloride diffusion coefficient at different compressive stress level (Wang et al., 2008)

Similarly, the relationship between stress level and chloride diffusion coefficient in the tension zone was also conducted by Wang (Wang et al., 2008) in Figure 2.21. It can be concluded that after bearing the compressive stress or tension stress, the chloride penetration into concrete will increase with increases in stress level.
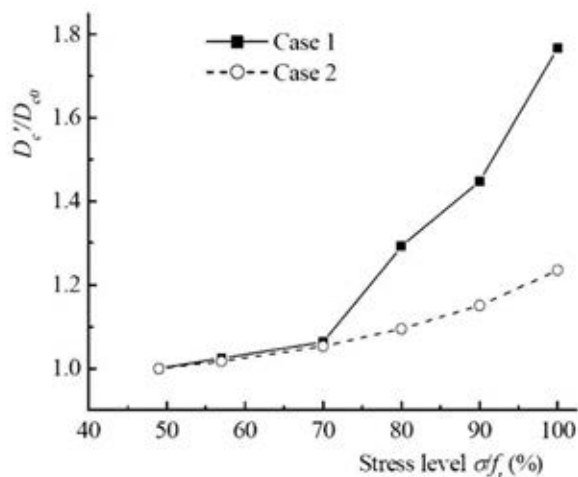
Figure 2.21. chloride diffusion coefficient at different tension stress level (Wang et al., 2008)

On the other hand, the chloride diffusion coefficient in the tensile zones was relatively found higher than that in the compression zone by several researchers when a concrete member was subjected to the combination of flexural loading and salt solution. Mien (Mien, 2008) indicated the chloride diffusion coefficient in the tension zone and compression zone of the concrete member under flexural loading are different and opposite. In the tension zone, when the flexural loading generated tensile stresses beyond elastic stress of concrete, the micro-cracks were widen

to lead porous volume as well as connectivity of concrete increases, so chloride diffusion coefficient increased. On the contrary, the concrete structure became denser in the compression zone and reduced the porous connectivity causing the lower chloride diffusion coefficient.
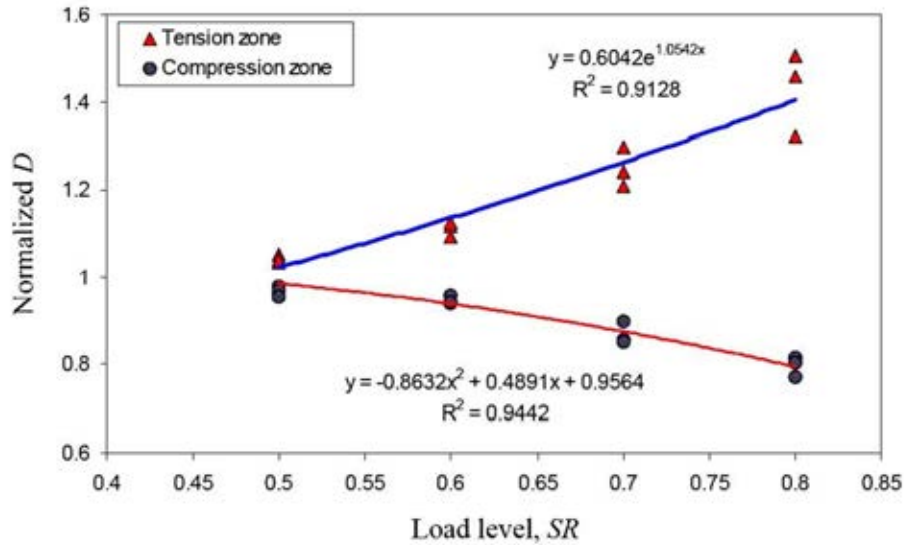
Figure 2.22. The chloride diffusion coefficient in tension zone and compressive zone under flexural loading (Mien, 2008).

Nevertheless, when increasing the steel bar in the tensile zones, that was not significantly an effect of the chloride diffusion coefficient but it was decreased in the compression zone (Gowripalan et al., 2000).

In addition to the effect of loading, the phenomenon of chloride penetration into concrete was also studied under different exposure conditions of marine environment. In submerged zone, the only chloride ion factor cannot damagingly cause corrosion of steel reinforcement. In order for the corrosion process to continue, there must be continues supply of water and oxygen. Consequently, the tidal and splash zones have been recognized as the high corrosion risk areas. In tidal environment, Mien (Mien, Stitmannaithum and Nawa, 2009a) experimented and developed model for chloride penetration into concrete subjected to wetting and drying cycles plenty oxygen supply. They suggested the governing equation describing the chloride penetration in plane concrete under tidal environment as follows:

$$\frac{\partial C_t}{\partial t} = D_a \frac{\partial^2 C_t}{\partial x^2} + \frac{C_t}{\phi} w_{sat} D_h \frac{\partial^2 h}{\partial x^2} + \frac{1}{\phi} \frac{\partial C_t}{\partial x} w_{sat} D_h \frac{\partial h}{\partial x} \tag{2.19}$$

Where:

$$D_a = D_{i,ref} . f_1(T) . f_2(t) . f_3(h) . f_4(SR) / \phi \tag{2.20}$$

$$D_h = 5 x 10^{-12} m / s^2 \qquad \text{(Saetta, Scotta and Vitaliani, 1993)} \tag{2.21}$$

$D_{i,ref}$, which was calculated under standard conditions: temperature 23°C, relative humidity (h=100%) and cement hydration degree after 28 days.

$$f_1(T) = \exp\left[\frac{U}{R}\left(\frac{1}{T_0} - \frac{1}{T}\right)\right] \tag{2.22}$$

With T and T_o expressed in deg K (T_o = 296K), R is the gas constant [kJ/(mol.K)], and U the activation energy of the diffusion process (KJ/mol).

$$f_2(t) = \left(\frac{28}{t}\right)^m \tag{2.23}$$

With t: the time (days), m: a constant that depends on the properties of the concrete mixtures.

$$f_3(h) = \left[1 + \frac{(1-h)^4}{(1-h_c)^4}\right]^{-1} \tag{2.24}$$

With h is the relative humidity in the concrete, h_c (h_c=0.75 at 25^{0}C) is the humidity at which the coefficient D_i drops to halfway between the maximum and minimum values.

$f_4(SR) = 0.0985e^{7.71SR}$ (Mien, Stitmannaithum and Nawa, 2009b), SR is the load level.

$$\tag{2.25}$$

h: is the relative humidity (%)

w_{sat}: represents liquid content (%).

In brief, if concrete structure is under loading and tidal environment, the chloride profile will be varied corresponding to the influence of fracture characteristic such as crack width, crack depth and the influence mechanical interaction between the fractured surfaces.

2.5   Models for chloride ingress into cracked concrete

Simulate a chloride penetration into cracked concrete is a challenge because the complicated characteristic and tortuosity of crack can cause a difficult task. In the literature, there are several models to simulate the chloride penetration into cracked concrete. However, most of these models are related to an influence of crack width on the chloride penetration ability of crack. Furthermore, the determination of chloride content in cracked concrete is very important for the evaluation of corrosion rate. Few proposed models can be applied to simulate the chloride profile in concrete structure caused by the penetration of chloride ions into crack.

For diffusion mechanism of chloride ions, Boulfiza (Boulfiza et al., 2003) proposed using equation of Fick's second Law to simulate the chloride diffusion into crack and matrix of

concrete under saturated condition. In Boulfiza's model, the chloride diffusion coefficient was approximately calculated by using an average chloride diffusion coefficient as equation follows:

$$D_{av} = D_0 + \frac{W}{l} D_{cr} \qquad (2.26)$$

where D_{av} is the average diffusion coefficient, D_0 is the diffusion coefficient of the uncracked concrete, W is the crack width, l is the crack spacing, and D_{cr} is the diffusion coefficient inside the crack, Figure 2.23.
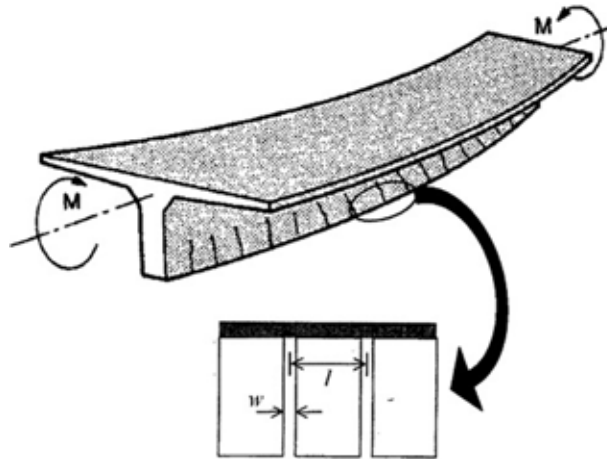
Figure 2.23. The schematic representation of crack spacing l and crack width W (Boulfiza et al., 2003).

However, in the equation of average chloride diffusion coefficient (Equation 2.26), it only mentioned crack width and was constant along crack plane, crack depth has not yet mentioned for evaluation of chloride penetration.
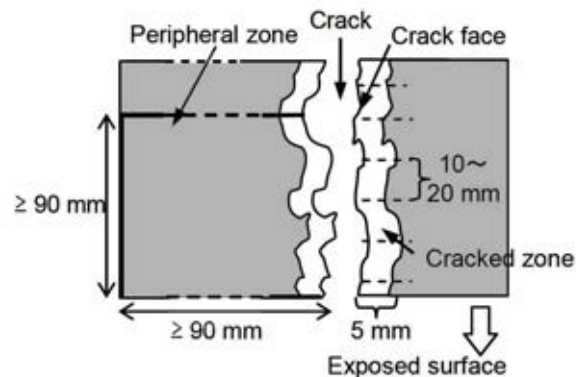
Figure 2.24. Concept for crack zone (Kato et al., 2005)

Contrary to model of Boulfiza, where the chloride profiles at crack and matrix of concrete were calculated by the average, Kato's model (Kato et al., 2005) proposed the chloride content of the

crack zone along the crack face to become the boundary of their model in addition to the exposed surface, Figure 2.24. The required input data for their model included the crack width, the boundary chloride content, the apparent diffusion coefficient of chloride ions in concrete, the apparent diffusion coefficient of chloride ions through the crack. In their model, they also assumed that the apparent diffusion coefficient of chloride ions through the crack was a constant along the crack depth.

Similarly, Paulsson-Tralla (Paulsson-Tralla and Silfwerbrand, 2002) also proposed the crack plane treating as the exposed surface and the chloride concentration on the crack plane also equaled to that on the exposed surface, Figure 2.25.
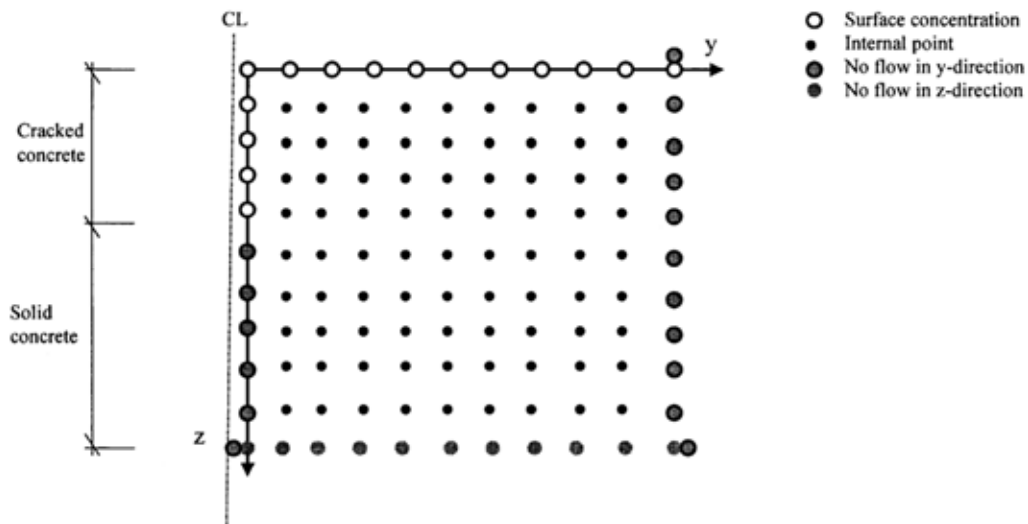
Figure 2.25. The space domain for model of chloride diffusion in cracked concrete, (Paulsson-Tralla and Silfwerbrand, 2002)

On another research, in order to approach a real crack, tapered crack (V-crack), Wang (Wang and Ueda, 2010) proposed a model to calculate the chloride penetration in cracked concrete with single tapered crack. However, this model is not clearly and has not yet validated.

Figure 2.26. Chloride ions spread in two (three) dimension (Paulsson-Tralla and Silfwerbrand, 2002)

Conclusively, in previous models, chloride ions have to diffuse into cracked concrete following at least two dimensions. However, there are several matters that should be consider again to approach for modeling the chloride diffusion into a real crack of concrete. Firstly, there is a lack of crack depth parameter; the proposed assumptions in previous model are suitable for cracks, which are throughout the concrete member and their crack planes are parallel each other. Secondly, the chloride diffusion coefficient through the crack must be a function of crack width. It cannot be a constant along the crack plane where crack width is varied, such as crack width of a real crack. Lastly, regarding the variation of chloride diffusion coefficient corresponding to crack width and the chloride binding capacity of crack plane, the boundary chloride content on the crack plane should also correspond to crack width varied along crack plane in addition to time.

2.6   Concluding remark

From all prior researches, in general view there is no doubt for signification of researching about the chloride penetration into reinforced concrete under service environment. In the field, chloride penetration is caused by combining factors such as kinds of cracks, crack characteristics, loading and marine environment and their influencing process each other. Because of the important role of significant topic, number of researches have been done to propose the models of chloride penetration in cracked and un-cracked concrete. However, these reports only concerned and conducted with the parallel crack walls or/and crack throughout the specimen or the artificial cracks. These cracks are not the real cracks in reinforced concrete structure. Except Win (Win et al., 2004), they investigated the chloride diffusion into cracked reinforced concrete inducted by bending moment. However, in their research the correlation between crack characteristics and chloride diffusion factors had not been obtained yet. As a conclusion, the chloride penetration into cracked concrete or reinforced concrete has been investigated with few influence factors of crack and not yet completely described the comprehension of these factors as the behaviors of a real concrete structure. For this reason, the purpose of this study will propose a model for chloride penetration into natural cracked reinforced concrete (V-shaped crack) under flexural loading and marine environment.

2.7   The objectives of study

- Study on the influence of crack characteristics, such as crack width and crack depth on the chloride penetration into cracked reinforced concrete.

- Develop a model to predict the chloride penetration into cracked reinforced concrete beam (with V-shaped crack) under marine environment.

- Experimental investigation of chloride penetration into cracked reinforced concrete in the simulated marine environment.

- Validate the proposed model by comparing the predicted results and experimental ones of chloride penetration into cracked reinforced concrete.

2.8 The scopes of study

To get the objectives above, the scopes of this study are included as follow:

- Propose a model to predict the chloride profile of cracked reinforced concrete under submerged zone impact.

- The crack studied will be generated as a natural crack having a varied crack width from zero to 0.15 mm by the experimental flexural loading of reinforced concrete beam.

- The marine environment will be simulated in the laboratory by the sodium chloride solution (NaCl 10%).

- The load case applied is static load combining with saturated marine environment in concrete structure will be carried out in this research.

- Under loading and marine environment, the experiments of chloride penetration are studied on reinforced concrete at crack and un-crack locations.

- From the experimental results, validate the proposed model for prediction of the chloride penetration into cracked reinforced concrete structures under marine environment.

CHAPTER III

DEVELOPMENT OF MODEL

3.1 Two dimensional chloride diffusivity model of cracked reinforced concrete

For cracked concrete, two-dimensional chloride diffusion should be assumed as shown in Figure 3.1. In modeling two-dimensional chloride diffusion, Fick's Second Law equation is expressed as follows:

$$\frac{\partial C_t}{\partial t} = D_a^x \frac{\partial^2 C}{\partial^2 x} + D_a^y \frac{\partial^2 C}{\partial^2 y} \qquad (3.1)$$

Where C_t: the total chloride content by the mass of cement content (%); D_a^x: the apparent chloride diffusion coefficient of matrix in x direction, along crack plane; D_a^y: the apparent chloride diffusion coefficient of matrix in y direction, perpendicular crack plane.
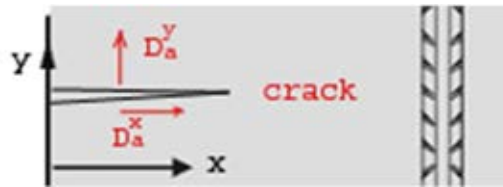
Figure 3.1. The two-dimensional chloride diffusion coefficient

When a crack appears on the concrete structure, the chloride profile in crack will strongly increase in correlation to the chloride diffusion coefficient of crack. By this way, chloride ions will penetrate into concrete through crack and un-crack concrete. As mention in previous chapters, there are several mechanisms for chloride transport in cracked concrete: capillary suction, permeation, diffusion or migration. In the field, only one type or mixed types of transport mechanisms will conduct for chloride ingress into cracked concrete, it depends on the saturate condition of concrete or the environment conditions. For instance, Paulsson-Tralla (Paulsson-Tralla and Silfwerbrand, 2002) proposed the main transport mechanisms for chloride penetration into cracked concrete in deicing environment were diffusion and convection due to capillary suction of deicing water. In their research, the saturate condition of concrete is a scope of research. Although, the chloride transport mechanism in concrete under the saturate condition is only the diffusion mechanism (Nagesh and Bhattacharjee, 1998; Boulfiza et al., 2003).

However, with cracked concrete, the chloride transport mechanisms become complicate due to the influence of crack walls acting as capillaries. Therefore, when cracked concrete is immerged into salt solution, the mechanism of chloride penetration is assumed, including the movement of bulk chloride solution into the whole crack by capillary suction and the diffusion of chloride ions into uncracked concrete regions at the same time. This assumption will be investigated as a simple approach (Vu, Hoang Quoc, Stitmannaithum, Boonchai and Takafumi, Sugiyama, 2011a). There are several matters regarding the assumption above, such as:

- How to simulate and evaluate the bulk chloride solution moved in the whole crack due to capillary suction?

- How to simulate a combination of capillary and diffusion mechanisms for chloride transport?

- How to simulate the diffusion of chloride ions into concrete through crack in which the crack width continues to vary with correlation to crack depth?

As a conclusion, it is very difficult and complicate to model or measure the chloride concentration, chloride diffusion coefficient inside and around crack because characteristics of crack are tortuous and roughness. Moreover, the chloride diffusion coefficient is continuously varied corresponding to crack width along the crack plane.

From the researches of Kato (Kato et al., 2005) and Djerbi (Djerbi et al., 2008b), they concluded that the chloride diffusion coefficient of a crack increased when crack width increased; and became steady when the crack width reached an threshold value of 75 µm or higher 80 µm; with Wang (Wang and Ueda, 2010), this value was 60 µm. On the other hand, Ismail (Ismail et al., 2004) also concluded that chloride profile, which was perpendicular to the crack plane, was similar to that of the surface when crack width was over 60 µm. In this research, to match with real crack characteristics, crack width was assumed to reduce linear from exposed surface to crack tip (Figure 3.2).

When crack appears on the concrete structure, the chloride transport mechanisms in cracked concrete are assumed as two main transport mechanisms in the saturated condition. They are a moving mechanism of bulk salt solution in whole crack in an initial stage, then, a diffusion of chloride ion from exposed surface into the whole crack and uncracked concrete region.

$D^3_{crack}=1/2(2 \times 10^{-10}+D_{uncr})$ (m^2/s)

$D^2_{crack}=2 \times 10^{-11}W-4 \times 10^{-10}$ (m^2/s)

$D^1_{crack}=D_0=2.03 \times 10^{-9}$ (m^2/s)

D_{uncr}

X

W = 30 μm

W = 60 μm

$0 \le C_s^y \le C_s$

$C_s^y = C_s$

Crack depth (L)

y

0

$C_s^x = C_s$
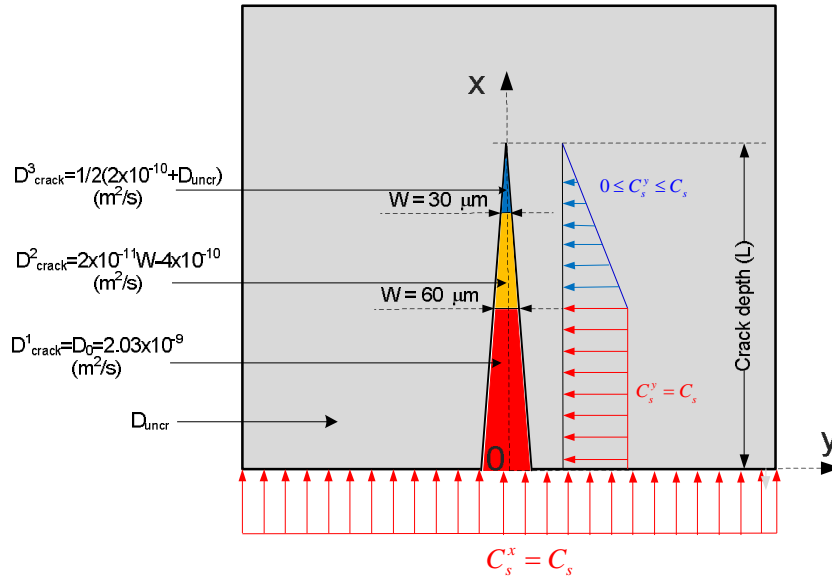
Figure 3.2. The concept of the 2D surface content and diffusion coefficient of chloride for cracked concrete

3.1.1 The movement mechanism of bulk salt solution

The movement mechanism of bulk salt solution is to transport the bulk salt solution from the exposed surface to inside whole crack by capillary suction. Then, the volume of this bulk salt solution will present and occupy between the crack planes. To approach simply with the moving mechanism of bulk salt solution by capillary suction, it will be instead by an assumption that the salt solution always present in the whole crack as a boundary condition. Because the time for movement of bulk salt solution from the exposed surface through the crack planes to the crack tip is very short when comparing with the exposed duration of concrete member, this movement of bulk salt solution with time-dependent will be ignored. By this assumption, the moving mechanism of bulk salt solution at initial stage is replaced by the chloride surface content located along the crack plane; it plays the boundary condition for the second dimensional diffusion. In this assumption, the chloride surface content located along the crack plane will be also assumed a function of crack width.

When crack width is larger than 60 μm, the environment in whole crack can be considered as the exposed surface. So, in this section, the chloride concentration depth being perpendicular to crack plane can be assumed to equal the chloride concentration depth from exposed surface of un-cracked concrete (Figure 3.2). This assumption was also proved by Win (Win et al., 2004). It also means the surface chloride content on crack plane is similar to that on the exposed surface.

In addition, when crack width reduces from 60 μm to zero along crack plane, the magnification of surface chloride content can be linearly reduced from chloride concentration on exposed surface to zero following Equation 3.2:

$$\begin{cases} C_s^y = C_s^x = C_s \text{ when } w \geq 60 \ \mu m \\ 0 \leq C_s^y < C_s \text{ when } 0 \ \mu m \leq w < 60 \ \mu m \end{cases} \tag{3.2}$$

3.1.2 The diffusion mechanism of chloride ions into cracked concrete

After the movement of bulk chloride solution takes place in whole crack completely, the diffusion mechanism for chloride ions through the crack will begin to act. In the diffusion mechanism, chloride ions will be diffused into concrete member by diffusion of higher chloride concentration of the exposed environment into lower that of cracked concrete and matrix (un-cracked concrete) at the same time, and specified by the chloride diffusion coefficients.

As mentioned in previous chapter, the chloride diffusion through a crack of concrete was very complicated and depended on the crack width opening. Consequently, the chloride diffusion coefficients of cracked concrete (D_{crack}) are assumed based on the lower and upper threshold values of crack width. In this assumption, the chloride ions will diffuse into concrete through whole crack having three zones divided by the lower and upper threshold values of crack width. In this research, the lower threshold value of crack width chosen is 30 μm and the upper threshold value of crack width chosen is 60 μm, Figure 3.2.

- In zone 1, from the exposed surface to the crack width of 60 μm, the environment is considered as the environment on exposed surface and the diffusivity of chloride ion in crack is assumed as in bulk water. So, the chloride diffusion coefficient in this zone will equal the diffusion coefficient of ions in bulk water (D_0), approximately 2.03 x 10^{-9} (m^2/s) (Kato and Uomoto, 2005; Sun et al., 2011):

$$D^1_{crack} = D_0 = 2.03 \text{ x } 10^{-9} \text{ } (m^2/s) \tag{3.3}$$

- For zone 2, where the crack width reduce from 60 μm to 30 μm, the chloride diffusion coefficient is assumed to reduce linear with reduce in crack width, expressed by equation below (Djerbi et al., 2008b):

$$D^2_{crack} = 2E\text{-}11*W - 4E\text{-}10 \text{ } (m^2/s), \text{ with } 30\mu m \leq W < 60\mu m. \tag{3.4}$$

- With zone 3, where the crack width reduce from 30 μm to crack tip ($0\mu m \leq W < 30\mu m$), in previous researches, the influence of crack on the chloride diffusion phenomenon can be ignored; it means the chloride diffusion coefficient in this zone will equal that in

uncracked concrete. In fact, the chloride diffusion coefficient must reduce linear from D^2_{crack} (at crack with (W) = 30 µm) to the chloride diffusion coefficient of un-crack concrete (D_{uncr}). However to simply calculate, it is calculated as the average of D^2_{crack} (at W = 30 µm) and D_{uncr}:

$$D^3_{crack} = (2E\text{-}11*30 - 4E\text{-}10 + D_{uncr})/2 = (2E\text{-}10 + D_{uncr})/2 \ (m^2/s). \tag{3.5}$$

About the chloride diffusion coefficient in uncracked concrete zone, an assumption is the concrete can be considered as being a quasi-homogeneous medium where the chloride diffusion coefficient of matrix in both x and y directions are similar and equal the chloride diffusion coefficients of un-crack concrete following two dimensions:

$$D_a^x = D_a^y = D_{uncr} \tag{3.6}$$

Conclusively, in this research the initial and boundary conditions for the chloride penetration into cracked reinforced concrete is applied as follow:

$$\begin{cases} \dfrac{\partial C_t}{\partial t} = D_a^x \dfrac{\partial^2 C}{\partial x^2} + D_a^y \dfrac{\partial^2 C}{\partial y^2} & x > 0, \ t > 0, \\ C(0, 0 \le y < L, 0) = C_s & \text{L: crack depth} \\ C(x, y, 0) = 0 & x > 0, \ y > 0. \end{cases}$$

3.2   Model for chloride diffusion at crack location of reinforced concrete

Generally, the chloride diffusion in cracked concrete must be recognized as two-dimensional diffusion. Because chloride ions diffuse not only from exposed surface to inside concrete but also from crack plane exposed with salt solution as second direction. However, under macro view, in tension surface of reinforced concrete structure, there are two regions obtaining the crack or uncrack locations. The crack and uncrack locations are defined under macro view as Figure 3.3.
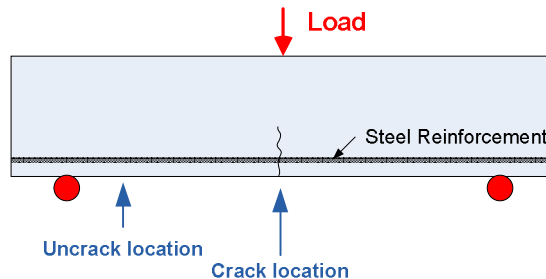
Figure 3.3. Definition for crack and uncrack locations.

At a crack location, the chloride profile is different to an uncrack location and more chloride concentration that induces more damage due to steel reinforcement corrosion than the uncrack

location. For this reason, with a proposed simple approach to predict the chloride profile at crack location of cracked concrete, the 1D model base on Fick's second Law (equation 3.1) will be proposed:

$$\frac{\partial C_t}{\partial t} = D_a \frac{\partial^2 C}{\partial x^2}$$
(3.7)

In the literature, for the plain concrete, under coupling cyclic load, the apparent diffusion coefficient of concrete was modified by Mien (Mien et al., 2009b) as:

$$D_a = D_{c,ref}.f_1(T).f_2(t).f_3(h).f_4(SR)/\phi$$
(3.8)

Where $f_4(SR)$ is a function of the dependence of $D_{c,ref}$ on the load levels (SR) and ϕ is the chloride binding capacity of a cement, it depend on the content component of C_3A in cement.

From the experiment program, Mien (Mien et al., 2009b) carried out the relationship between chloride diffusion coefficient and load level of cyclic loading on $f_4(SR)$:

$$f_4(SR) = 0.0985e^{7.71SR}$$
(3.9)

The equation (3.8) was applied to model the chloride penetration in plain concrete under combination of cyclic load in case of appearing invisible crack. However, in the real structure, with a embedded steel reinforcement in concrete the visible crack will occur on the reinforced concrete structure under varying load level, the ratio of applied load and ultimate load. The rate of chloride diffusion will increase and the chloride profile in concrete will be changed by the increasing chloride diffusion coefficient.

However, to evaluate the chloride ingress into visible crack of concrete structure, the chloride diffusion coefficient (D_a) must be updated to become the chloride diffusion coefficient at crack location (D_{cr}). Up to now, many researchers have concluded that crack width played the role of increasing the chloride penetration into cracked concrete. Moreover, with the cylinder specimens, they also pointed out that when crack width reached to the threshold value, the chloride diffusion coefficient could be considered constant or independent on the crack width. These proposed threshold value of the crack width are 60 µm (Wang and Ueda, 2010), 75 µm (Kato et al., 2005) or higher 80 µm (Djerbi et al., 2008b).

However, in the real reinforced concrete structure under flexural load, cracks can occur on the surface of tension zone and propagate from the tension surface to the neutral axis due to the increasing magnitude of loading or number of load cycles. In a naturally cracked reinforced concrete structure, crack width has an important role in chloride penetration, but crack depth should also be recognized as a key parameter affecting chloride penetration and chloride profile. The different depths of cracks can influence on the chloride penetration depth and causing the variation of the chloride diffusion coefficient. For instance, a deeper crack depth will have a

deeper chloride penetration depth than a shallower crack depth, although these cracks have the same crack width and concrete proportion, Figure 3.4
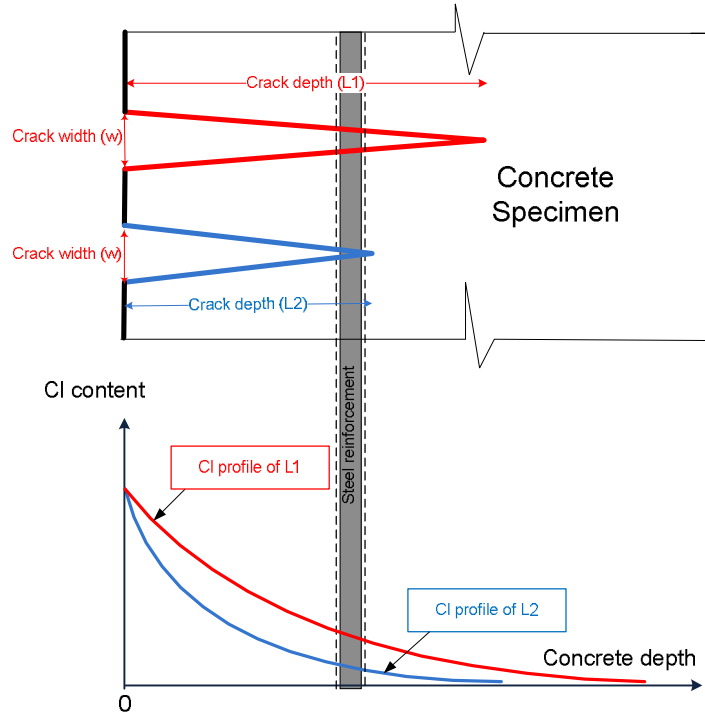
Figure 3.4. The concept for the influence of crack depth on the chloride profile

The illustration of updated chloride diffusion coefficient of the plain and reinforced concrete with the load can be presented as follow, figure below.
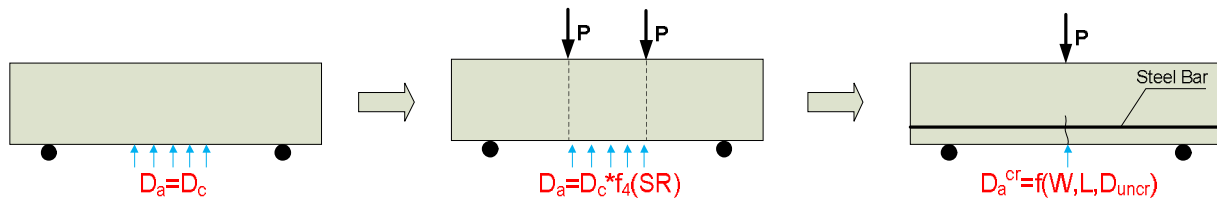
Figure 3.5. The illustration of updating chloride diffusion coefficient

Consequently, the chloride diffusion coefficient of concrete at crack location is expressed as equation below:

$$D_a^{cr} = f(W, L, D_{uncr}) \tag{3.10}$$

where D_a^{cr} is the chloride diffusion coefficient at crack location, is a function considering the dependence of chloride diffusion coefficient at crack location on that at uncrack location (D_{uncr}), the crack width (W) and crack depth (L).

The concept of chloride diffusion though a crack is illustrated in Figure 3.6. Chloride ions will diffuse in cracked concrete following two states. Firstly, chloride ions will diffuse through the crack and governed by the chloride diffusion coefficient of crack (D_{cr}). Then, chloride ions continually diffuse in the un-cracked concrete region at the tip of crack and governed by the chloride diffusion coefficient of un-cracked concrete (D_{un-eff}), which has the effect of crack depth to it. In this research, crack depth is defined as the straight length from the crack mouth along crack plane to where a crack width is 30 µm. Because when the crack width is less than 30 µm, there is insignificant for chloride diffusion (Djerbi et al., 2008b; Ismail et al., 2008). Therefore, in this study, it is termed as respective crack depth.
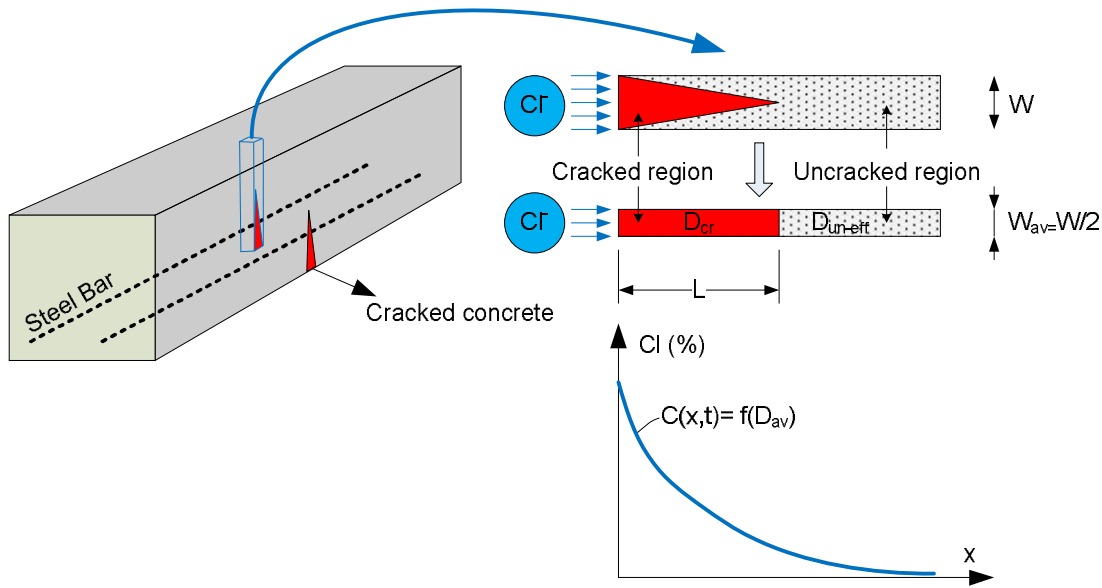
Figure 3.6. The concept for chloride diffusion coefficient at crack location of reinforced concrete

By the assumption above, the chloride diffusion in cracked concrete using equation of Fick's 2nd Law in which the proposed average coefficient (D_{av}) is used:

$$D_{av} = \frac{D_{cr} + D_{un-eff}}{2} \tag{3.11}$$

where D_{cr} is calculated based on crack width (w) and followed equation below (Djerbi et al., 2008b):

$$\begin{cases} D_{cr}(m^2/s) = (2x10^{-11})w - 4x10^{-10}, & \text{when } 30\mu m \leq w \leq 80\mu m \\ D_{cr}(m^2/s) \approx 14x10^{-10}, & \text{when } w > 80\mu m \end{cases} \tag{3.12}$$

However, in the research of Djerbi (Djerbi et al., 2008b) the crack walls are separate and parallel, but in this research with reinforced concrete, crack width is reduced in correlation to crack depth. Therefore, the average crack width (W_{av}) is proposed as equation (3.13) and is approximately calculated by average of W_1 and W_2.

$$W_{av} = \frac{W_1 + W_2}{2} = \frac{W_1 + 30}{2} \tag{3.13}$$

where W_1 is crack mouth (μm); $W_2 = 30\,\mu m$.

With the effect of crack depth, the chloride diffusion coefficient of an uncracked concrete region, which is the region above the crack tip (Figure 3.6), will be assumed a function of crack depth and this function will be found by the experiment program, as equation follows:

$$D_{un-eff} = f(L, D_{uncr}) \tag{3.14}$$

where L (mm) is the respective crack depth; D_{uncr} is the chloride diffusion coefficient of uncracked concrete.

CHAPTER IV

SIMULATION OF CHLORIDE PENETRATION INTO CRACKED REINFORCED CONCRETE

This chapter aims to carry out the results of analytical computation applied by the proposed model to predict the chloride penetration in cracked reinforced concrete in marine environment. The chloride transport will be simulated and chloride profile will be predicted by the 1D model and 2D model as well.

4.1 Simulation for chloride diffusion at crack location of reinforced concrete

The simulation of one dimensional chloride diffusivity based on the proposed model which is discussed in Chapter 3. The proposed model is developed from the Fick's 2nd Law with the chloride diffusion coefficient at crack location; it was modified as the average of the chloride diffusion coefficient in the whole cracked concrete and un-cracked concrete at the tip of crack. The surface chloride content at crack location was obtained by fitting curve of Fisk'2nd Law equation from the experiment results. The input data of analytical computation model is shown in table 4.1

Table 4.1. The input data for analytical computation following 1D chloride diffusivity model

Beam series	W/C	Crack no.	Crack mouth (w_1), μm	Crack depth (L), mm	D_{uncr} (m^2/s)	C_s (% Wt. of concrete)	Immerged duration (week)
		1	58	32.5		0.6	
1	0.4	2	51	18.5	3.26E-11	0.5	
		3	59	35		0.49	
2	0.5	1	77	36	5.33E-11	0.55	2
		2	67	34		0.47	
		1	106	49.5		0.72	
3	0.6	2	81	32	8.85E-11	0.6	
		3	102	45.5		0.48	
2	0.5	1	93	41.5	3.16E-11	0.46	4
3	0.6	1	83	41.5	4.74E-11	0.56	
1	0.4	1	53	30.5	2.43E-11	0.52	6

		2	45	21.5		0.52	
		3	60	32.5		0.54	
		1	52	27.5		0.63	
2	0.5	2	41	17.5	2.19E-11	0.71	
		3	41	21		0.71	
		1	54	29		0.65	
3	0.6	2	50	26.5	2.77E-11	0.58	
		3	72	33		0.52	
1	0.4	1	89	42	2.47E-11	0.60	
		2	88	41.5		0.52	8
2	0.5	1	74	31.5	2.43E-11	0.70	
3	0.6	1	80	40.5	3.25E-11	0.76	
2	0.5	1	107	45.5	1.72E-11	0.61	16
		2	101	45		0.61	

Note: beam series 1, 2, 3 are noted for W/C = 0.4, 0.5 and 0.6, respectively.

The analytical computation results of chloride profile at crack locations of reinforced concrete under variation of the exposed time are plotted in the figures below.
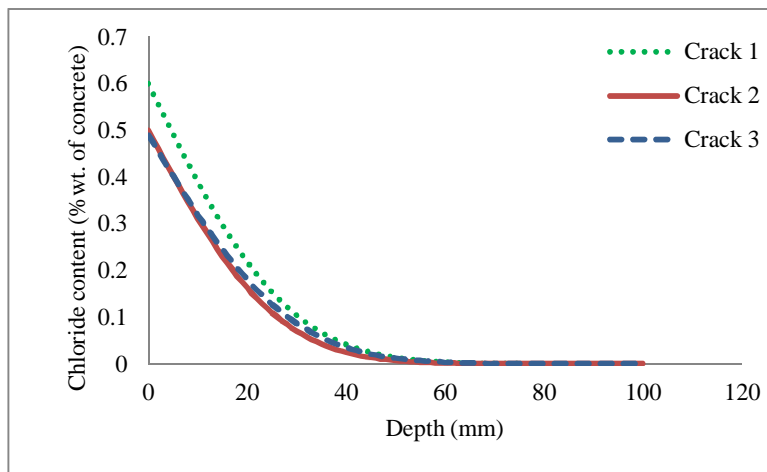
Figure 4.1. Predicting chloride profile of beam series 1 after 2-week immersion in salt solution
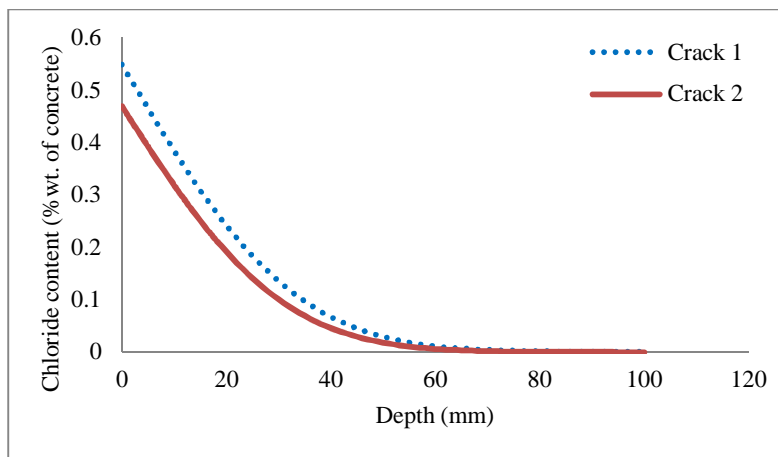
Figure 4.2. Predicting chloride profile of beam series 2 after 2-week immersion in salt solution
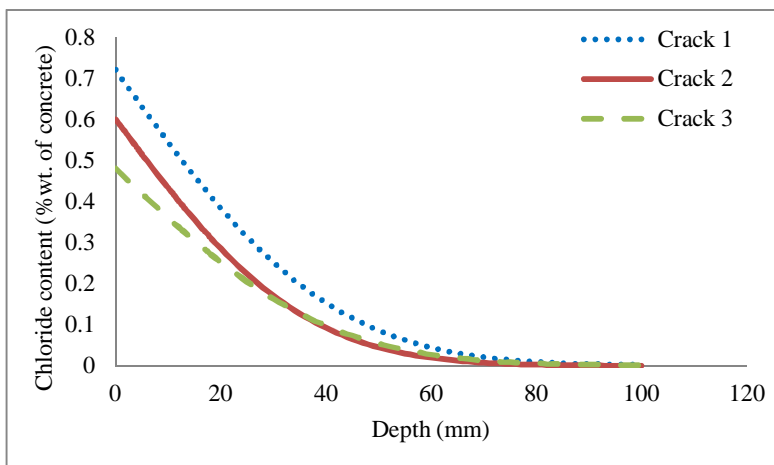
Figure 4.3. Predicting chloride profile of beam series 3 after 2-week immersion in salt solution
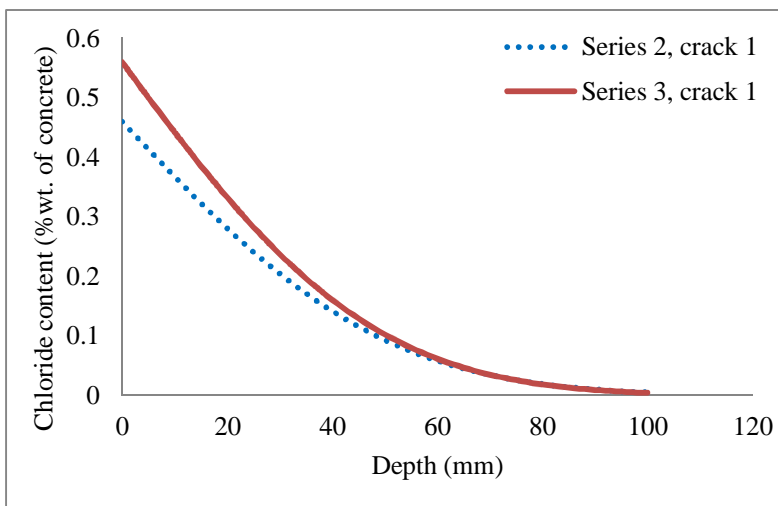
Figure 4.4. Predicting chloride profile of beam series 2 and 3 after 4-week immersion in salt solution
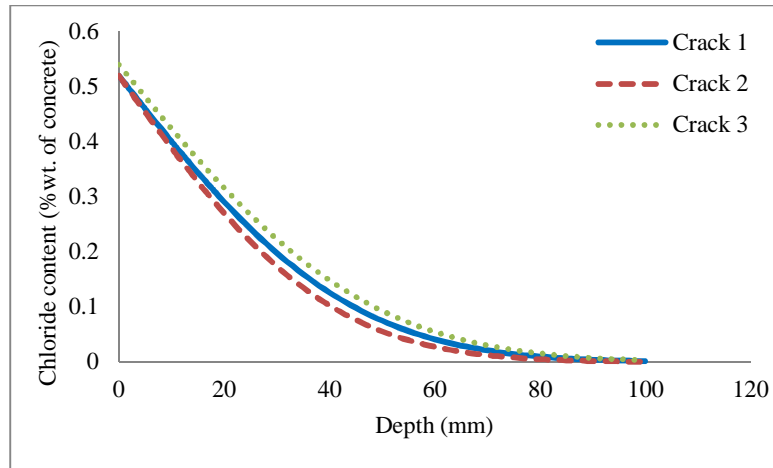
Figure 4.5. Predicting chloride profile of beam series 1 after 6-week immersion in salt solution
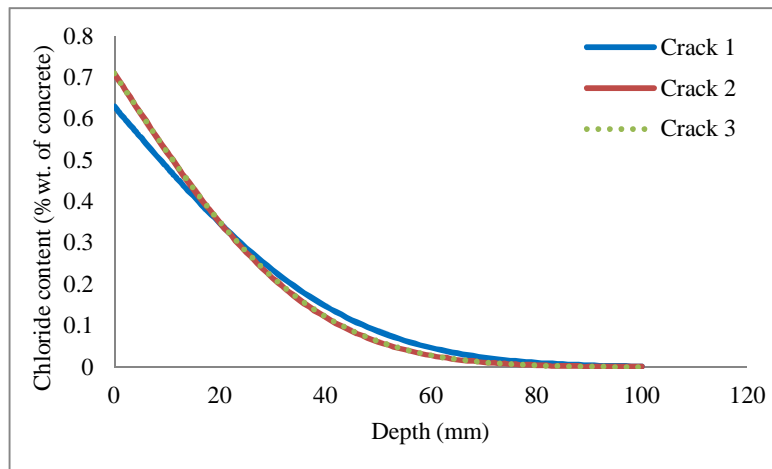
Figure 4.6. Predicting chloride profile of beam series 2 after 6-week immersion in salt solution
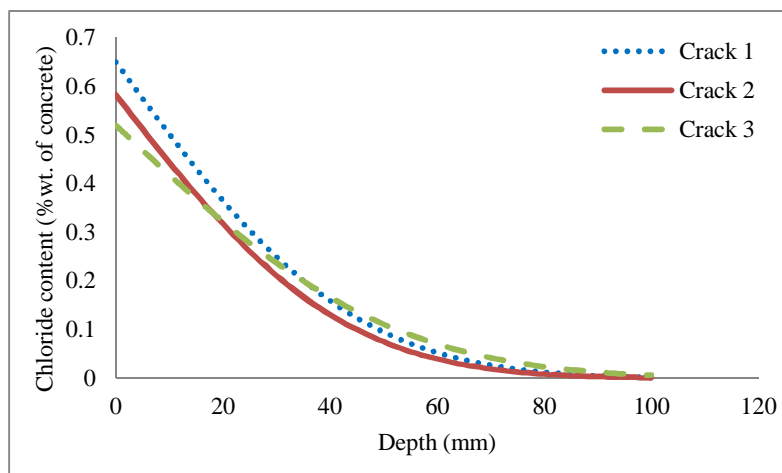
Figure 4.7. Predicting chloride profile of beam series 3 after 6-week immersion in salt solution
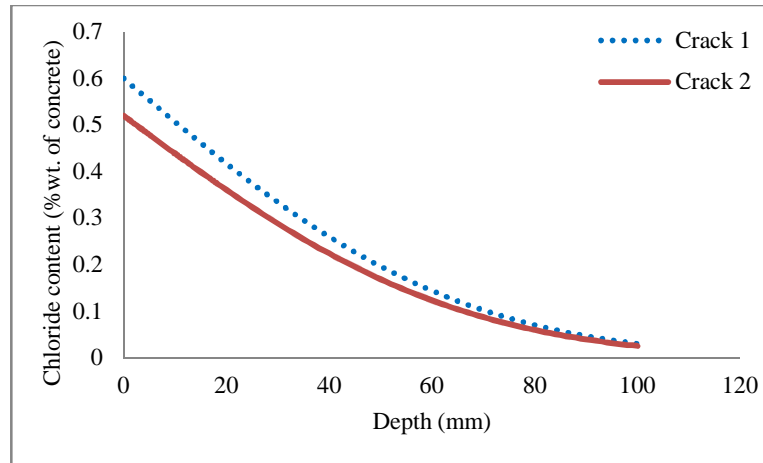
Figure 4.8. Predicting chloride profile of beam series 1 after 8-week immersion in salt solution
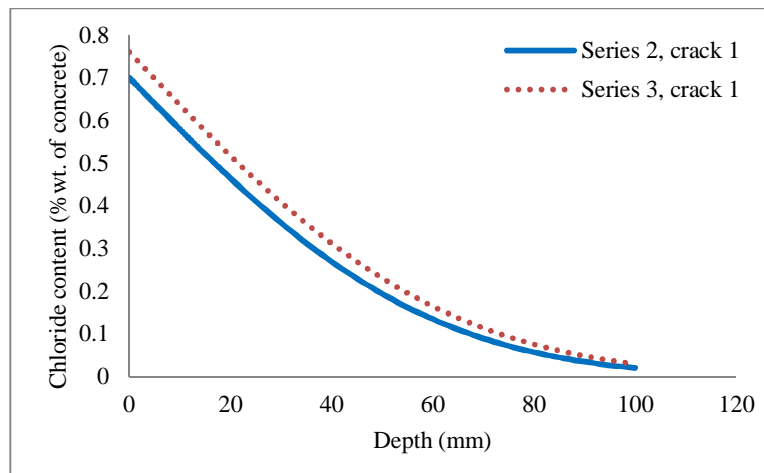
Figure 4.9. Predicting chloride profile of beams after 8-week immersion in salt solution
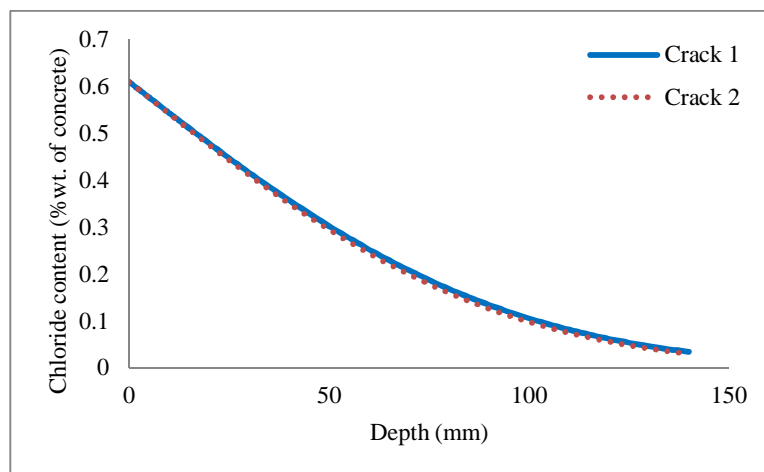
Figure 4.10. Predicting chloride profile of beam series 2 after 16-week immersion in salt solution

Regarding the predicted model, it is recognized that in the same concrete proportion (same beam series) the chloride profiles at each cracks are different and they are strongly affected by the characteristics, crack width and crack depth.

4.2   Simulation for 2D chloride diffusivity in crack concrete

To describe the diffusion of chloride ions into concrete member under saturate condition, the Fick's second Law equation is applied:

$$\frac{\partial C_t}{\partial t} = D_a \frac{\partial^2 C}{\partial x^2} \tag{4.1}$$

Equation (4.1) is valid only for one-dimensional diffusion where the chloride diffusion is leaded following one direction that is along the depth of the concrete member. In modeling two-dimensional chloride diffusion, equation (4.1) will must be modified to become a given equation as follows:

$$\frac{\partial C_t}{\partial t} = D_a^x \frac{\partial^2 C}{\partial^2 x} + D_a^y \frac{\partial^2 C}{\partial^2 y} = D_a \left[\frac{\partial^2 C}{\partial x^2} + \frac{\partial^2 C}{\partial y^2} \right] \tag{4.2}$$

The equation (4.2) accompanies with an assumption that the concrete structure is homogeneous and chloride diffusion coefficients are similar following two directions:

$$D_a^x = D_a^y = D_a$$

The boundary conditions are:

$$\begin{cases} C(x, y, t) = C_0 & \text{on S, at } t = 0, \\ D_a \frac{\partial C}{\partial x} l + D_a \frac{\partial C}{\partial y} m + c = 0 & \text{on S.} \end{cases} \tag{4.3}$$

where l and m are direction cosines; c is the boundary chloride flux.

In developing a finite element approach to two-dimensional conduction (Lewis, Nithiarasu and Seetharamu, 2004), the distribution of chloride concentration in the element having M nodes is described by:

$$C(x, y, t) = \sum_{i=1}^{M} N_i(x, y) C_i(t) = [N]\{C\} \tag{4.4}$$

where $N_i(x,y)$ is the interpolation function associated with the time dependent nodal chloride concentration, $C_i(t)$; [N] is the row matrix of interpolation functions, and {C} is the column matrix (vector) of nodal chloride concentration.

Applying Galerkin's finite element method, the residual equations corresponding to equation (4.2) are:

$$\int_A N_i(x,y)\left(D_a\frac{\partial^2 C}{\partial x^2}+D_a\frac{\partial^2 C}{\partial y^2}-\frac{\partial C_t}{\partial t}\right)dA=0 \tag{4.5}$$

Using integration by parts, the variational statement of equation (4.4) is written as:

$$-\int\left[\left(D_a\frac{\partial N_i}{\partial x}\frac{\partial C}{\partial x}+D_a\frac{\partial N_i}{\partial y}\frac{\partial C}{\partial y}-N_i\frac{\partial C_t}{\partial t}\right)\right]dxdy+\int_S N_i D_a\frac{\partial C}{\partial x}ldS+\int_S N_i D_a\frac{\partial C}{\partial y}mdS=0 \tag{4.6}$$

On substituting the spatial approximation from Equation 4.3, Equation 4.5 becomes

$$-\int\left[\left(D_a\frac{\partial N_i}{\partial x}\frac{\partial N_j}{\partial x}C_j(t)+D_a\frac{\partial N_i}{\partial y}\frac{\partial N_j}{\partial y}C_j(t)\right)\right]dxdy-\int N_i\frac{\partial N_j}{\partial t}C_j(t)dxdy-\int_S N_i c\,dS=0 \tag{4.7}$$

With i and j represent the nodes. Equation (4.7) can be expressed in a more convenient form as:

$$\left[C_{ij}\right]\left\{\frac{\partial C_i}{\partial t}\right\}+\left[K_{ij}\right]\left\{C_j\right\}=\left\{f_i\right\} \tag{4.8}$$

Where

$$\left[C_{ij}\right]=\int N_i N_j dxdy \tag{4.9}$$

$$\left[K_{ij}\right]=\int\left[\left(D_a\frac{\partial N_i}{\partial x}\frac{\partial N_j}{\partial x}C_j(t)+D_a\frac{\partial N_i}{\partial y}\frac{\partial N_j}{\partial y}C_j(t)\right)\right]dxdy \tag{4.10}$$

$$\left[f_i\right]=-\int_s N_i c\,dS \tag{4.11}$$

The equation describing the two dimensional diffusivity of chloride has the form being similar to the thermal equation. In order to solve this equation, the ANSYS program based on the finite element method can be employed. By using thermal module of ANSYS program, the input data include the chloride diffusion coefficient of cracked and un-cracked concrete, the chloride surface content of un-cracked concrete, and crack characteristics (Table 4.2).

In ANSYS program, the analysis type of transience is chosen to calculate the chloride concentration at a given point in the medium with time dependent. The solid 2D - 4 node liner element is chosen to mesh the model. With the size of 100 mm for beam model, the element size of 1mm is chosen to modeling. The elements of model after meshing are plotted in Figure 4.11. By the offered assumption in Chapter 3, the initial and boundary conditions are used for modeling as follow:

$$\begin{cases} \dfrac{\partial C_t}{\partial t} = D_a \left(\dfrac{\partial^2 C}{\partial x^2} + \dfrac{\partial^2 C}{\partial y^2} \right) & x > 0,\ t > 0, \\ C(0, 0 \le y < L, 0) = C_s & \text{L: crack depth} \\ C(x, y, 0) = 0 & x > 0,\ y > 0. \end{cases}$$
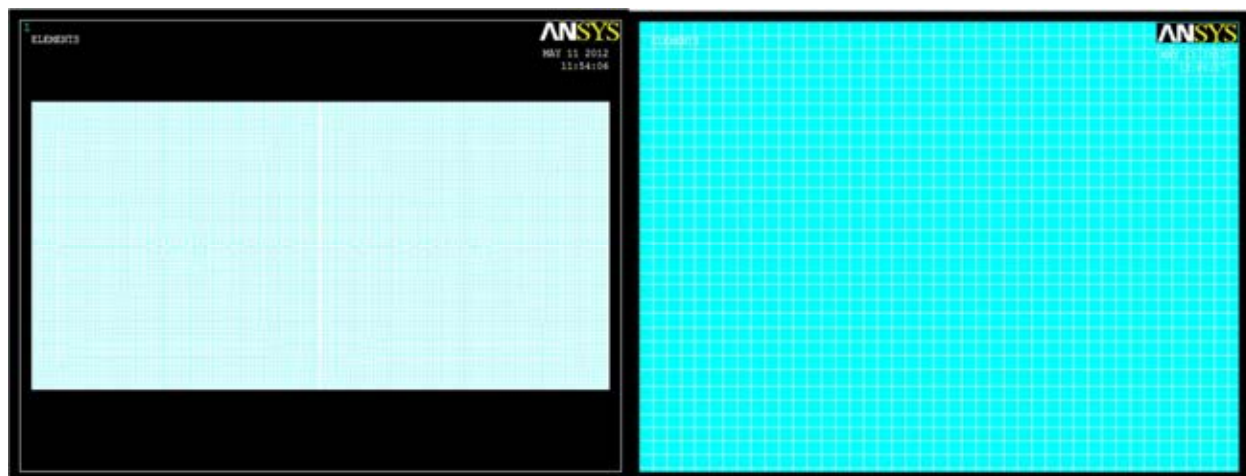
Figure 4.11. The elements of model by ANSYS

Table 4.2 The input data for ANSYS program analysis.

Beam No.	W/C	Crack depth at (mm)			D_{uncr}^{app} (m²/s)	Cs (% weight of concrete)	Exposed duration (week)
		W = 60 (µm)	W = 30 (µm)	Tip			
1	0.5	23.5	41.5	57	3.16E-11	0.59	4
2	0.6	19	41.5	64	4.74E-11	0.82	4
3	0.4	23	42	57.5	2.46E-11	0.97	8
4	0.5	11.5	31.5	50	2.43E-11	1	8
5	0.6	28.5	40.5	72	3.25E-11	0.86	8
6 (EPMA)	0.4	34.5	54.5	72.5	1.36E-11	0.528	12
7 (EPMA)	0.5	25.5	44	65.5	1.79E-11	0.54	12
8 (EPMA)	0.6	Crack mouth = 50 µm	27	67.5	3.13E-11	0.559	12
9	0.5	27.5	45.5	64	1.65E-11	0.85	16

4.2.1 Model for 2D chloride diffusivity

In this part, chloride ions will penetrate into crack and matrix of concrete at the same time. The surfaces exposed to chloride solution are the tension surface and crack plane Figure 4.12, all remaining surface of concrete specimen will be covered by epoxy layers.

In this model, the exposed surfaces will be attributed by the surface chloride content as the boundary conditions.

The experimental results of chloride diffusion coefficient of uncracked concrete beams are used for two -dimensional analysis of chloride penetration using finite element formulation from ANSYS program. The experimental results of chloride diffusion coefficient above are determined from one-dimensional diffusion of Fick's second Law using non-linear regression where the highest coefficient of regression gave an indication of the best fit. The crack plane is treated as an exposed surface where the surface chloride content is a function of crack width varying along crack plane, presented in Chapter 3, while chloride concentration at the exposed surface is assumed constant.
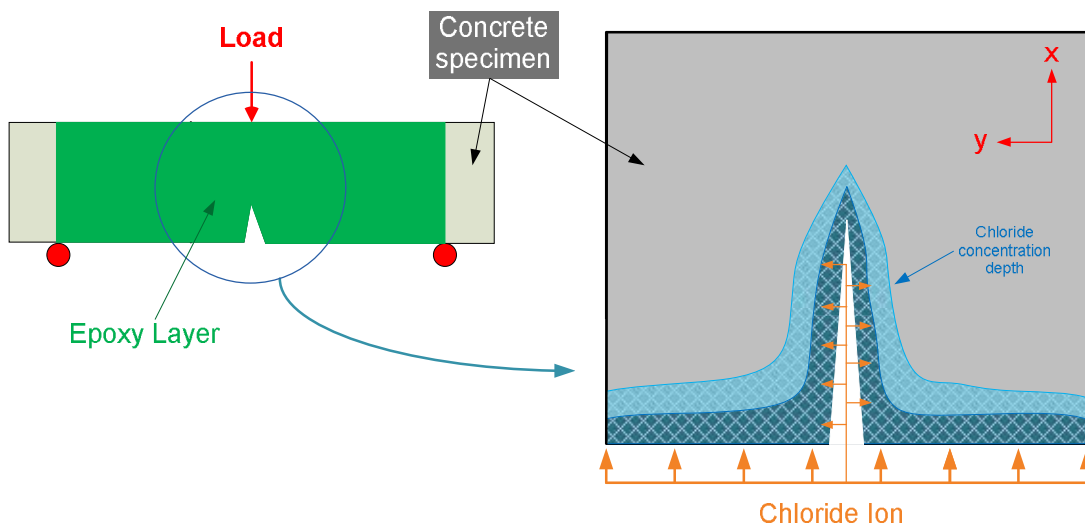
Figure 4.12. The surfaces exposed to chloride solution (2D chloride diffusivity)

The analytical computation results are illustrated in these figures below:
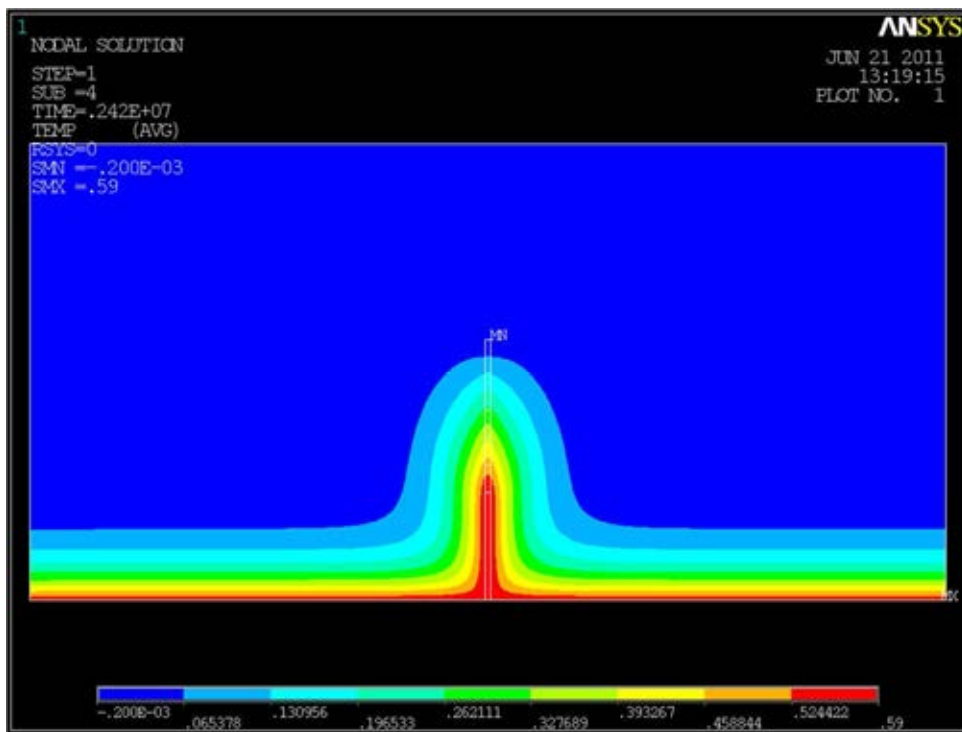
Figure 4.13. The analytical result of 2D chloride diffusivity of cracked concrete beam 1
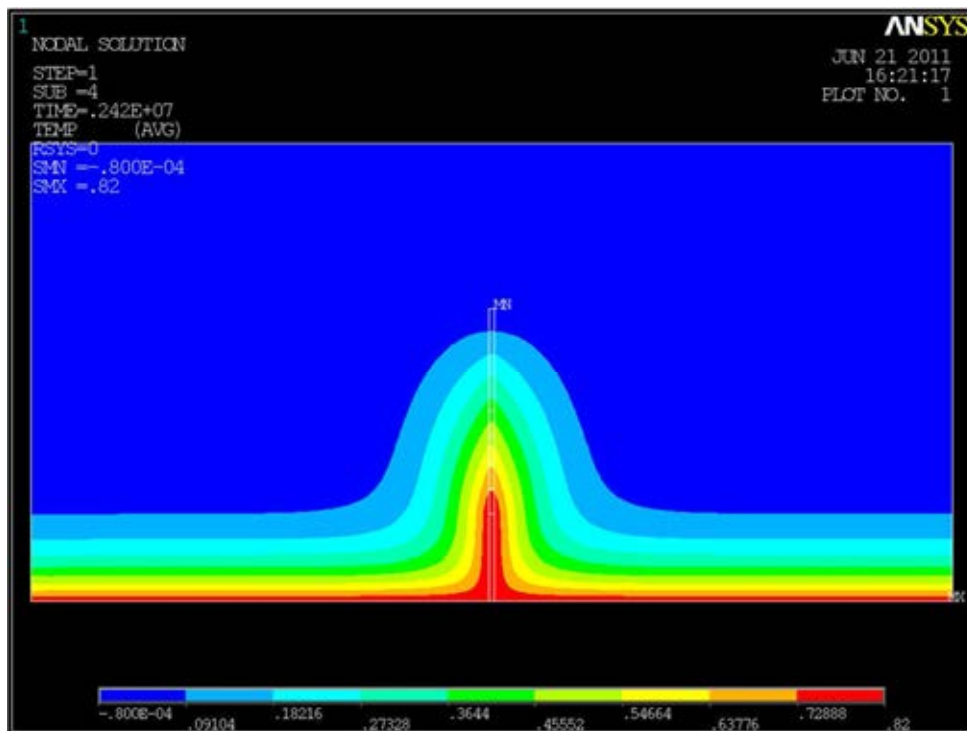
Figure 4.14. The analytical result of 2D chloride diffusivity of cracked concrete beam 2
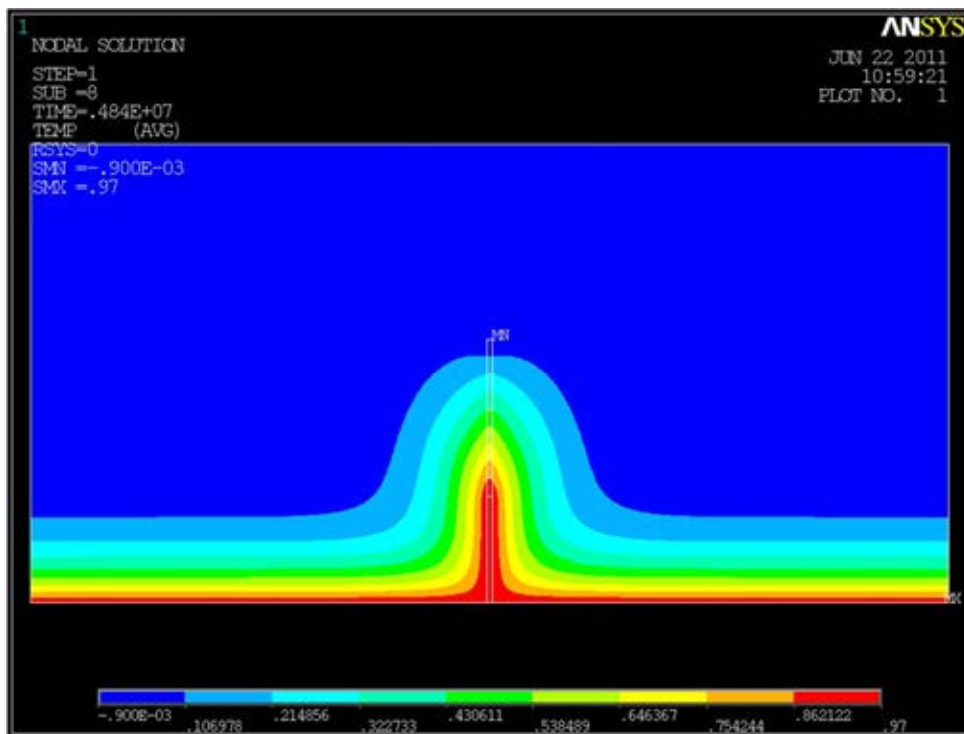
Figure 4.15. The analytical result of 2D chloride diffusivity of cracked concrete beam 3
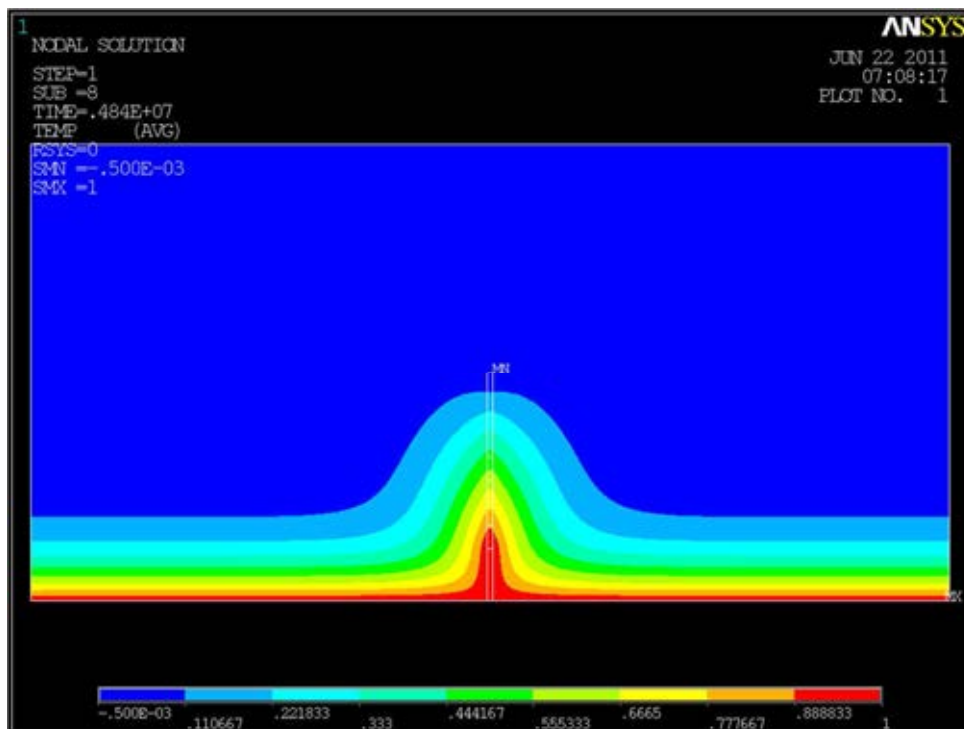
Figure 4.16. The analytical result of 2D chloride diffusivity of cracked concrete beam 4
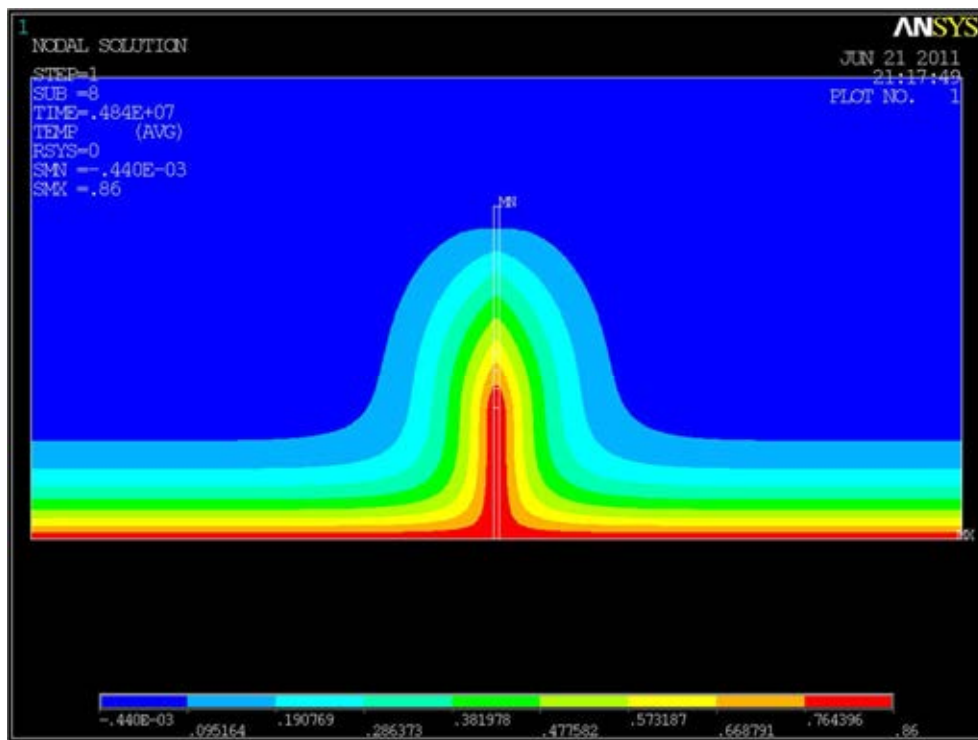
Figure 4.17. The analytical result of 2D chloride diffusivity of cracked concrete beam 5
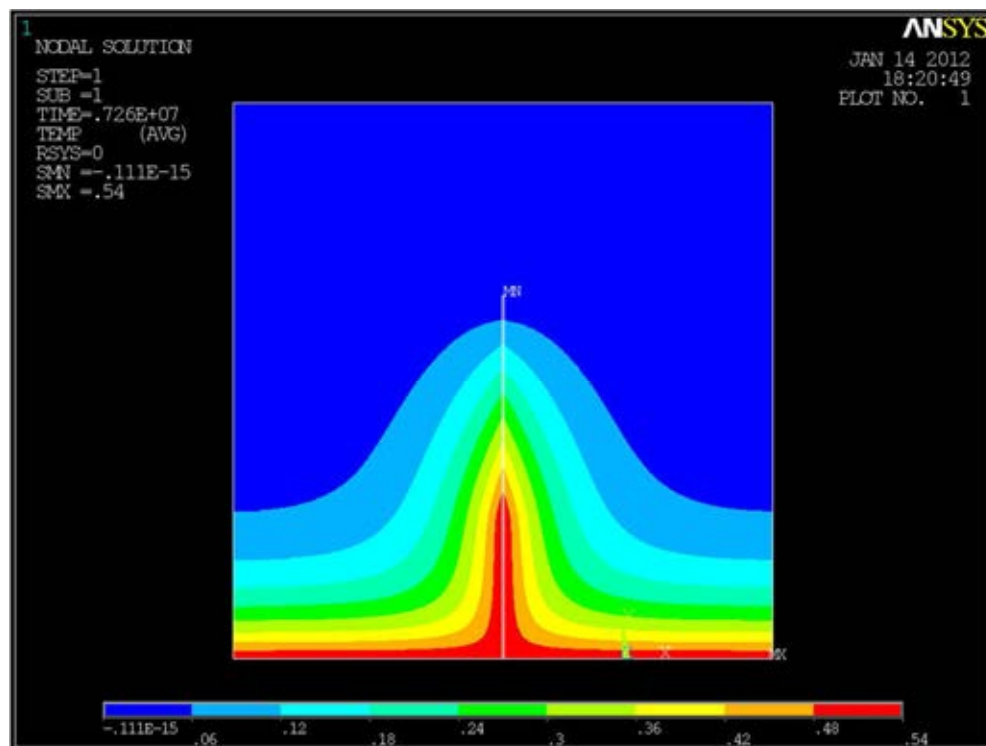
Figure 4.18. The analytical result of 2D chloride diffusivity of cracked concrete beam 7

4.2.2 Model for chloride diffusivity only perpendicular crack plane
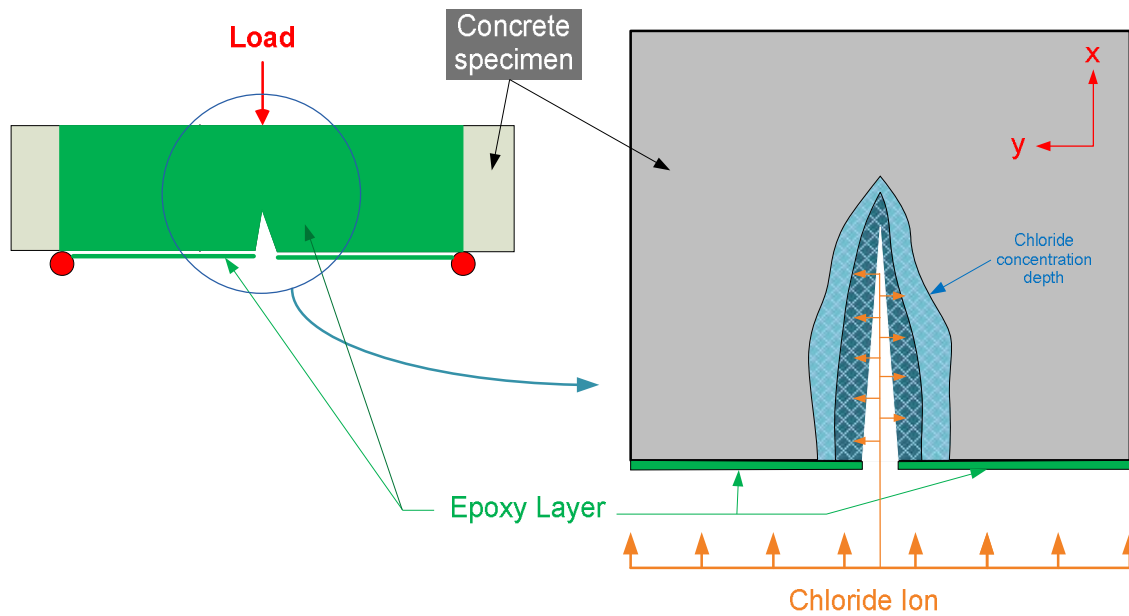
Figure 4.19. The crack plane surface exposed to chloride solution

In this part, to observe the chloride diffusion into matrix upon only crack plane, all the surface of concrete specimen (including the tension surface, except crack paths) will be coated by epoxy layers. The chloride ions from environment on the tension surface only diffuse through crack path to inside concrete, then, they will diffuse perpendicular to crack plane into matrix Figure 4.19.

In this model, the environment between crack planes, acting as exposed surfaces, will be attributed by the surface chloride content as the boundary conditions. In this research, beam no. 6 and 8 are performed for the chloride diffusion perpendicular to crack plane. The analytical computation results are illustrated in figures below:
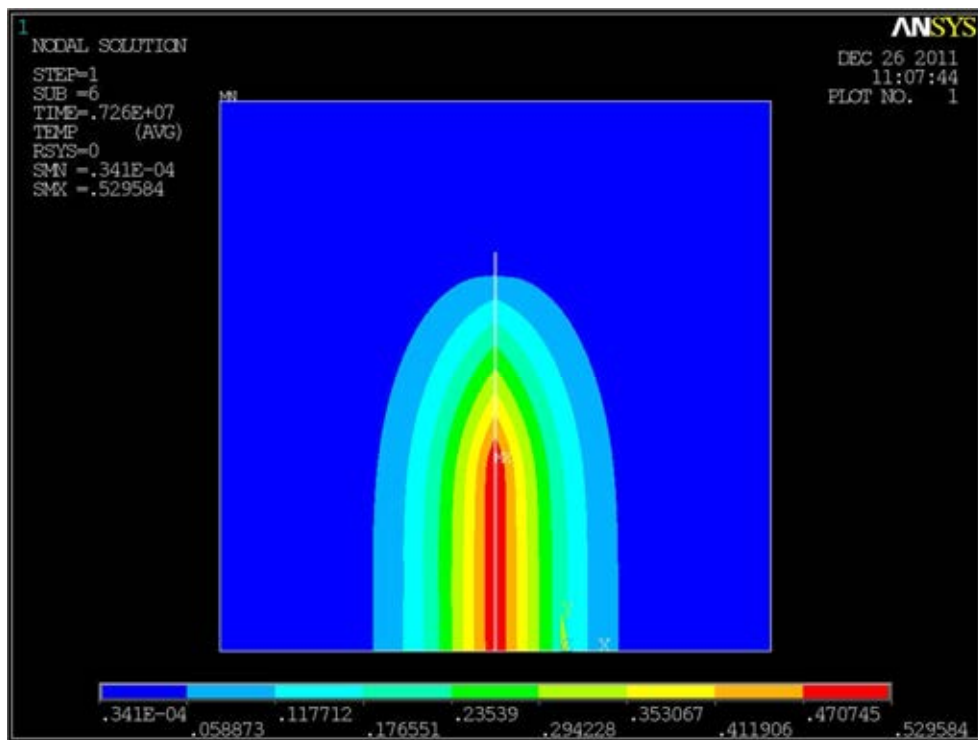
Figure 4.20. The analytical result for chloride diffusivity perpendicular to crack plane of beam 6
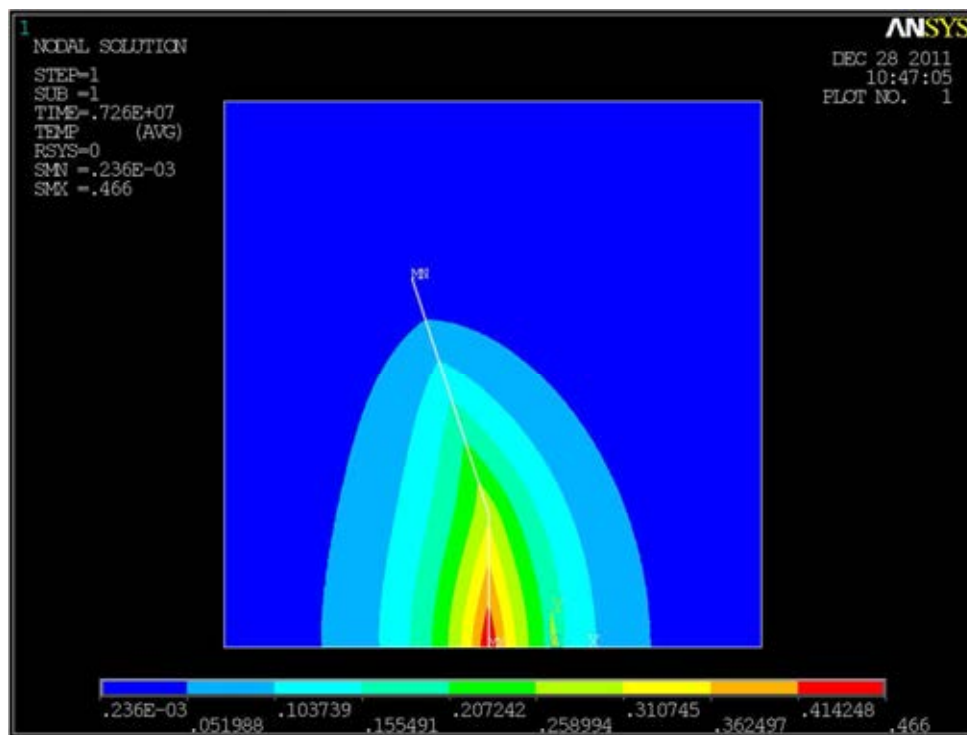
Figure 4.21. The analytical result for chloride diffusivity perpendicular to crack plane of beam 8.

CHAPTER V

MODEL VALIDATION

The research process is described in figure below:

Figure 5.1. The sketch of process research.

5.1   Experimental procedures

In this research, materials used include cements, fine aggregate and coarse aggregate. Cement type is Ordinary Portland cement (OPC, ASTM type I). Coarse aggregate, crushed limestone aggregate, has a maximum size of 20mm. Fine aggregate is river sand having fineness modulus of 2.6. Both of coarse and fine aggregates satisfy the American Society for Testing and Materials (ASTM-C33, 1999). Mixture concrete design follows a standard of American Concrete Institute (ACI-211.1, 2002). Three types of water to cement ratio (W/C) of concrete proportion investigated are 0.4, 0.5, and 0.6. With each mixture, the workability is checked by slump test; cylinder specimens, ϕ150 x 300mm, are prepared for the evaluation of the compression strength. The concrete mixture proportions for studying are presented in Table 5.1. The fine and coarse aggregate was washed and dried prior to casting to remove the initial chloride content.

Table 5.1 Mix proportion per 1 cubic meter of concrete

Mix	W/C	Cement (kg)	Water (kg)	Sand (kg)	Coarse Agg. (kg)	av. Comp. Str. (MPa)	av. Slump (cm)
1	0.4	513	205	664.14	1,024	48.1	7.5
2	0.5	410	205	748.62	1,024	39.3	8.5
3	0.6	342	205	804.93	1,024	32.8	8

5.1.1   Experiment procedures to perform the effect of crack depth on the chloride penetration
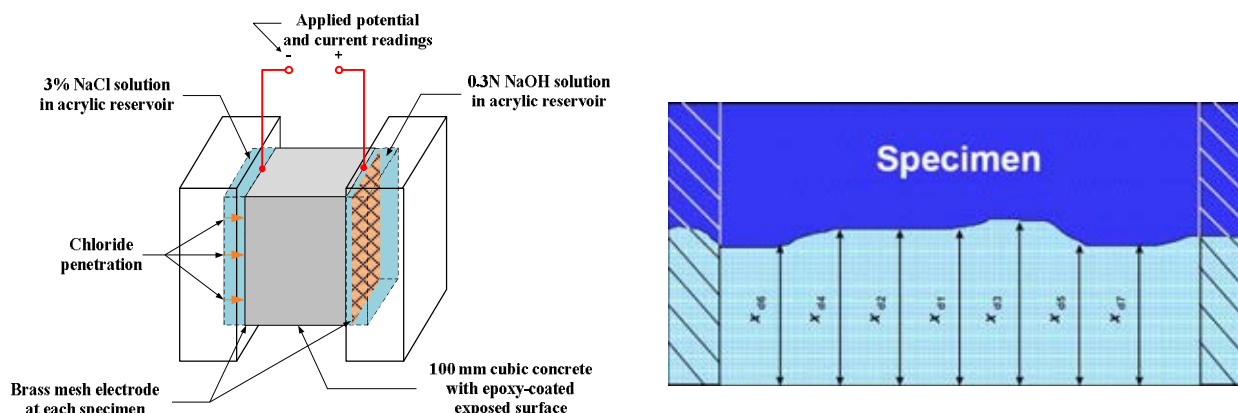
Figure 5.2. Set up of short-term diffusion test combined by ASTM C1202 and Nordtest NT 492

The purpose of this experiment is to determine a correlation of the chloride diffusion coefficient ($D_{un\text{-}eff}$) to crack depth (L). The concept of this test reflects the relationship between chloride penetration depth at crack and uncrack locations in correlation to crack depth. This experiment will be based on the short-term diffusion test (STDT) (Mien et al., 2011), a basis of chloride migration test, which is modified by combination of ASTM C1202 and Nordtest NT build 492 (Figure 5.2).

An assumed shape result of chloride penetration depth is expressed on Figure 5.3, where: x_{uncr} is the chloride penetration depth of un-cracked concrete, L is crack depth, x_{un-eff} is the chloride penetration depth at crack tip.
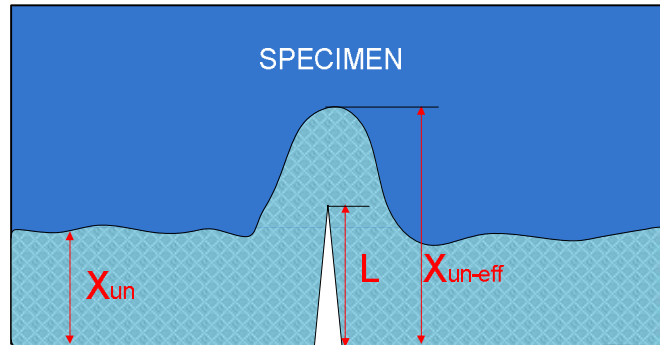
Figure 5.3. The concept of the penetration depth at crack location of reinforced concrete

Based on Nordtest NT build 492, the chloride diffusion coefficient is determined as follows:

$$D_{un} = \frac{Rt}{zFE} \cdot \frac{x_{un} - \alpha\sqrt{x_{un}}}{t} \qquad (5.1)$$

And:

$$D_{un-eff} = \frac{Rt}{zFE} \cdot \frac{x_{un-eff} - \alpha\sqrt{x_{un-eff}}}{t}$$

(5.2)

Where:

$$\alpha = 2\sqrt{\frac{RT}{zFE}} \cdot erf^{-1}\left(1 - \frac{2c_d}{c_0}\right), \quad E = \frac{U-2}{L}$$

z: absolute value of ion valence, for chloride, z = 1; F: Faraday constant, F = 9.648 ×104 J/(V.mol); U: absolute value of the applied voltage, V; R: gas constant, R = 8.314 J/(K.mol); T: average value of the initial and final temperatures in the anolyte solution, K; L: thickness of the specimen, m; t: test duration, seconds; erf–1: inverse of error function; cd: chloride concentration at which the color changes, cd ≈ 0.07 N for OPC concrete; c0: chloride concentration in the catholyte solution, $c_0 \approx 2$ N.

In the same conditions of environment and concrete proportion, a relationship between x_{un-eff} and x_{un} is assumed the linear relation to crack depth (L). The penetration depth of crack tip concrete (x_{un-eff}) is expressed by a function of L and x_{un}.

Moreover, if crack depth equals zero (no crack), the x_{un-eff} will equals x_{un} ($x_{un-eff} = x_{un}$). Consequently, the penetration depth of crack tip concrete (x_{un-eff}) is expressed by equation below:

$$x_{un-eff} = a.L + x_{un}$$

$$(5.3)$$

Similarly, we have:

$$D_{un-eff} = a_1.L + D_{un} \qquad\qquad (5.4)$$

where a and a_1 are the experiment coefficient; L is crack depth from the exposed surface to crack tip.

Conclusively, with the equation (5.4), the chloride diffusion coefficient of uncrack region at crack tip (D_{un-eff}) will be predicted by chloride penetration depth (x_{un}) or chloride diffusion coefficient (D_{un}) of un-crack concrete and crack depth (L).

a. Generate the single crack by bending beam.

b. Sawing cubic concrete specimen from cracked beam.

c Cubic concrete specimen containing single crack

f. Chloride penetration depth at crack

e. Splitting specimen

d. STDT test
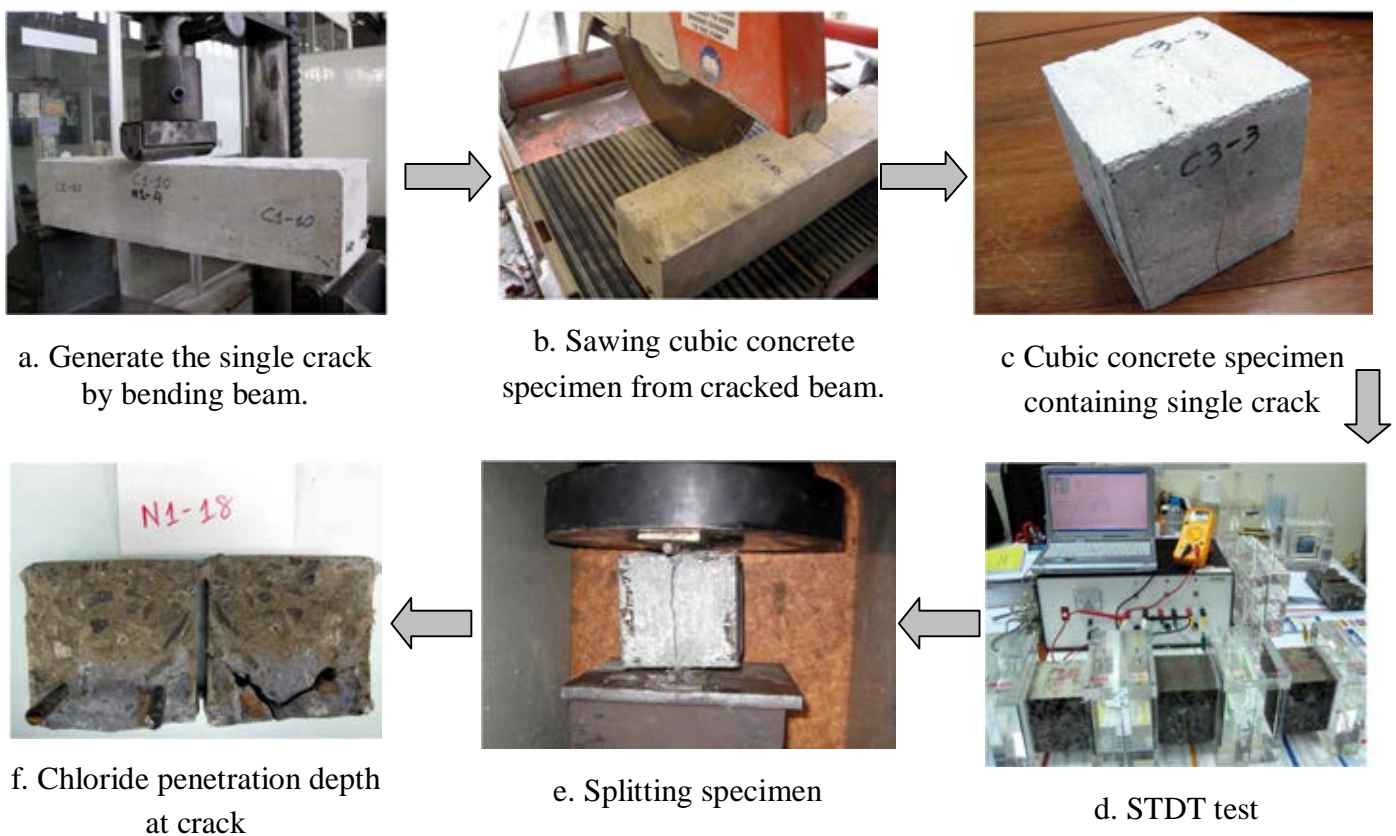
Figure 5.4. The schematically experimental procedure

For each type of concrete proportions, beams of 100x100x500 (mm) were cast, and then cured in the mold for one day. After removed from the mold, they were cured in tap water for 27 days at room temperature. Following curing, a single crack was generated in each beam by a bending test with three-point load. Crack depth was modified by varying the magnitude of the applied load. Cubic specimens containing a crack were sawed from the cracked reinforced concrete beams. Before conducting the chloride migration test, a correlation of crack depth to crack width along crack depth of the cubic specimen is measured on both crack sides of the cubic specimen

by digital microscope. Due to the complicated torturous crack plane, it is very difficult to determine by eye where crack tip is. So in this study the respective crack depth would be used and measured from tension surface to where the crack width would equal 30 µm. Another reason is the influence of crack on chloride diffusion will be ignored when the crack width less than 30 µm. The measurements for crack width and crack depth correlation (Figure 5.5) will be used to determine the respective crack depth as it relates to the crack width of 30 µm. The crack mouth on the tensile surface of cubic specimen was measured at 9 points of interval distance of 1 cm.
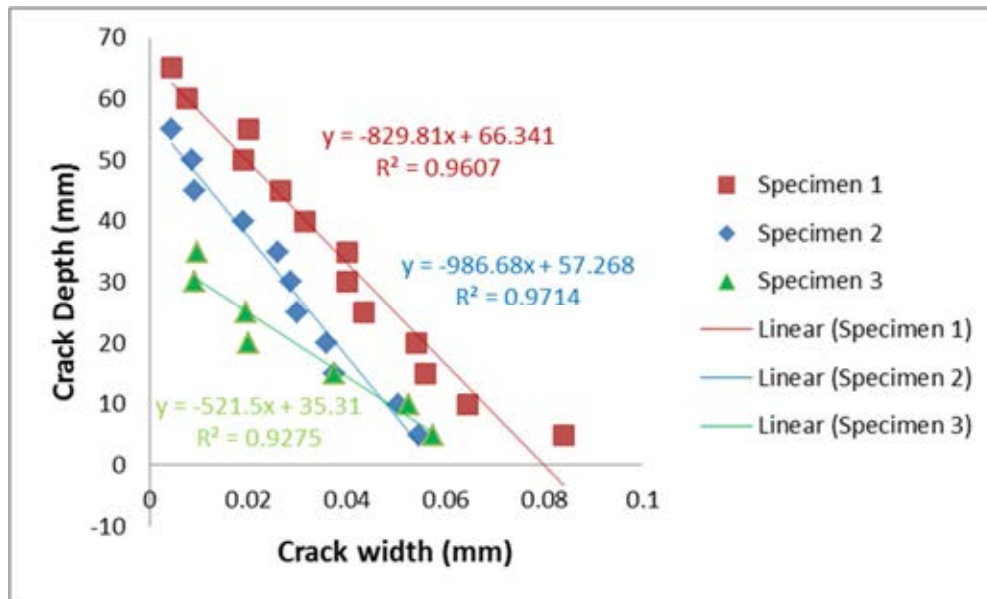
Figure 5.5. An example of results for the correlation between crack width and crack depth

The chloride ion migration of these cubic specimens was tested by STDT. Moreover, in this test, the shape of applied voltage cell was modified to change from cylinder-shape specimen to cubic-shape specimen. The applied voltage for testing was 60 V. The duration time of testing was 10 hours. Following the STDT, the cubic specimens were split into two parts. The silver nitrate 0.1 M was then sprayed on the split surface of the concrete. After 15 minutes, the chloride concentration depth was measured as visible white precipitation of silver chloride at the crack tip. A summary of the experiment process is illustrated in the Figure 5.4.

5.1.2   Determination for chloride profile by chemical analysis method

The chloride profile is found by chemical analysis method, that bases on a Standard Test Method for Acid-Soluble Chloride in Mortar and Concrete (ASTM-C1152, 1997). This test will result the total chloride content in each concrete sample. For the tests of total chloride content, 10g of powder sample passing a 850µm sieve is dispersed in a 250ml beaker with 75ml of deionized water, 25ml of dilute (1+1) nitric acid added slowly, then 3ml of hydrogen peroxide (30% solution), and 20 drops of acid nitric (1+1) added in excess, and heat the covered beaker rapidly

to boiling. After removal of the beaker from the hot plate and filtering the solution, the chloride concentration in the filtrate will be analysed by titration method (ASTM-C114, 2000).

5.1.3   Determination for chloride profile by EPMA test

The chemical analysis method is only shown the content of chloride at specific points which are collected by the required amount of concrete powder. To increase the accuracy of experimental results and model, besides the chemical analysis method, an electron probe microanalysis (EPMA) will be employed to plot the chloride concentration distributed around crack region.

EPMA is a non-destructive testing method by using a focused beam of high energy electrons, which interact with the atoms in the sample, Figure 5.6. It will yield X-ray characteristics which are quantified and compared with counts from standards. The results of elemental composition, quantify and distribution are plotted as digital images where a colour scale of each element indicate its composition and distribution on a sample (Mohammed, Yamaji and Hamada, 2002; Mori, Yamada, Hosokawa et al., 2006; Sugiyama, Kenta, Masahiro et al., 2008).
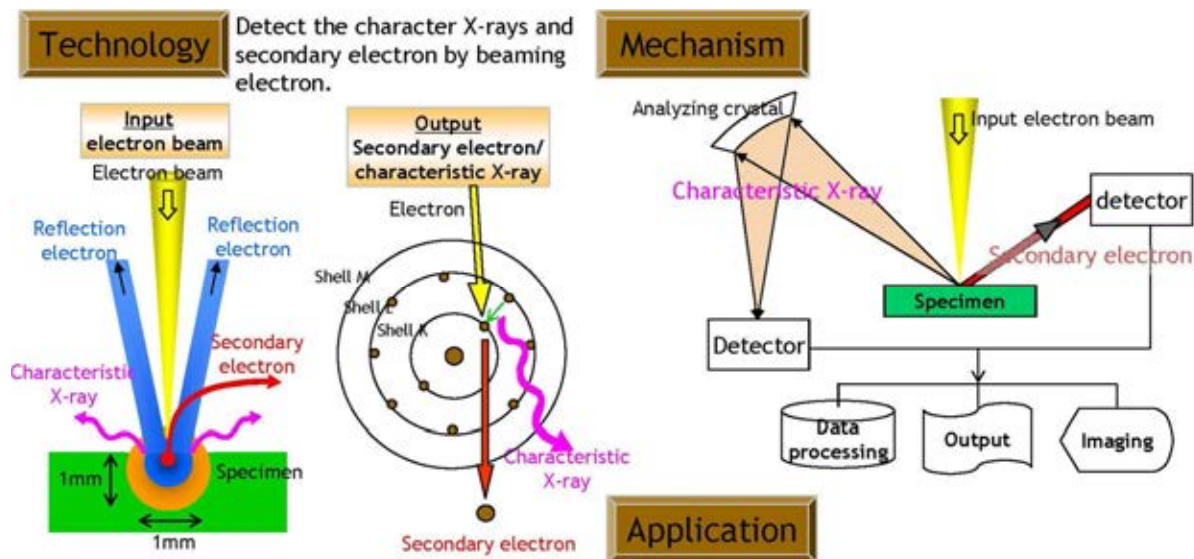
Figure 5.6. The mechanism and technology of EPMA (http://jp.fujitsu.com)

In this research, to prepare the samples for EPMA test, the beam specimens were coated on all surfaces, except the exposed surface, by the epoxy layers. There are two types of beams with different exposed surface:

- The exposed surface includes the tension surface and the crack plane surface for 2D chloride diffusivity (Figure 4.12).

- And, the exposed surface is only crack plane surface for 1D chloride diffusivity (Figure 4.19).
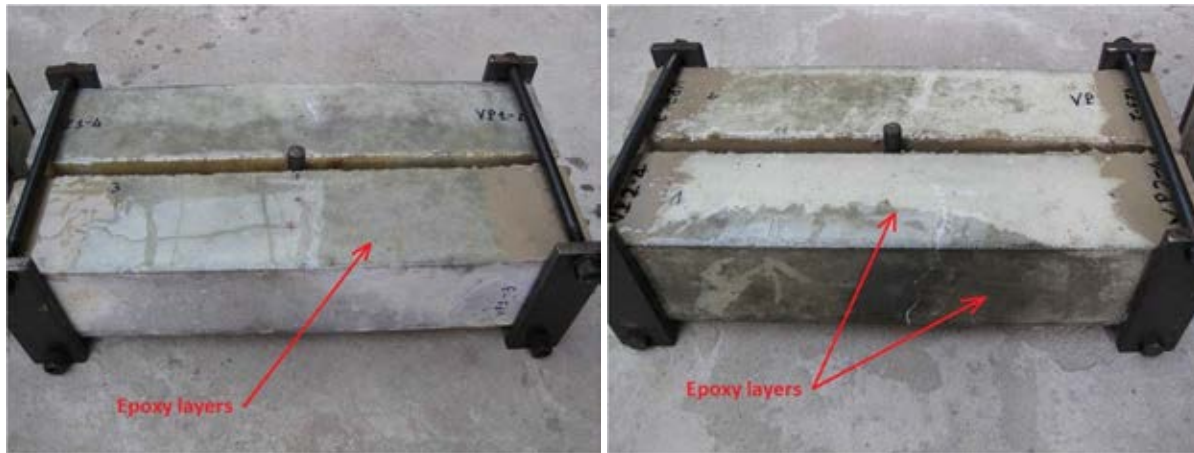
(a) 2D chloride diffusivity   (b) 1D chloride diffusivity

Figure 5.7. Cracked reinforced concrete beam with coated epoxy layers

After coating with epoxy layers (Figure 5.7) for 3 days hardening and immersion in the salt solution of 10% NaCL, specimen slice containing crack is sawed in dry condition, Figure 5.8. The slice 40 mm in width, 70 mm in depth and 12 mm in thickness are cleaned by ultrasonic waves with propanol solution for 5min, dry them in vacuum dry for 1 day. Then vacuuming 1 day, slices are covered with acrylic solution and let them stable for 24 hours so that acrylic can harden. Then, again, coat one more layer of acrylic on the surface of sample, where the measurement will be, and let samples dry for 48 hours. Polish the surface of sample by alumina and sand paper. After polishing, wash sample again with propanol solution and ultrasonic machine for 5 min, vacuum sample in deciator for 48 hours, finally, coat sample with carbon for measurement. The conditions of EPMA measurement in current research involved: the size of each pixel was 130 µm x 130 µm, the acceleration voltage was 15 KV, the probe diameter was 50 µm and unit measurement time was 50ms.
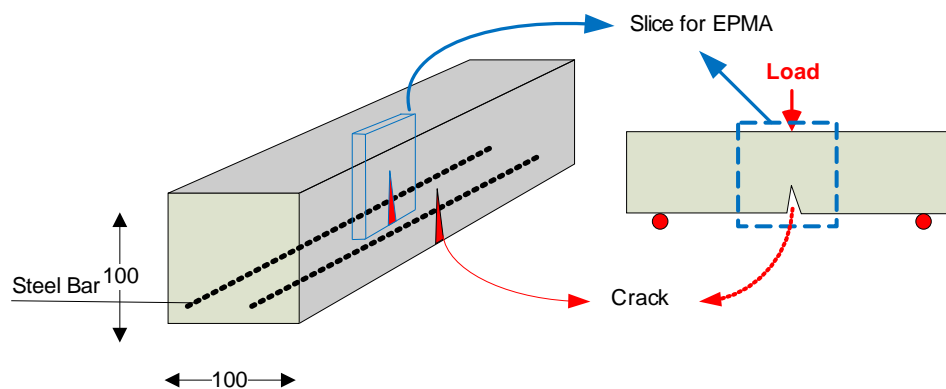
Figure 5.8. The location of the slice for EPMA test

5.2 Experimental Results

5.2.1 Correlation of the applied load (SR) to crack width opening
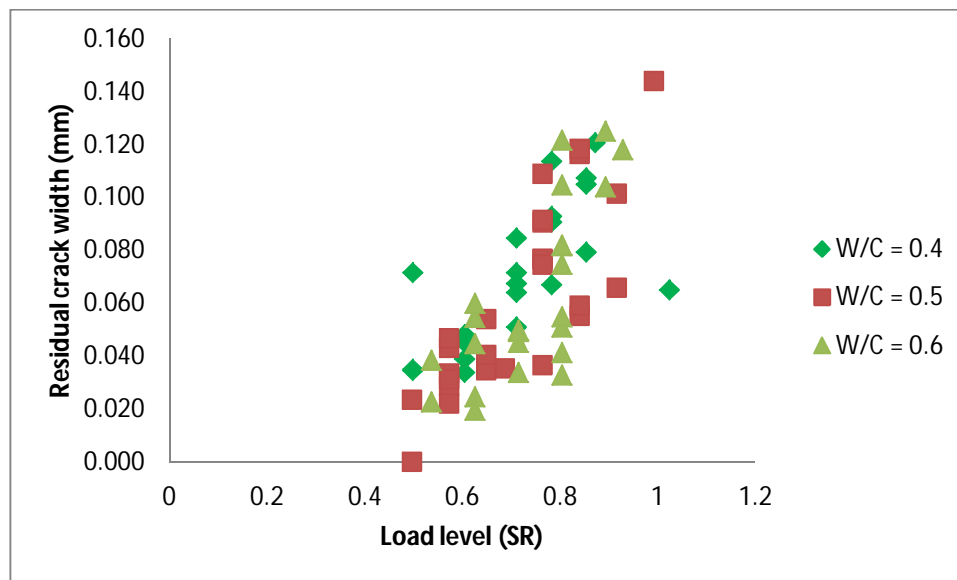
Figure 5.9. The correlation between load level (SR) and residual crack mouth opening

In this research, the load level (SR) is defined as the applied load to ultimate load ratio. Generally, the opening of crack width would increase with increases in the load level or applied load. In Mien's research (Mien, 2008), his model for chloride diffusion into plain concrete under loading related to load levels because the cracks in plain concrete occurred as micro crack, invisible crack. Furthermore, the correlation of the applied load (load level) to cracks of plain concrete could easily be obtained. Therefore, with plain concrete it is better to survey the influence of micro crack on chloride diffusion by conveying to the influence of load level on the chloride diffusion. However, in this research, under loading on reinforced concrete, the cracks will occur under visible cracks, that why it is the best for studying on the crack characteristics and chloride diffusion. Another reason is under loading the characteristics of crack, such as crack width and crack depth, will be varied due to the distribution of steel reinforcement inside the reinforced concrete structure. It results the relationship between crack width, crack depth and applied load is typically nonlinear. Conclusively, in current research the influence of loading will be ignored, the crack width and crack depth instead of loading will be studied on the chloride diffusion. In fact, the crack characteristics and applied load have had a relationship that should be investigated in structural engineering field for a design assignment.

5.2.2   The correlation between crack depth and crack width

$y = -2364.1x^2 + 829.96x - 17.006$
$R^2 = 0.9158$

$y = -2358x^2 + 904.61x - 22.152$
$R^2 = 0.9271$

$y = -2180.2x^2 + 885.57x - 24.001$
$R^2 = 0.7364$
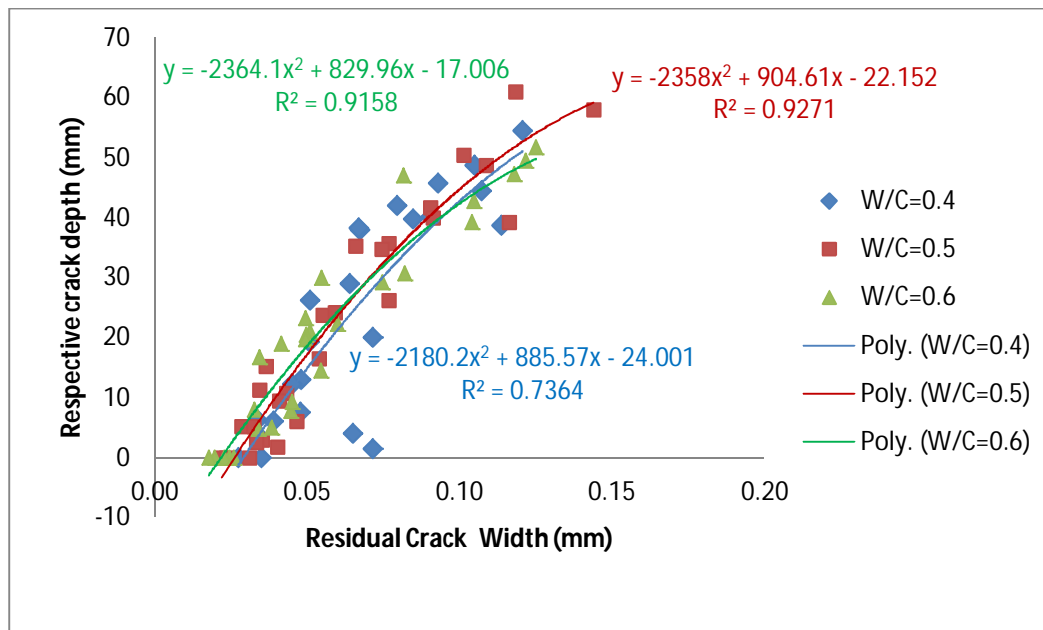
Figure 5.10. The correlation between respective crack depth and residual crack width

Regarding the experimental results, Figure 5.10, it is not difficult to recognize the trends of influence of respective crack depth on the residual crack width with the variation of W/C ratio are similar. Because mix proportions of concrete beams are similar, except W/C ratio, it causes the differences of compressive strength. However, its influence on the opening crack width is not much; because varying crack width is primarily affected by the bond strength, as well as the slip value is a main parameter. In this study, the round reinforcement steel was used, so the compressive strength did not promote ability for the bond strength so much, when compared with the bond strength between deformed steel bar and concrete. Moreover, the results of measurement for residual crack width and crack depth and are measured as the applied load retired.

5.2.3   The influence of water-cement ratio (W/C) on the chloride penetration depth

The experimental results of chloride concentration depth in uncracked concrete with the W/C of 0.4, 0.5 and 0.6 are presented in Figure 5.11. The result showed that the chloride concentration depth increased when the W/C ratio increased. When the water content increase, it will cause more porosity for concrete matrix. Furthermore, the water to cement ratio is recognized to be one of the key factors inducing the increasing permeability of concrete (Sanjuán and Muñoz-Martialay, 1996). In addition, the chloride concentration depth of specimens with and without embedded steel bars was similar, Figure 5.12.
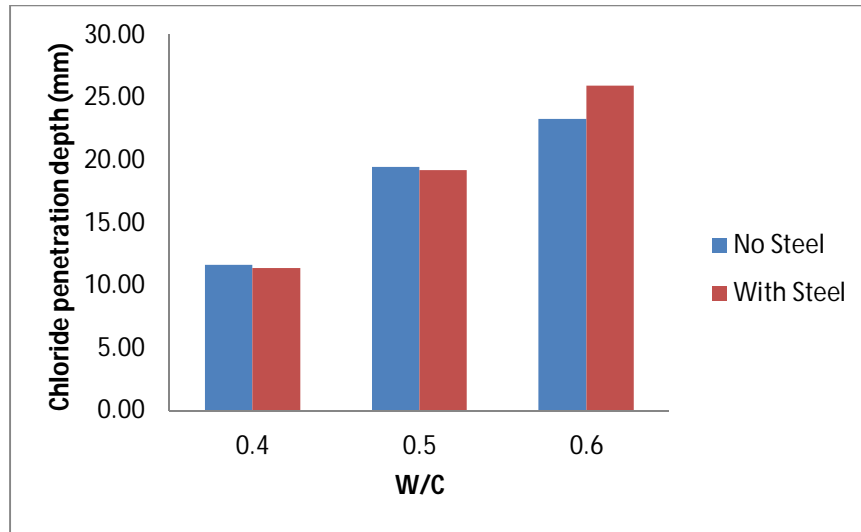
Figure 5.11. The chloride penetration depth at uncrack location versus the W/C ratio

| (a) | (b) |
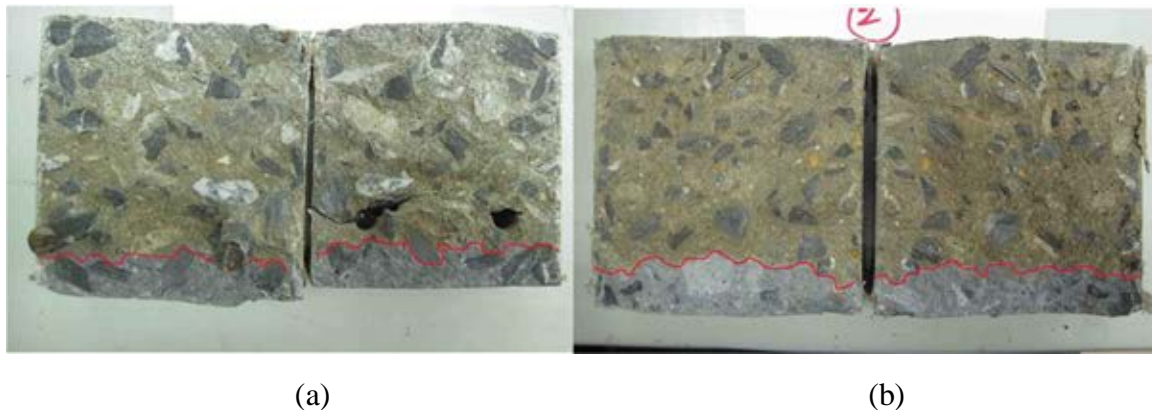
Figure 5.12. The chloride concentration depth of specimens with (a) and without (b) steel bars

5.2.4   The influence of crack depth on the chloride penetration depth

The cracks caused the strong influence on the chloride concentration depth. Generally, chloride ions penetrate through crack path into concrete; it causes the increasing depth of chloride penetration at the crack location, as shown in Figure 5.13.

The experimental results for the influence of respective crack depth on the chloride penetration depth are shown in Figure 5.14. The chloride penetration depth increased linear with respective crack depth varied from zero to 60 mm. The results also showed that the chloride penetration depths of W/C of 0.6 were higher than W/C of 0.5 and 0.4 at the same depths of cracks. It is explained by the influence of the concrete density on the chloride penetration depth. Normally, the density of concrete with W/C of 0.6 is less than the concrete with W/C of 0.5 and 0.4.

(a)   **(b)**
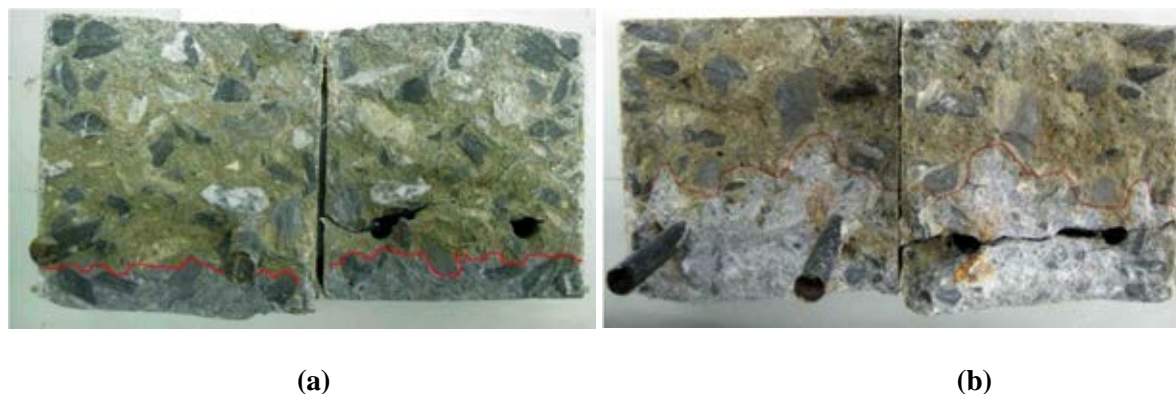
Figure 5.13. The chloride penetration depth at uncrack (a) and crack (b) locations.
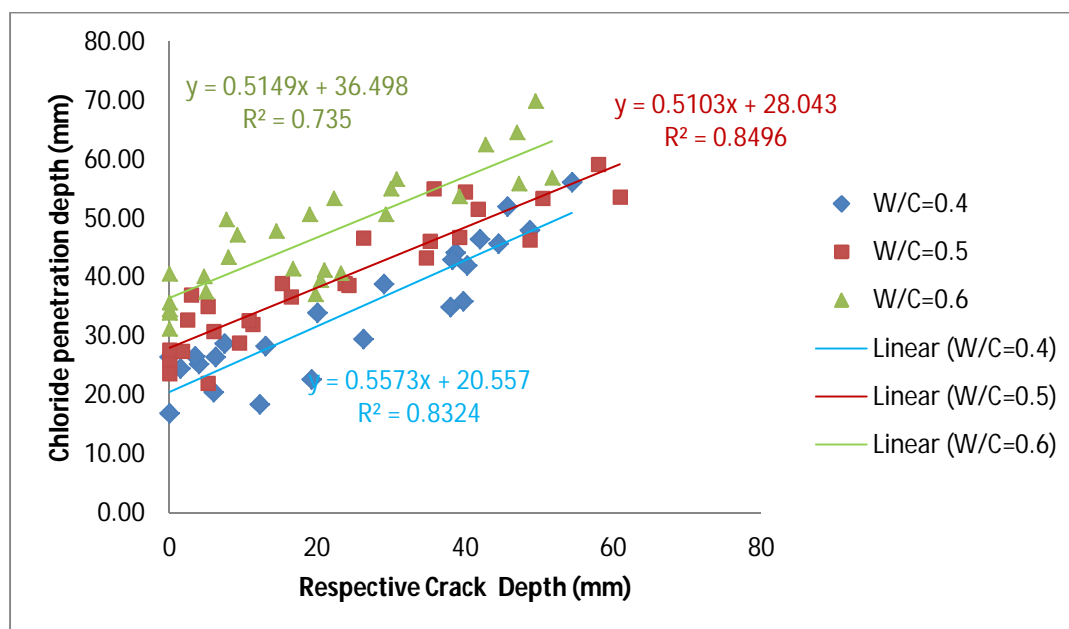
Figure 5.14. The chloride penetration depth at crack location versus the respective crack depth

Regarding experimental results, it is easy to show that the rates of increasing the chloride concentration depth are similar when the W/C varies from 0.4 to 0.6. From these results, the coefficient of 'a' of equation (5.3) was found to equal 0.53, as follows:

$$a_1 = \frac{0.51 + 0.52 + 0.56}{3} = 0.53$$

The experimental results also show that the chloride penetration depth at crack location (x_{cr}) could be expressed by a function of respective crack depth (L) and the chloride penetration depth at uncrack location of concrete (x_{uncr}). Furthermore, the x_{cr} and x_{uncr} would be considered the linear relation to respective crack depth (L). In addition, if crack depth equals zero (no crack) as the boundary condition, the x_{cr} will equal x_{uncr}.

Consequently, the equation (5.3) describes the influence of crack depth on the chloride concentration depth at crack location is as follows:

$$x_{cr} = 0.53 * L + x_{uncr} \qquad (5.5)$$

where x_{cr} is the chloride penetration depth at crack location (mm); x_{uncr} is the chloride penetration depth at uncracked location (mm); L is the respective crack depth (mm).

It also show that the trend of chloride penetration through a crack of concrete was not dependent on the concrete proportions but it is dependent on the characteristics of crack (Vu, Hoang Quoc, Stitmannaithum, Boonchai and Takafumi, Sugiyama, 2011b).

5.2.5   The influence of residual crack width on the chloride concentration depth
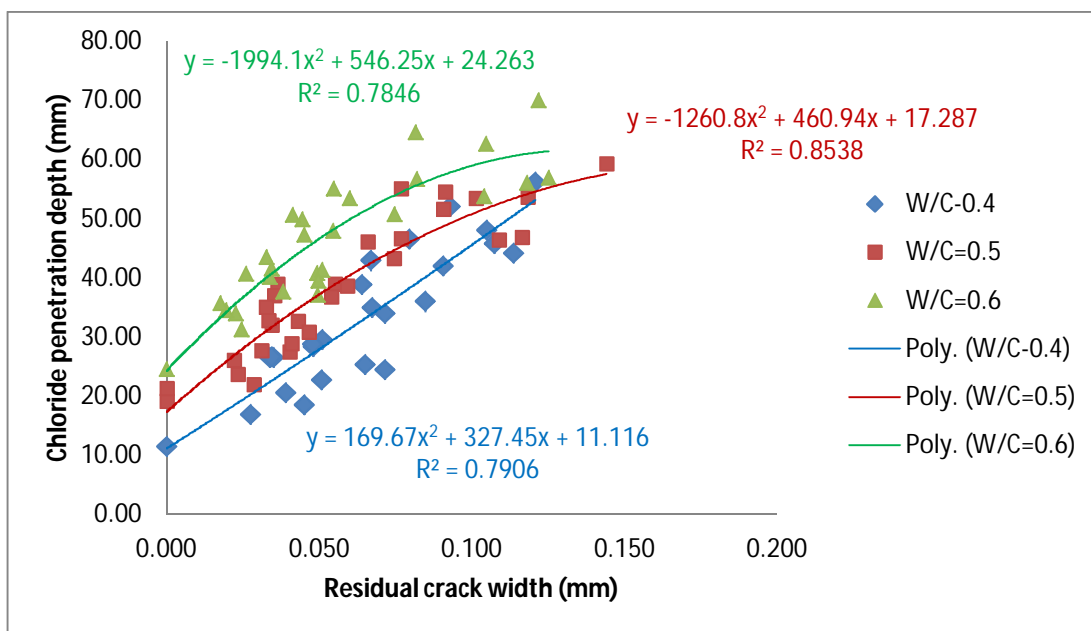
Figure 5.15. The influence of crack width on the chloride concentration depth.

Similarly with the influence of crack depth on the chloride penetration depth, the experimental results also pointed out that the chloride penetration depth increases in increase of residual crack width. However, it seems that the rate of the increasing chloride penetration depth will reduce when the crack width increasing. It can be explained by the influence of the crack depth on that. Viewing back the correlation of crack width to crack depth, Figure 5.10; the rate of the increasing crack depth correlating to that values of residual crack width also reduce. It means that the influence of crack depth on the chloride penetration depth is more significant than the crack width. It is easy to understand that the chloride penetration depth of a deeper crack depth is larger than that of a shallow crack depth, although they have the same crack width.

5.2.6   The influence of crack depth on the chloride diffusion coefficient at crack location
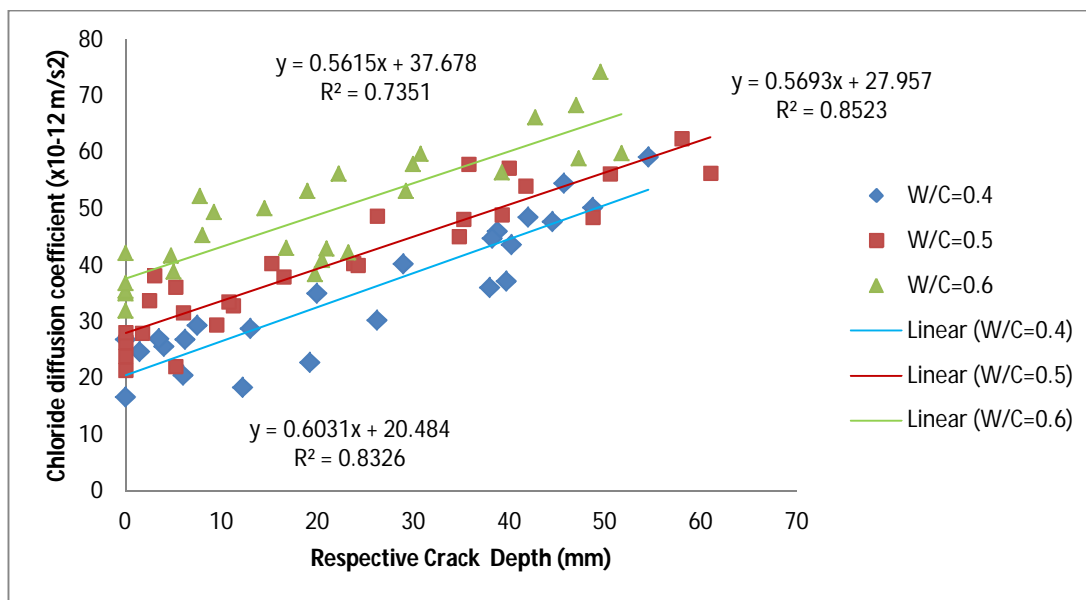
Figure 5.16. The influence of crack depth on the chloride diffusion coefficient by STDT.

Figure 5.16 shows the experimental results of the influence of crack depth on the chloride diffusion coefficient by STDT. At the same depths of cracked concrete, the chloride diffusion coefficients are still govern by effects of concrete proportion, typically, water-cement ratio. Because the chloride diffusion takes place not only in the crack but also in the matrix of concrete, the differences among the performance of matrix concrete types caused the variation of chloride diffusion coefficient. Normally, a higher concrete performance will bring out a lower chloride diffusion coefficient (Suryavanshi, Swamy and Cardew, 2002).

Similar with the experimental results of chloride penetration depth, the chloride diffusion coefficient at cracked concrete also increased with increasing the crack depth. Furthermore, the trends of increasing chloride diffusion coefficient with crack depth are similar when the water to cement ratios varied. It can be concluded that the trend of increasing the penetration depth and diffusion coefficient of chloride is independent with the proportion of concrete (W/C), when the crack depth varies.

From the experimental results of Figure 5.16, the coefficient 'a_1' of the equation (5.4) is found as follows:

$$a_1 = \frac{0.56 + 0.57 + 0.6}{3} = 0.58$$

So, the equations (3.14) describing the influence of crack depth (L) on the chloride diffusion coefficient of uncracked concrete can be presented as below:

$$D_{un-eff} = f(L, D_{uncr}) = 0.58L*10^{-12} + D_{uncr} \qquad (5.6)$$

where L is crack depth (mm).

5.2.7 The tortuosity and constrictivity of crack

Marsavina (Marsavina et al., 2009) also conducted the effect of chloride penetration on the cracked concrete. In his research, the study performed on the artificial crack (a notch) that was generated by a steel sheet put on the fresh surface specimen (Figure 5.17). His results took into the account of the influence of crack depth on the chloride penetration depth, were expressed in Figure 5.18 and Figure 5.19. In their research, the OPC cement was used and the water-cement ratio was 0.5.

(a)   (b)
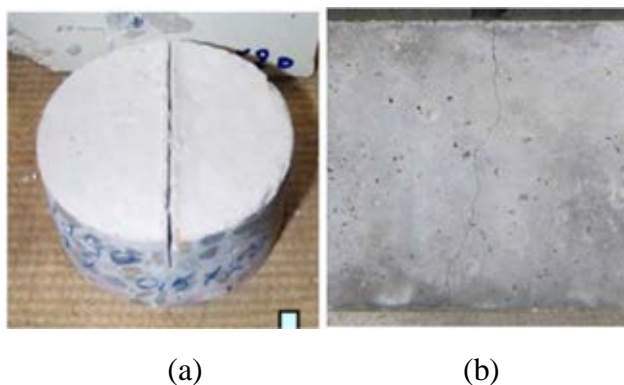
Figure 5.17.The artificial crack by Marsavina (Marsavina et al., 2009) (a) and natural crack of current research (b).
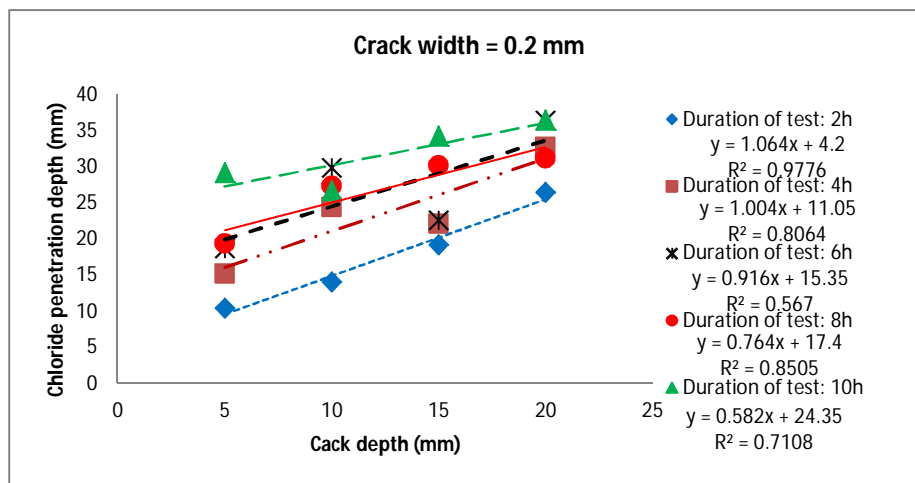
Figure 5.18. Influence of the notch depth on chloride penetration depth (W=0.2 mm) (Marsavina et al., 2009)
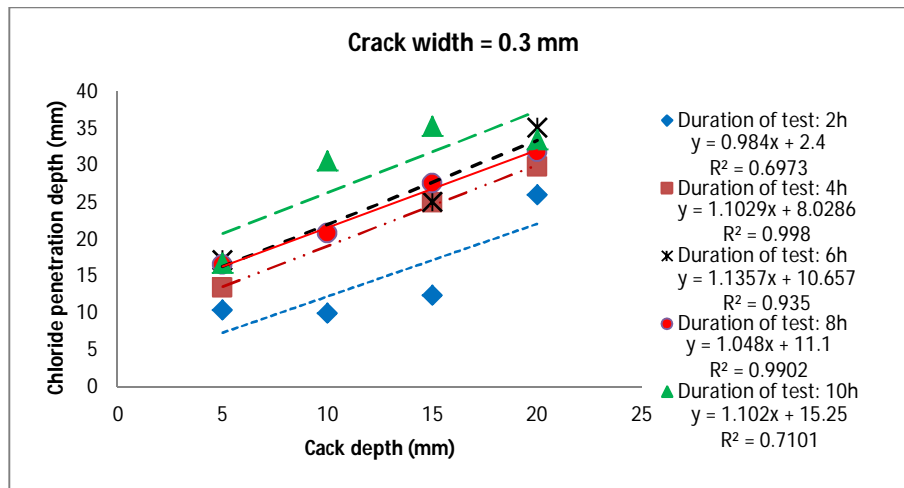
Figure 5.19. Influence of the notch depth on chloride penetration depth (W=0.3 mm) (Marsavina et al., 2009)

In Marsavina's results above, the influence of crack width seemed insignificant to the chloride penetration depth because the crack width in their research was large. If the crack width is larger than 80 μm, the chloride diffusion coefficient of crack could be consider constant (Djerbi et al., 2008b). Moreover, the trends (slopes) of the regression lines are similar when the crack depth varied. So, by approximately averaging of the slope coefficients of the regression lines, the equation describing the influence of crack depth on the chloride penetration depth for the artificial crack is expressed as follow:

$$x'_{cr} = 0.97 * L + x_{uncr} \tag{5.7}$$

where x'$_{cr}$ is the chloride penetration depth at crack tip of artificial crack.

Call back the equation (5.5) described the influence of crack depth on the chloride penetration depth conducted by natural crack of reinforced concrete in part 5.2.4:

$$x_{cr} = 0.53 * L + x_{uncr}$$

Where: x$_{cr}$ is the chloride penetration depth at crack tip of natural crack.

From equation (5.5) and (5.7), it is simple to recognize that the reducing of the slope coefficient is from 0.97 to 0.53, although both of experiments have the same concrete proportion (W/C), kind of test... Hence, the difference is only due to the generation methods of crack between the artificial cracks and natural cracks (Figure 4.16). The different points of crack characteristics between the artificial crack and natural crack are listed on Table 5.2. The reasons causing the reducing slope of experimental curves in these researches are assumed the tortuosity of crack and the constrictivity of crack.

Table 5.2. The different characteristics of crack and the affected coefficients

Characteristics	Crack plane surface	Crack plane trend	Shape
Marsavina (**Marsavina et al., 2009**)	Smooth	Parallel	
Present research	Roughness	Slope	
Affected coefficient	Tortuosity (τ)	Constrictivity (δ)	

To compare with the influence of artificial crack (Figure 5.18, Figure 5.19), the results for the influence of natural crack characteristics on the chloride penetration depth (Figure 5.14) is called back and is converted by the tortuosity and constrictivity parameters following equations (2.16) and (2.18); the converted results is illustrated on Figure 5.20

W/C=0.5

$y = 0.7844x + 11.457$
$R^2 = 0.9313$
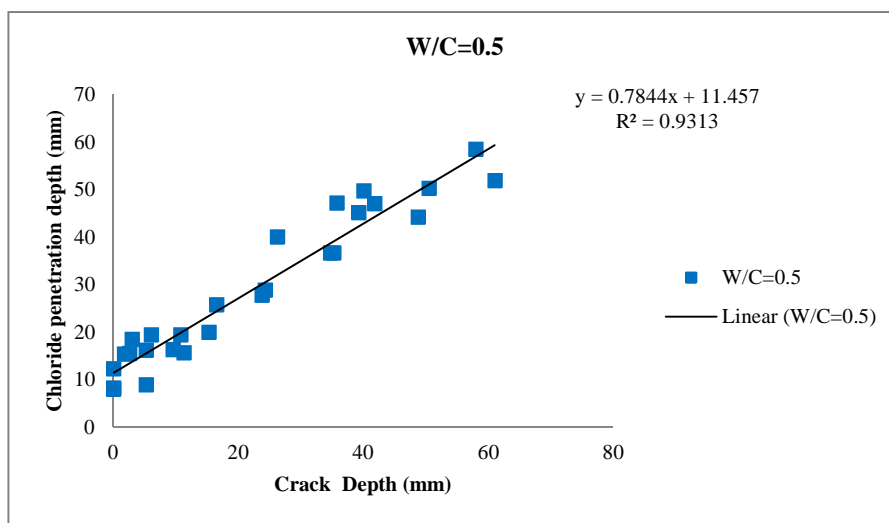
Figure 5.20. The influence of crack depth on the chloride penetration depth after converted by the tortuosity and constrictivity parameters of crack.

Regarding the result of Figure 5.20, after coverted by the tortuosity and constrictivity parameters, the slope of curve increases from 0.53 in Figure 5.14 to 0.784 in Figure 5.20 and trends to reach to 0.97 (slope coefficient of the artificial crack) in Figure 5.18 and Figure 5.19. However, there is an error between the influence of artificial crack and natural crack on the chloride penetration depth (after converted by the tortuosity and constrictivity parameters): the deviation of slope coefficients of 0.784 and 0.97. An explanation is the assumption of the crack tortuosity

parameter value (τ_{cr}) of 1.0 proposed by Ishida (Ishida et al., 2009), equation (2.16), could not be suitable and should be considered again.

According the experiments of current research and Marsavina's research (Marsavina et al., 2009), the experimental tortuosity parameter of natural crack should be proposed again for chloride penetration as follow:

$$\tau_{cr} = \frac{0.97}{0.784} \simeq 1.24 \qquad (5.8)$$

With natural crack (visible crack), the tortuosity parameter of natural crack should be larger than value of 1.0 because the natural crack plane has never been straight and smooth like the artificial crack.

The tortuosity coefficient of natural crack, equation (5.8), will be used for a visibly natural crack having a crack width less than 225 µm; because the crack tortuosity will not influence on chloride diffusion in this large crack (Ismail et al., 2008).

5.3   Experiment verification

5.3.1   Validation for model of chloride diffusion at crack location of reinforced concrete

5.3.1.1   Experimental results of chloride profile at crack and uncrack locations

(a)   (b)

Figure 5.21. Immersion (a) and after immersion (b) of cracked beam in salt solution

The cracked concrete beams were immerged during different periods of 2, 4, 6, 8 and 16 weeks. After immersion in salt solution, the chloride profiles were collected at cracked and un-crack location of these beams (Figure 5.22). The chemical analysis method (ASTM-C1152, 1997) is employed to analyse the chloride content. The experimental results of chloride content at crack and uncrack location at interval depth are presented in Appendix A. The experimental results of

crack characteristics, surface chloride content and chloride diffusion coefficient at crack and uncrack location are shown in Table 5.3.
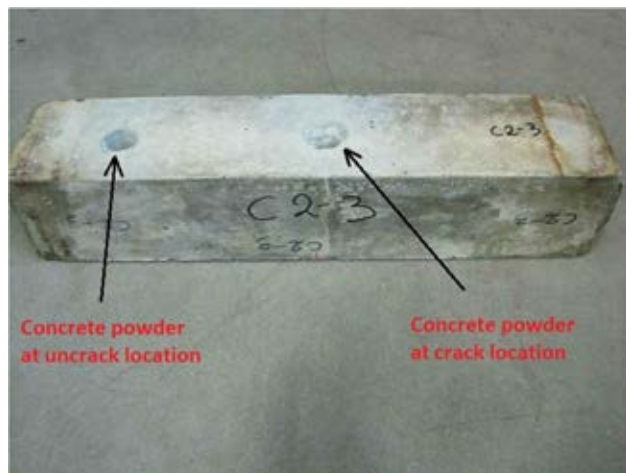
Figure 5.22. The location for collecting the concrete powder to analyze chloride content

Table 5.3. The surface chloride content and chloride diffusion coefficient at crack and uncrack locations.

Immersion periods	Beam series	W/C	Crack	Crack width (mm)	Crack depth (mm)	Cs (% Wt. of concrete)	Da (m^2/s)
2	1	0.4	1	0.058	32.5	0.6	5.77E-10
			2	0.051	18.5	0.5	3.20E-10
			3	0.059	35	0.49	5.37E-10
			Uncrack	-	-	0.91	3.77E-11
	2	0.5	1	0.077	36	0.55	6.76E-10
			2	0.067	34	0.47	8.02E-10
			Uncrack	-	-	0.72	5.33E-11
	3	0.6	1	0.106	49.5	0.72	4.49E-10
			2	0.081	32	0.6	6.77E-10
			3	0.102	45.5	0.48	7.62E-10
			Uncrack	-	-	0.6	8.87E-11
4	2	0.5	Crack	0.093	41.5	0.46	4.21E-10
			Uncrack	-	-	0.59	3.16E-11
	3	0.6	Crack	0.083	41.5	0.56	2.63E-10
			Uncrack	-	-	0.82	4.74E-11
6	1	0.4	1	0.053	30.5	0.52	2.20E-10
			2	0.045	21.5	0.51	1.86E-10
			3	0.06	32.5	0.54	1.67E-10
			Uncrack	-	-	0.91	3.77E-11
	2	0.5	1	0.052	27.5	0.63	1.30E-10

			2	0.041	17.5	0.71	1.07E-10
			3	0.041	21	0.71	1.14E-10
			Uncrack	-	-	0.71	2.19E-11
	3	0.6	1	0.054	29	0.65	1.81E-10
			2	0.05	26.5	0.58	1.45E-10
			3	0.072	33	0.72	2.21E-10
			Uncrack	-	-	0.6	2.28E-11
8	1	0.4	1	0.089	42	0.6	2.26E-10
			2	0.088	41.5	0.52	2.75E-10
			Uncrack	-	-	0.97	2.47E-11
	2	0.5	Crack	0.074	31.5	0.7	1.58E-10
			Uncrack	-	-	1	2.43E-11
	3	0.6	Crack	0.096	50.5	0.86	1.63E-10
			Uncrack	-	-	0.76	3.25E-11
12	1	0.4	Uncrack	-	-	0.53	1.35E-11
	3	0.6	Uncrack	-	-	0.56	3.13E-11
16	2	0.5	1	0.107	45.5	0.61	2.85E-10
			2	101	45	0.61	2.61E-10
			Uncrack	-	-	0.85	1.65E-11

Note: beam series 1, 2, 3 are noted for W/C = 0.4, 0.5 and 0.6, respectively.

5.3.1.2   Validation for chloride diffusion coefficient at crack location

The numerical calculation of chloride diffusion coefficient at crack location of reinforced concrete is found by using equation (3.11), (3.12) and (5.6). The average chloride diffusion coefficient (D_{av}), equation (3.11), is proposed as the diffusion coefficient of concrete age referred at 28 days. To evaluate the time-dependent chloride diffusion coefficient, using an aging exponent to take into account the variation of chloride diffusion coefficient with the time of service life:

$$D(t) = D_0 \left(\frac{28}{t} \right)^a \tag{5.9}$$

where D_0 is the chloride diffusion coefficient at 28 days; $D(t)$ is the chloride diffusion coefficient at t days; a is the experiment coefficient, 0.3 for OPC (Bermudez and Alaejos, 2010).

The input data for the calculation analysis of the chloride diffusion coefficient at a crack comes from the experimental results, which include crack width, crack depth and apparent chloride diffusion coefficient of uncracked concrete (Table 5.3).
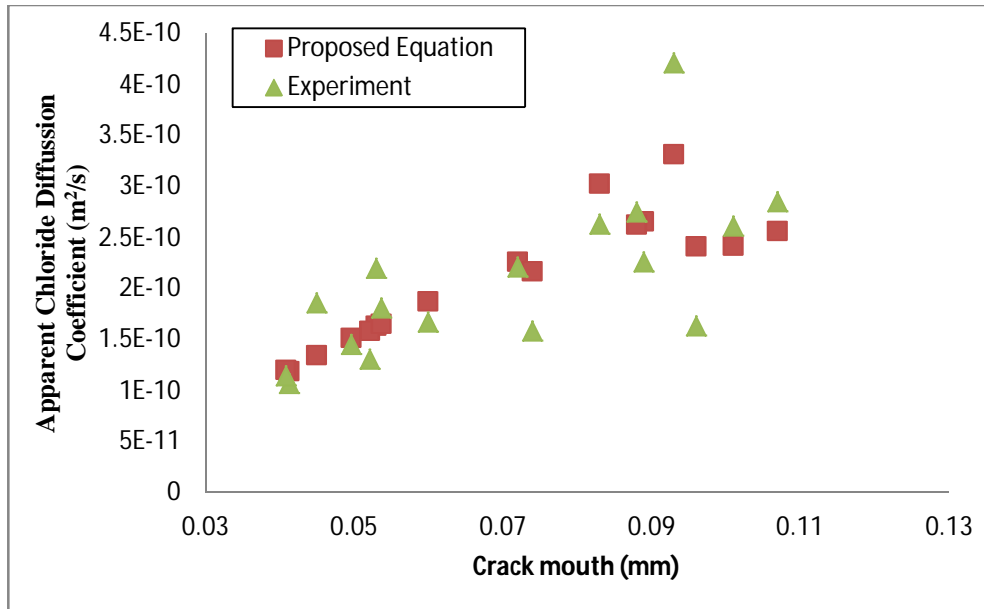
Figure 5.23. Comparison between the predicted results and experimental results affected by crack mouth
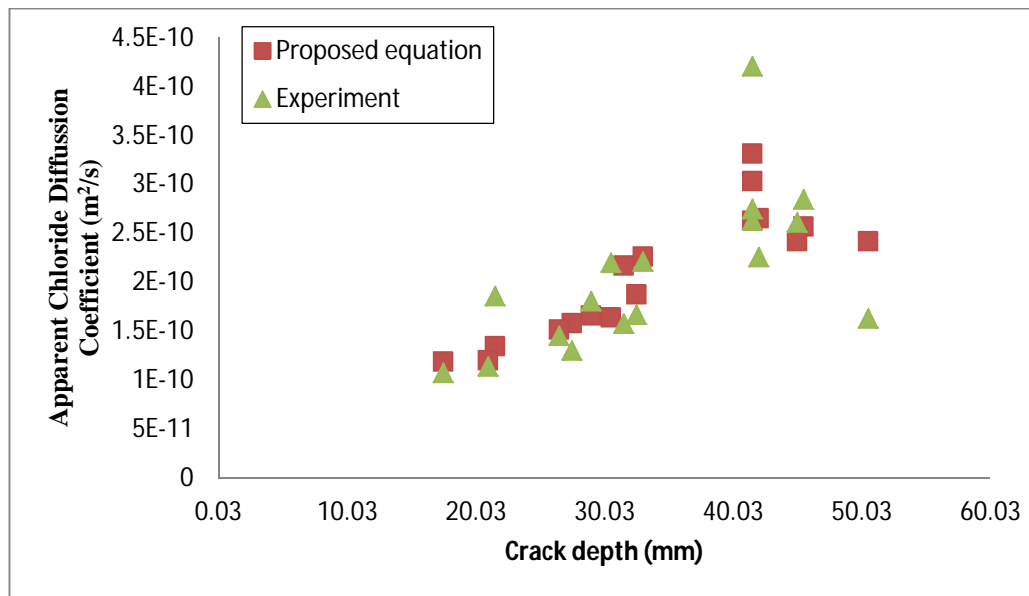
Figure 5.24. Comparison between the predicted results and experimental results affected by crack depth

The predicted results of apparent chloride diffusion coefficient are compared with the results from a self-conducted experiment and are given in Figure 5.23 and Figure 5.24. The chloride diffusion coefficient of a natural crack increases with increase in crack width (Figure 5.23). Similarly, the chloride diffusion coefficient is also strongly increased with increase in crack depth (Figure 5.24). Crack depth creates a path for the movement of chloride ions and diffusion inside concrete structure, by this way it increases and propagates the chloride concentration.

Table 5.4. The deviation between predicted and experimental results

Immersion periods (week)	Beam series	W/C	Crack No.	Chloride diffusion coefficient, (m^2/s)		Deviation (%)
				Experimental results	Predicted results	
4	2	0.5	1	4.21E-10	3.316E-10	21.27
	3	0.6	1	2.63E-10	3.029E-10	-15.18
6	1	0.4	1	2.20E-10	1.634E-10	25.74
			2	1.86E-10	1.342E-10	27.85
			3	1.67E-10	1.871E-10	-12.04
	2	0.5	1	1.30E-10	1.579E-10	-21.21
			2	1.07E-10	1.186E-10	-10.87
			3	1.14E-10	1.196E-10	-4.79
	3	0.6	1	1.81E-10	1.654E-10	8.63
			2	1.45E-10	1.515E-10	-4.48
			3	2.21E-10	2.261E-10	-2.32
8	1	0.4	1	2.26E-10	2.655E-10	-17.46
			2	2.75E-10	2.623E-10	4.63
	2	0.5	1	1.58E-10	2.165E-10	-37.01
	3	0.6	1	1.63E-10	2.415E-10	-48.14
16	2	0.5	1	2.85E-10	2.565E-10	9.99
			2	2.61E-10	2.418E-10	7.34

The deviations between predicted and experimental results are shown in Table 5.4. It appears that the deviation between predicted and experimental results increases when the crack mouth and crack depth increase. There are two reasons: first is the effect of the tortuosity of the crack, and, second is the effect of the straightness of crack. The deeper cracks are normally not straight or perpendicular to the exposed surface when compared with shallower cracks, but the direction of hole drilled to collect concrete powder is always straight and perpendicular to the exposed surface. That is why there is a difference between the predicted and experimental results. It is very difficult to collect an exact sample at a crack for experiments. Therefore, these deviations of the study are quite good under macro scale investigation. Comparably, under micro scale, Sun

(Sun et al. 2011) conducted the study on chloride diffusion coefficient of concrete involving four-phase composite materials and the deviation of Sun's research results was up to 25%.

Through the experimental and predicted results, it is interested to see that the influence of the W/C ratio and immersion periods on the chloride diffusion coefficient is not much when compared with the influence of the crack width and crack depth on the chloride diffusion coefficient. The influence of crack characteristics on the chloride diffusion coefficient is more significant than the proportion or age of concrete. When a crack width is increased, the chloride diffusion coefficient of cracked concrete may increase from 10 to 100 time when compared with that of uncracked concrete (Takewaka et al., 2003). Therefore, the influence of concrete proportion or concrete age on the chloride diffusion coefficient is less significant when compared with the influence of crack width and crack depth. In conclusion, the characteristics of crack, such as crack width and crack depth, have an important role for the chloride penetration into cracked reinforced concrete beam.

5.3.1.3   Validation for model of chloride diffusion at crack location of reinforced concrete.

By applying the Fick's 2nd Law and the average chloride diffusion coefficient, equation (3.11), the chloride profile at crack location is calculated. Then, the comparisons between the predicted results and experimental results are plotted in figures below.

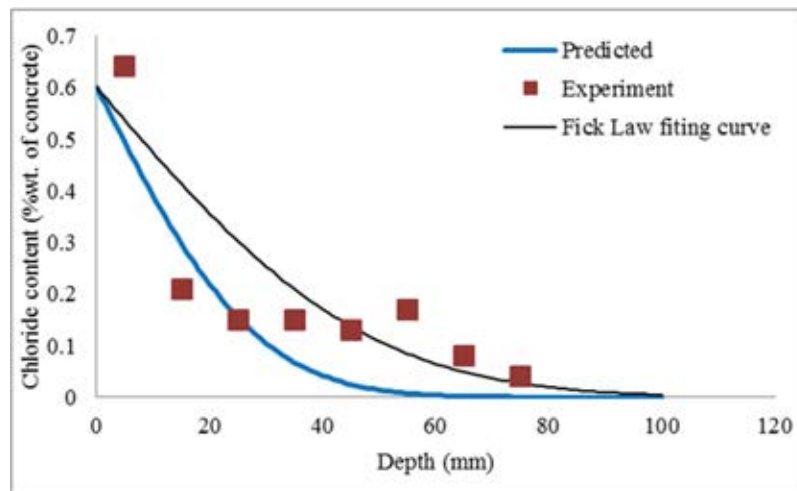- 2 weeks immersed in salt solution:

Figure 5.25. Comparision between predicted and experimental results (Beam series 1, crack 1)
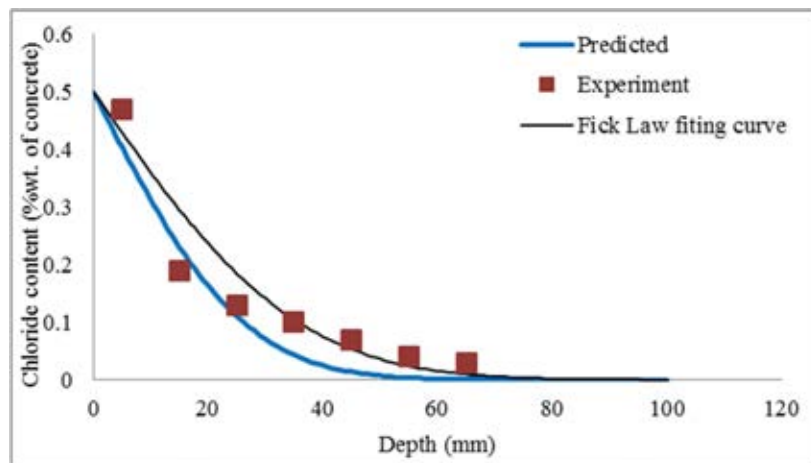
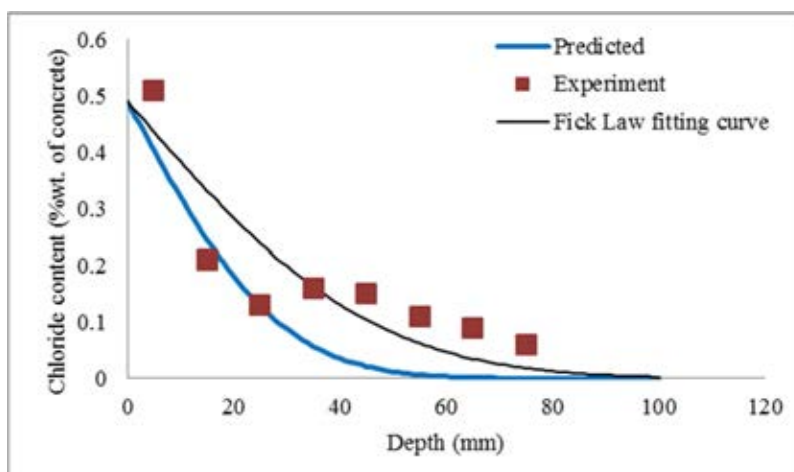**Figure 5.26. Comparision between predicted and experimental results (Beam series 1, crack 2)**

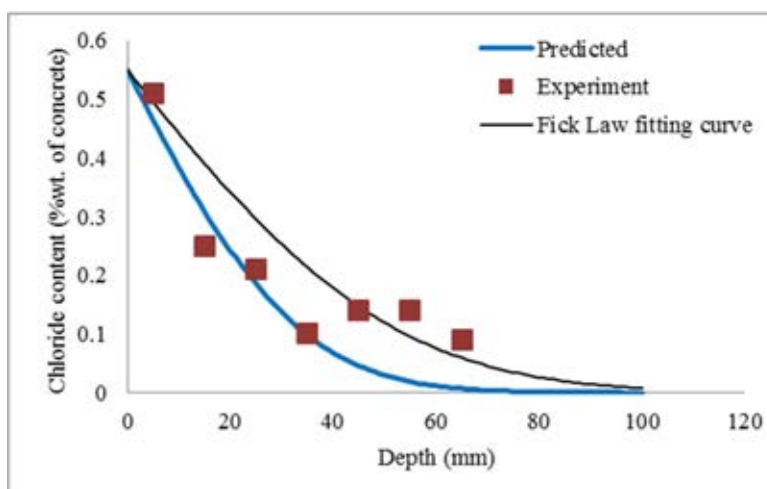**Figure 5.27. Comparision between predicted and experimental results (Beam series 1, crack 3)**

Figure 5.28. Comparision between predicted and experimental results (Beam series 2, crack 1)
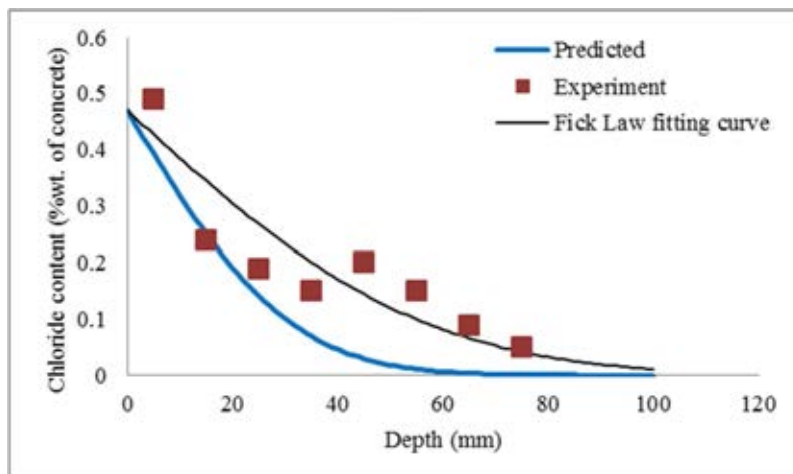
Figure 5.29. Comparision between predicted and experimental results (Beam series 2, crack 2)
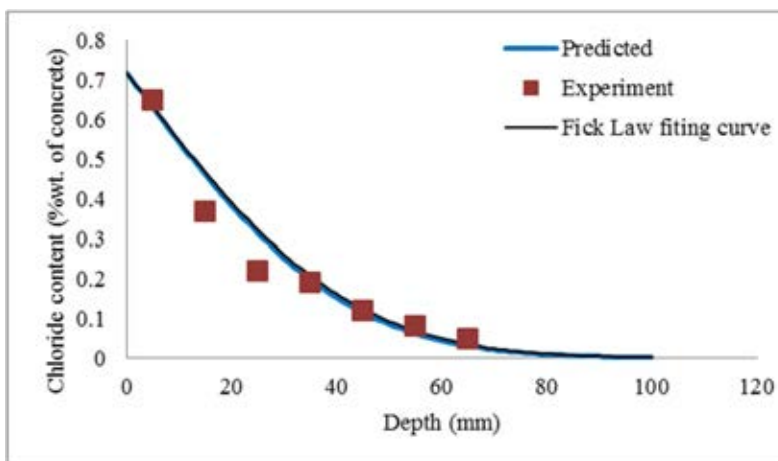

Figure 5.30. Comparision between predicted and experimental results (Beam series 3, crack 1)

Figure 5.31. Comparision between predicted and experimental results (Beam series 3, crack 2)

Figure 5.32. Comparision between predicted and experimental results (Beam series 3, crack 3)

- 4 weeks immersed in salt solution

Figure 5.33. Comparision between predicted and experimental results (Beam series 2, crack 1)

Figure 5.34. Comparision between predicted and experimental results (Beam series 3, crack 1)
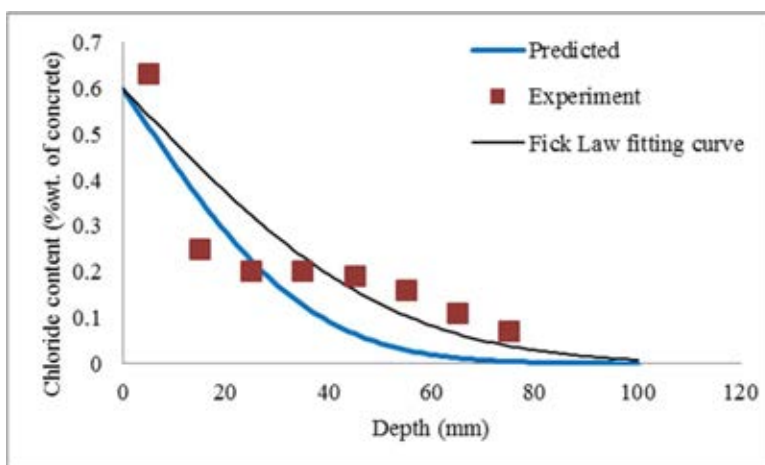
- 6 weeks immersed in salt solution

Figure 5.35. Comparision between predicted and experimental results (Beam series 1, crack 1)

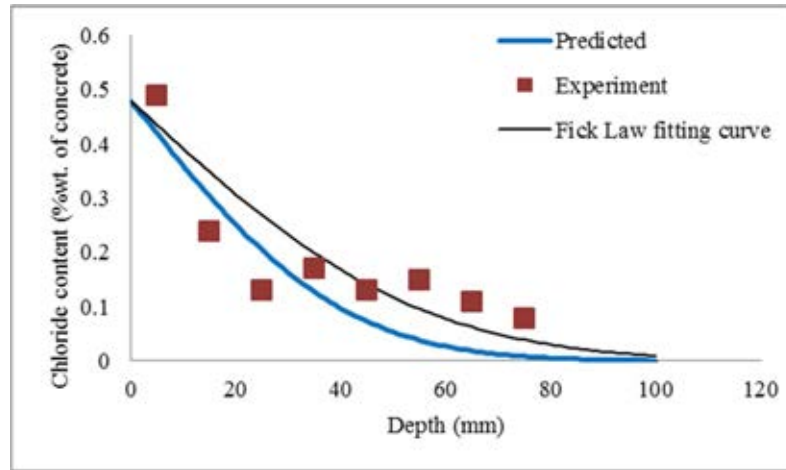**Figure 5.36. Comparision between predicted and experimental results (Beam series 1, crack 2)**

Figure 5.37. Comparision between predicted and experimental results (Beam series 1, crack 3)
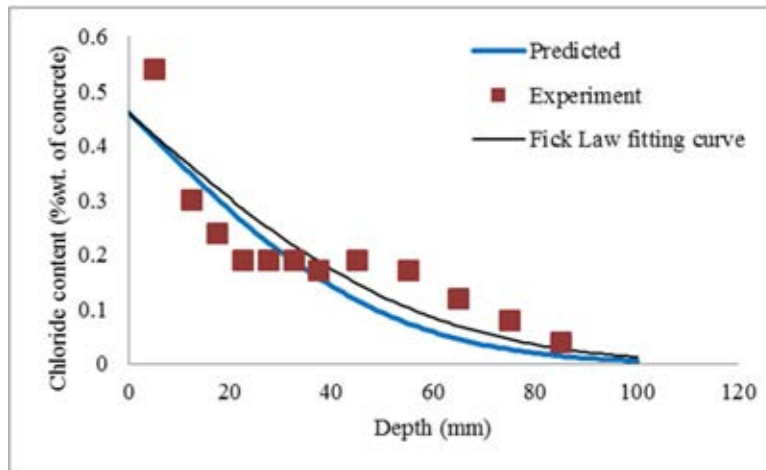
Figure 5.38. Comparision between predicted and experimental results (Beam series 2, crack 1)
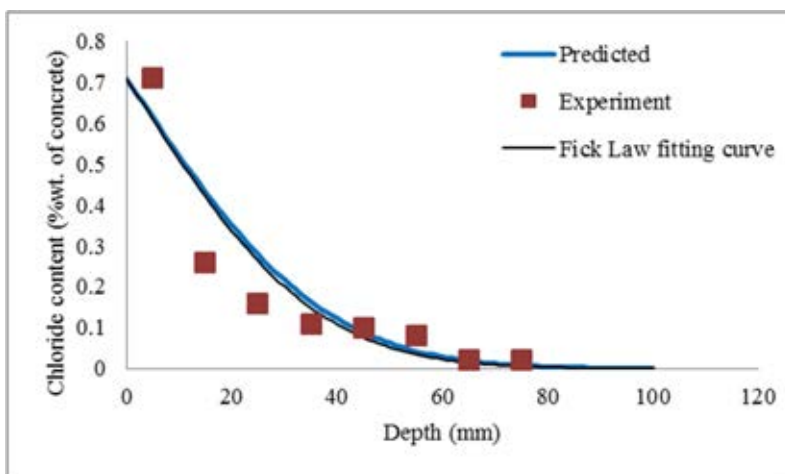
Figure 5.39. Comparision between predicted and experimental results (Beam series 2, crack 2)
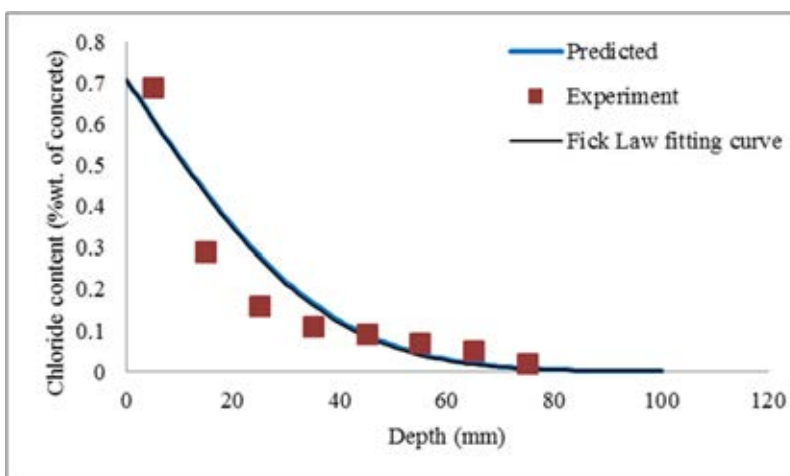
Figure 5.40. Comparision between predicted and experimental results (Beam series 2, crack 3)
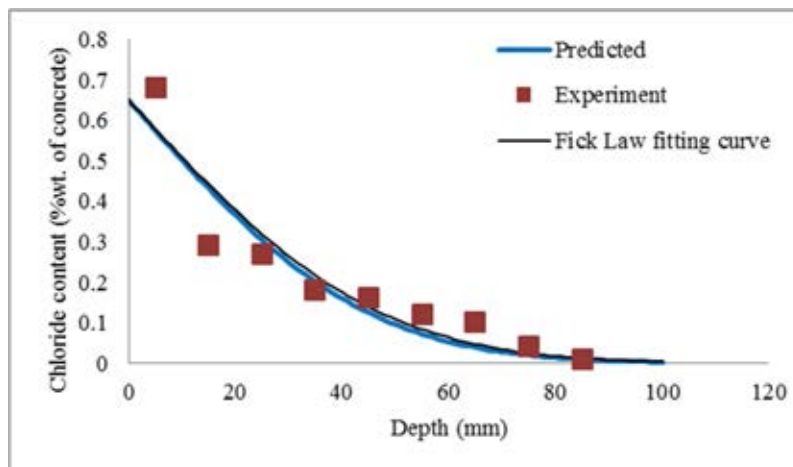
Figure 5.41. Comparision between predicted and experimental results (Beam series 3, crack 1)
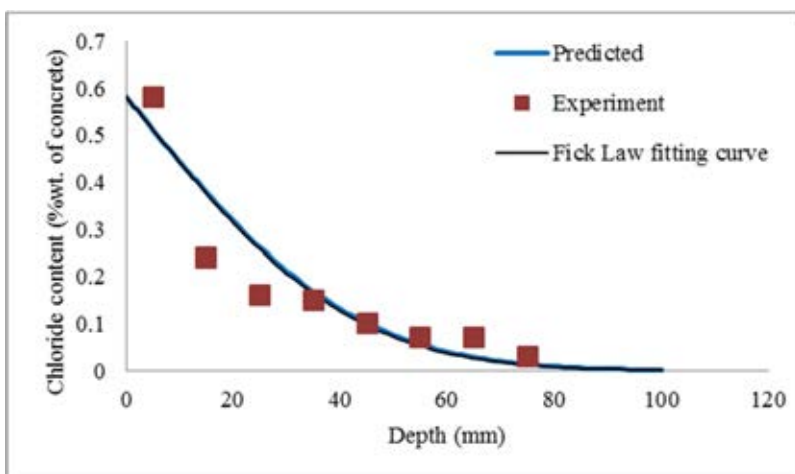
Figure 5.42. Comparision between predicted and experimental results (Beam series 3, crack 2)
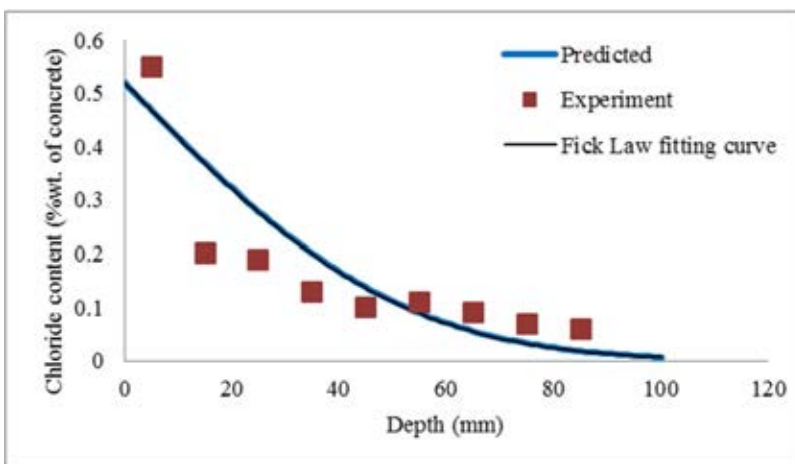
Figure 5.43. Comparision between predicted and experimental results (Beam series 3, crack 3)

- 8 weeks immersed in salt solution

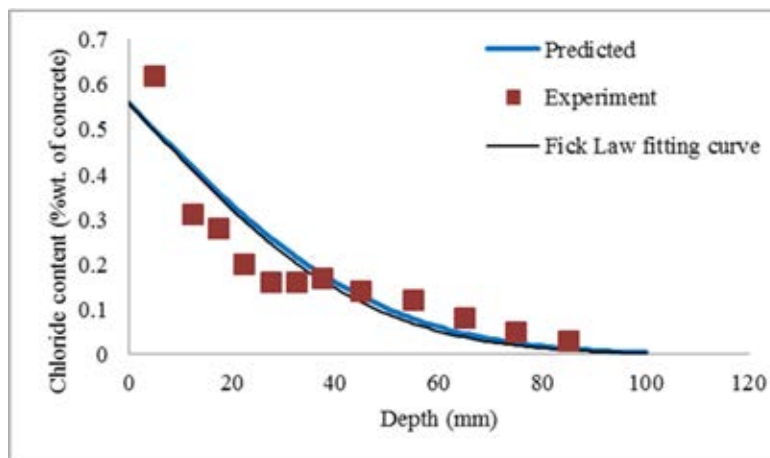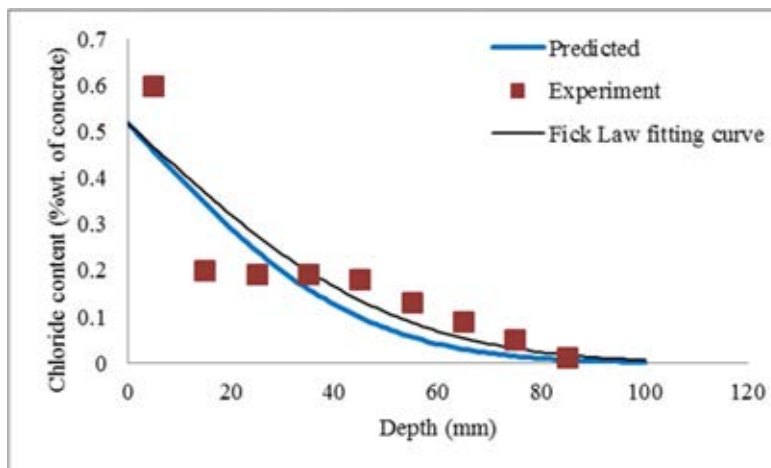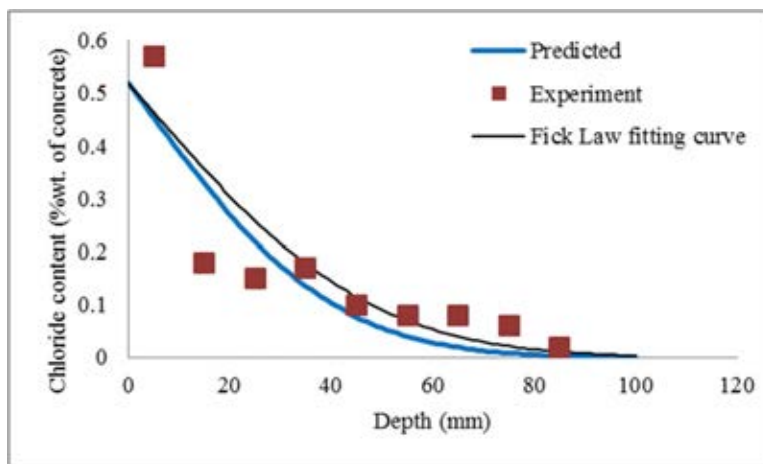**Figure 5.44. Comparision between predicted and experimental results (Beam series 1, crack 1)**

Figure 5.45. Comparision between predicted and experimental results (Beam series 1, crack 2)

Figure 5.46. Comparision between predicted and experimental results (Beam series 2, crack 1)

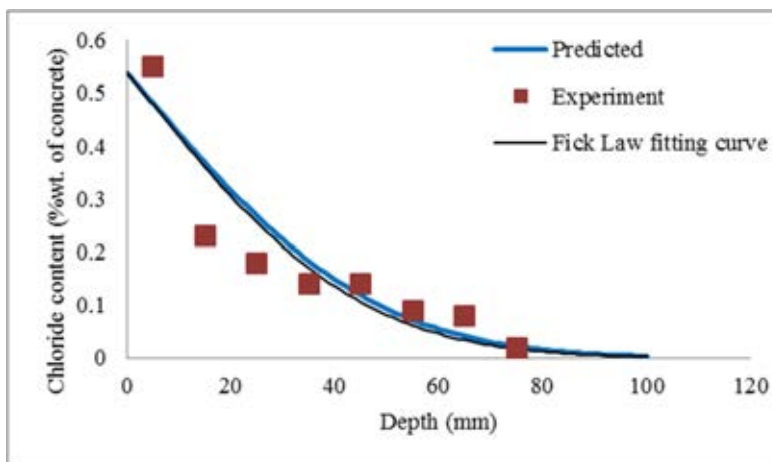**Figure 5.47. Comparision between predicted and experimental results (Beam series 3, crack 1)**

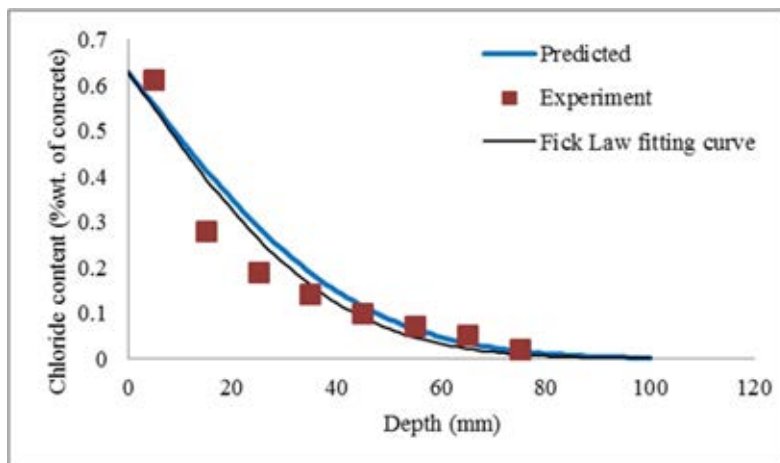- 16 weeks immersed in salt solution

Figure 5.48. Comparision between predicted and experimental results (Beam series 2, crack 1)

Figure 5.49. Comparision between predicted and experimental results (Beam series 2, crack 2)
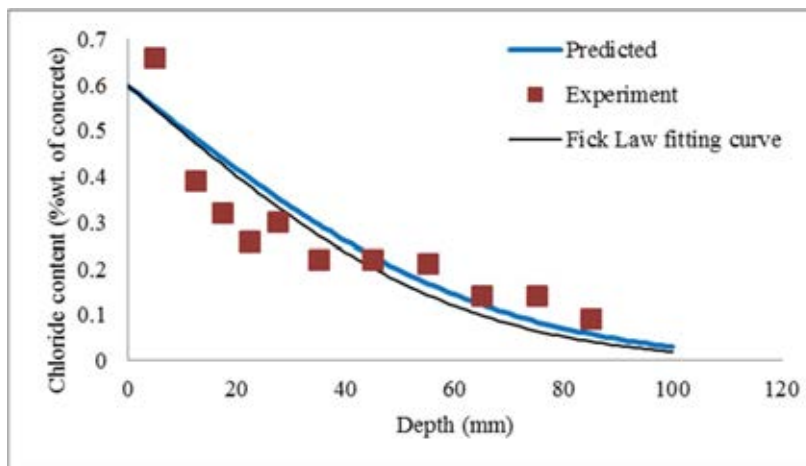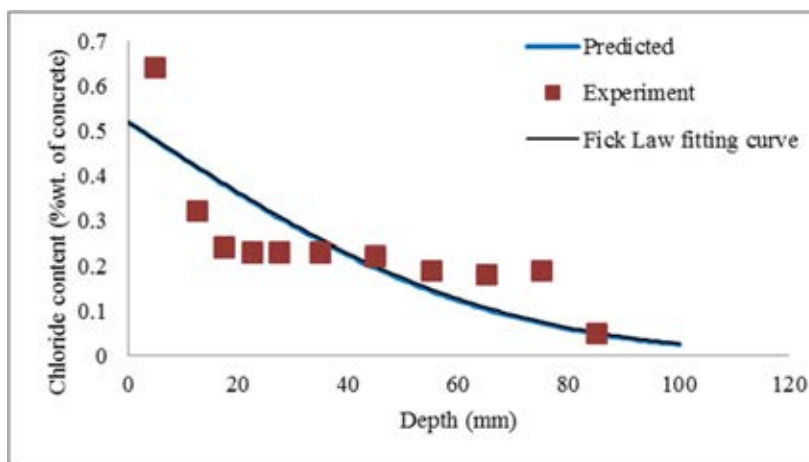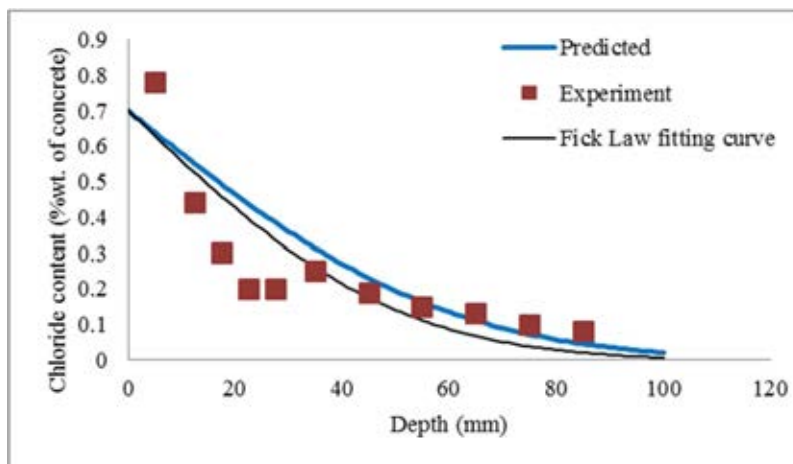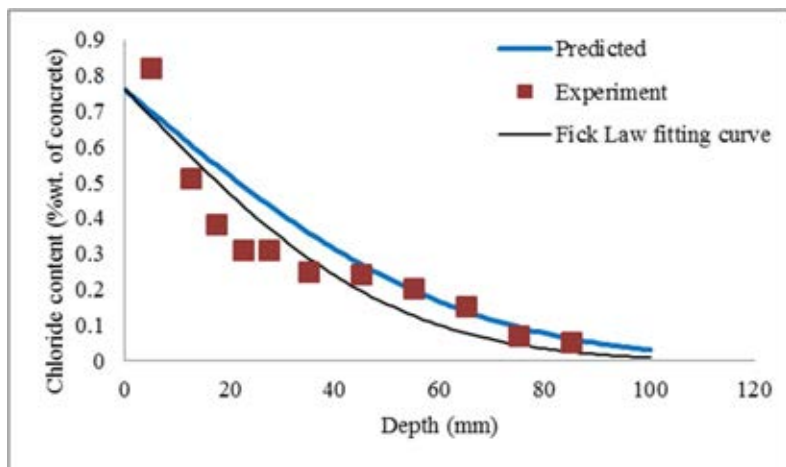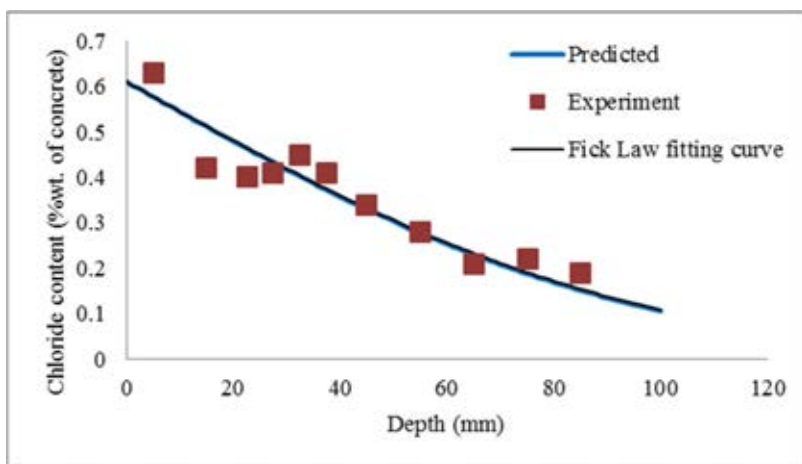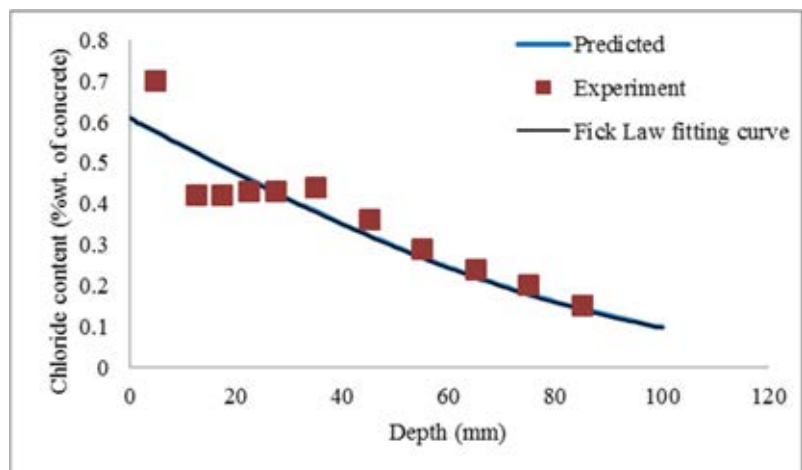
The 1D model used the surface chloride concentration at crack location and average chloride diffusion coefficient (D_{av}) to estimate the chloride content at crack location. The results of 1D diffusivity chloride model fitted very well with the experimental results, except the samples immerged in salt solution during 2 weeks.

In theory, a chloride diffusion mechanism takes place when there is a concentration gradient of chloride ions. Typically, the concentration of chloride ions in the environment is higher than the concentration of these ions in the concrete pores. In current research, the chloride penetration into cracked concrete is assumed to be governed by only diffusion process. While in fact, the chloride penetration into concrete might be governed by several combined mechanisms due to a involvedly complex interaction of physical and chemical processes. For instance, in current research, there are two chloride transport mechanisms into cracked concrete, capillary suction and diffusion. However, in current experiment, it is assumed that the diffusion is the primary transport mechanism of the chloride into concrete. Because it is accepted in many conditions, the trend of the observed chloride profile curve can be fitted by using diffusion theory. Moreover, Polder (Polder, 1996) justified this assumption for the following reasons: the capillary suction is only significant for concrete with low cover depths and the capillary suction occurs only during the early ages of concrete exposure. This is able to explain for the case of 2-week immersion of current research. In this case, the predicted results are not fitted with the experimental results. An explanation is proposed that the experimental results for chloride penetration are governed by the mechanism of movement of bulk chloride solution due to capillary suction, which primarily controls the chloride transport thought the whole crack at the initial ages of immersion. Then, the mechanism of chloride diffusion would be taken as following Fick's Second Law. Inversely, the predicted results are obtained by derivation of Fick's second Law equation, which is applied for only diffusion mechanism. However, as a sufficient long age of immersion, in case of immersion periods larger than 4 weeks, only diffusion mechanism still controls the chloride penetration into concrete. That is why there is a good agreement between the experimental results and predicted results.

5.3.2   Two dimensional chloride ingress in cracked concrete

It is very difficult to validate the two dimensional diffusivity of chloride by the complication of preparing and comparing with the experimental results. Furthermore, because the distributions of chloride concentration around the crack are extremely complicate and difficult to evaluate, these are a lack for finding a method to determine the chloride concentration around the crack plane. In this research, two experiment programs are proposed for determination of chloride concentration distribution. These experimental results will be used to compare with the predicted results for validating the proposed model. In first experiment program, the concrete powder samples will be collected by drilling hole at interval depth near crack plane. Then, these concrete powder samples will be analyzed to determine the chloride content by conventional chemical analysis method. Second experiment program is using the electron probe microanalysis (EPMA) to plot

the image map of chloride concentration corresponding with a colorimetric. This experiment applies for concrete area around the crack plane where the concrete powder samples could not collect to analyze by chemical method.

5.3.2.1   Validation program by chemical analysis method

The concrete powder samples were collected at locations near crack plane of crack beam. On each cracked reinforced concrete beam (Table 4.2), drilling two holes have the different distances from the crack plane as figures below. The diameter of the hole was 25 mm. The interval depth for collecting the concrete powder was 10 mm. The minimum weight of each sample of concrete powder was 10 g. Then, the conventional chemical analysis method (ASTM-C1152, 1997) was employed to find out the total chloride content at interval depth in each concrete samples.
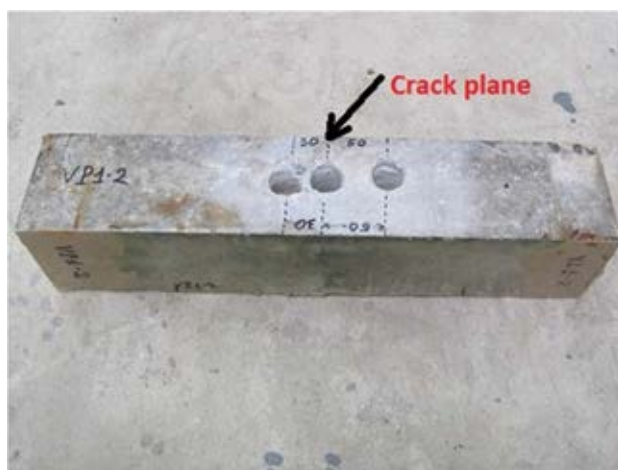
Figure 5.50. Beam 3 - The chloride profile locations at 30mm and 50 mm away from crack plane.
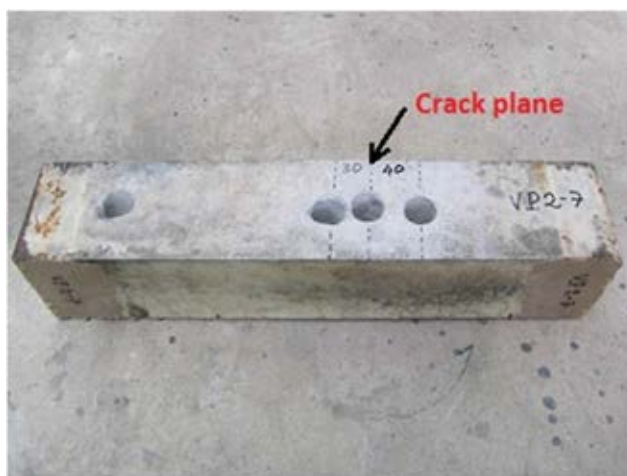
Figure 5.51. Beam 4 - The chloride profile locations at 30 mm and 40 mm away from crack plane
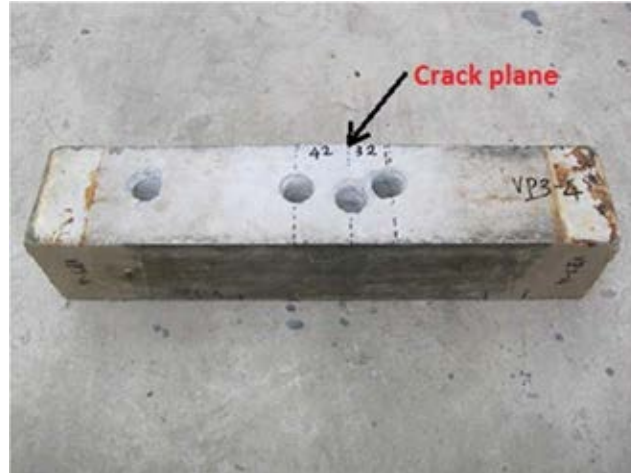
Figure 5.52. Beam 5 - The chloride profile locations at 32 mm and 42 mm away from crack plane
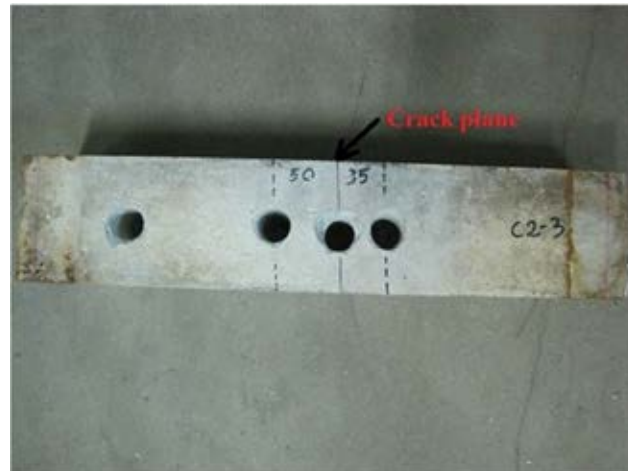
Figure 5.53. Beam 9 - The chloride profile locations at 35 mm and 50 mm from crack plane

The predicted results of total chloride content were extracted from model of ANSYS program. The advantage of ANSYS program is able to plot the magnitude of chloride content of computation model at any wanted locations. Then, these predicted results are compared with the experimental results of concrete powder samples near the crack plane. They are expressed in figures below:
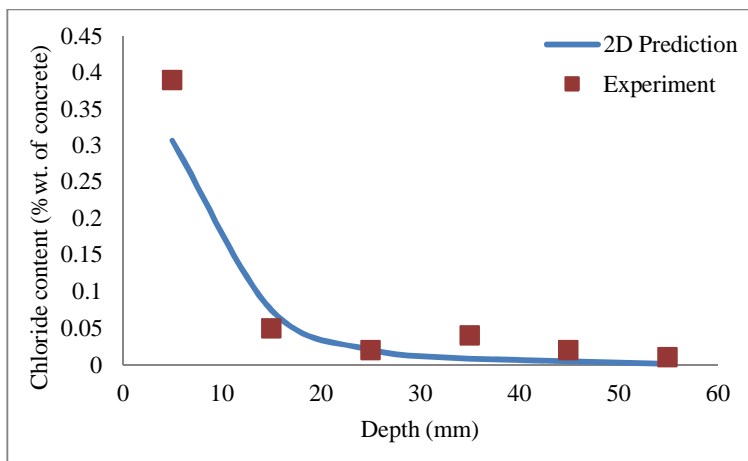
Figure 5.54. Beam 1 - The comparison of predicted and experimental results at 30mm away from crack plane
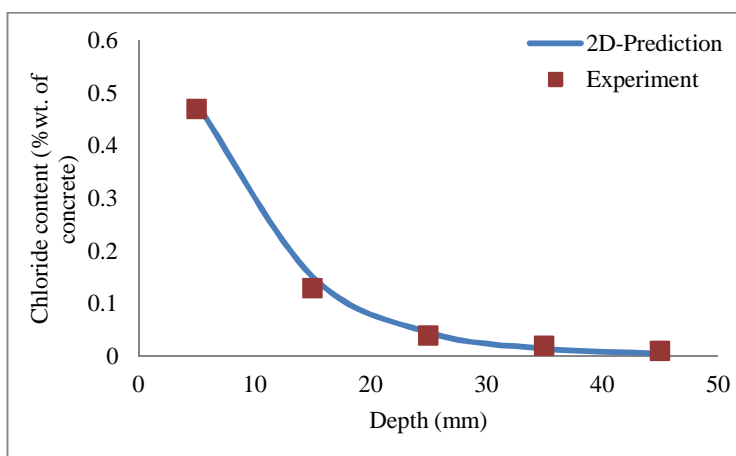
Figure 5.55. Beam 2 - The comparison of predicted and experimental results at 41mm away from crack plane
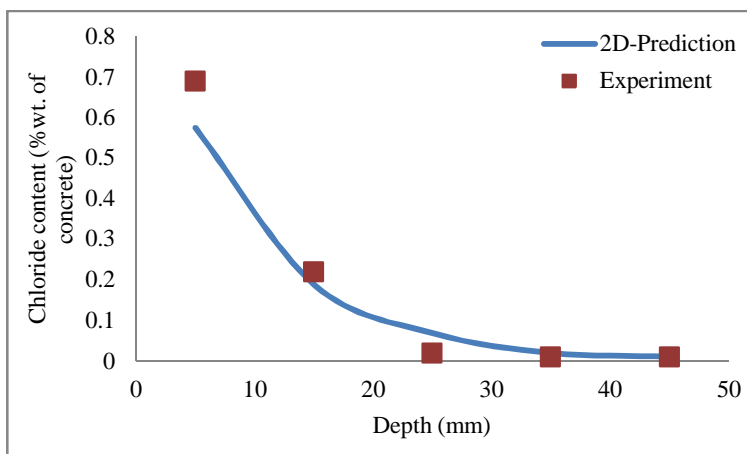
Figure 5.56. Beam 3 - The comparison of predicted and experimental results at 30mm away from crack plane

Figure 5.57. Beam 3 - The comparison of predicted and experimental results at 50mm away from crack plane
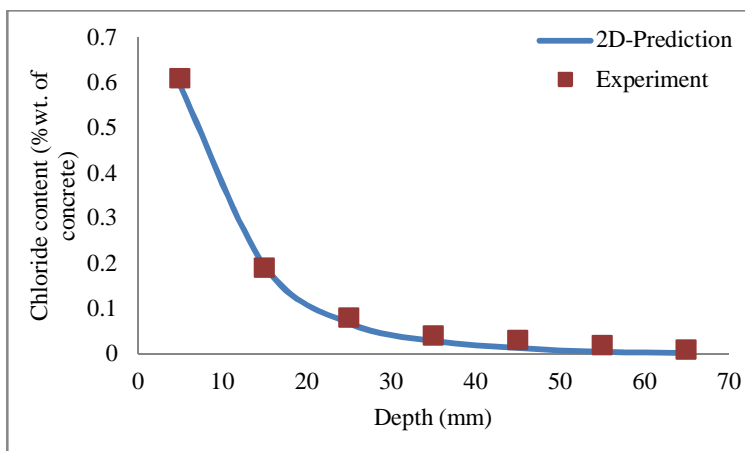
Figure 5.58. Beam 4 - The comparison of predicted and experimental results at 30mm away from crack plane
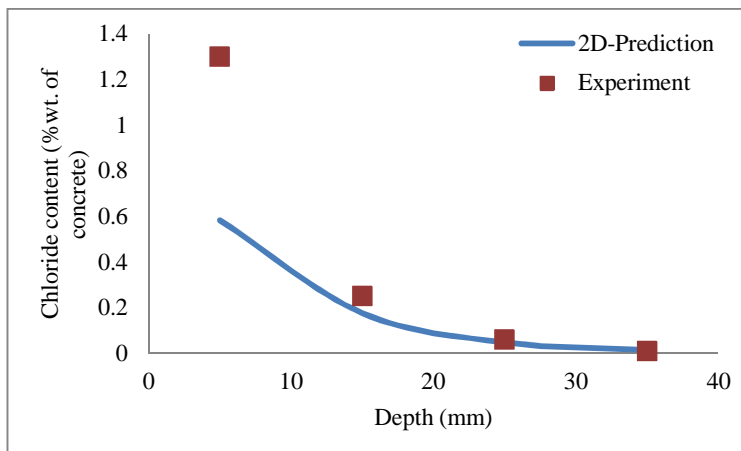
Figure 5.59. Beam 4 - The comparison of predicted and experimental results at 40mm away from crack plane
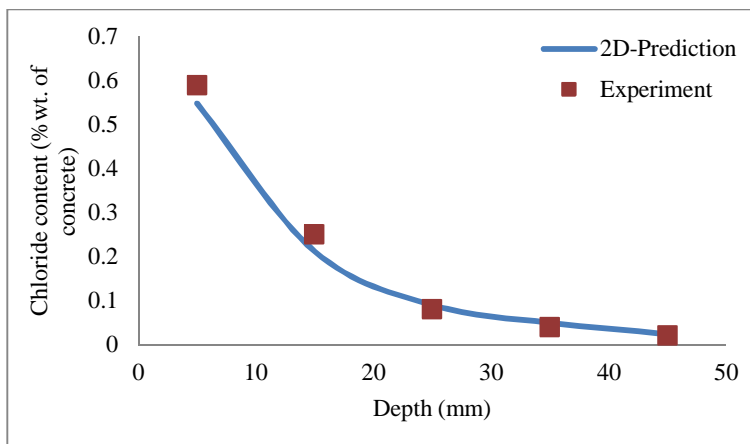
Figure 5.60. Beam 5 - The comparison of predicted and experimental results at 32mm away from crack plane
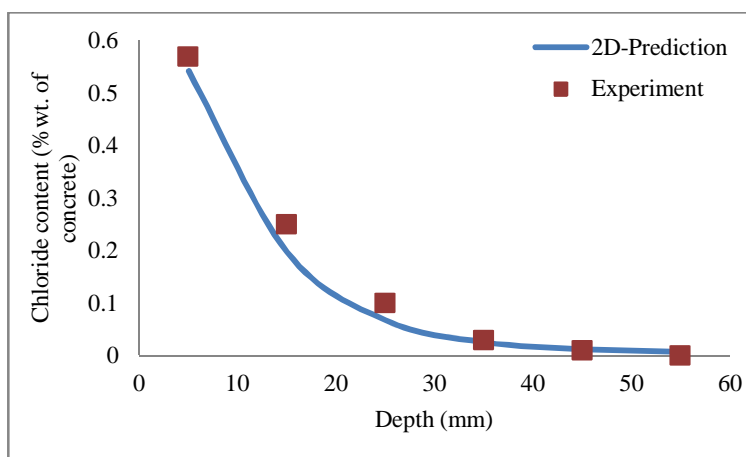
Figure 5.61. Beam 5 - The comparison of predicted and experimental results at 42mm away from crack plane
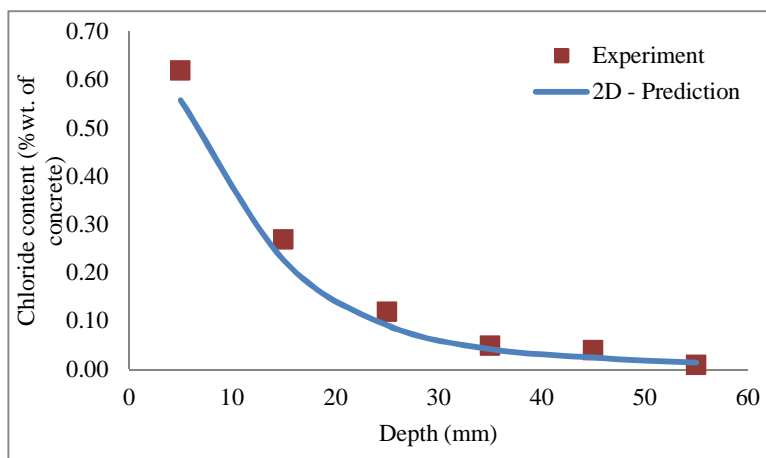
Figure 5.62. Beam 9 - The comparison of predicted and experimental results at 35mm away from crack plane

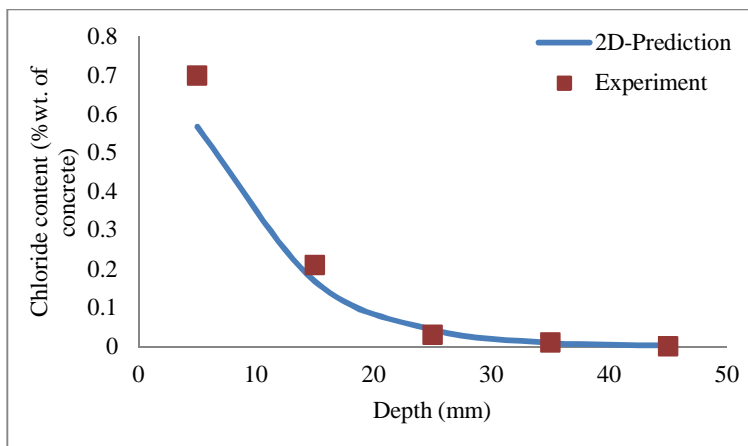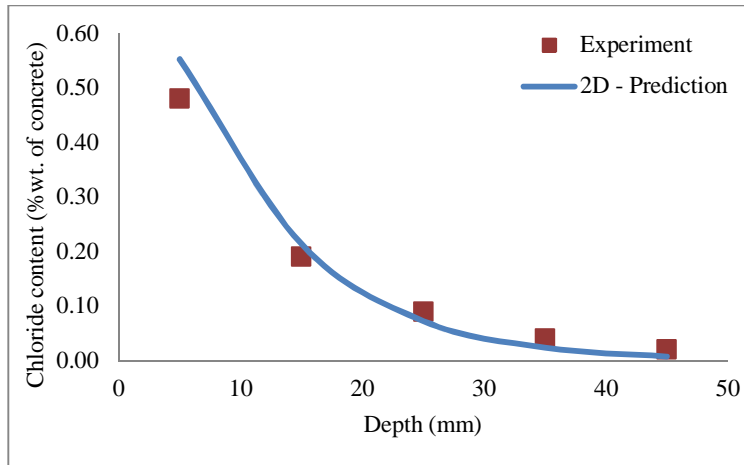**Figure 5.63. Beam 9 - The comparison of predicted and experimental results at 50mm away from crack plane**

By applying the proposed 2D chloride diffusivity model, presented in Chapter 3, with using the surface chloride content (Cs) of experiment results at the uncrack location, chloride diffusion coefficient of uncrack concrete and the crack characteristics, the distribution of chloride content near the crack plane of reinforced concrete can be predicted. Regarding figures above, it can be recognized that both the experiment results and predicted ones show the chloride content corresponding to the depth of concrete were reducing from exposed surface to inner concrete. In addition, the experiment results and predicted results of chloride content fit well for almost cases. Their deviations are accepted although the errors could be obtained by the influence of crack tortuosity. From the verify program and comparison with the experiment results, the reliability of the proposed model could be accepted because of the tortuosity, unity, straight of crack plane that can influence on accuracy of the experimental results at compared locations.

5.3.2.2   Validation program by EPMA test

The specimens after prepared following the procedure in part 5.1.3 are shown in Figure 5.64. There are totally three specimens for EPMA analysis: one specimen (W/C = 0.5) for 2D chloride diffusivity and two specimens (W/C = 0.4 and 0.6) for only chloride diffusivity perpendicular to crack plane. The specifications of specimens were shown in (Table 4.2).

(a) W/C = 0.4   (b) W/C = 0.5   (c) W/C = 0.6
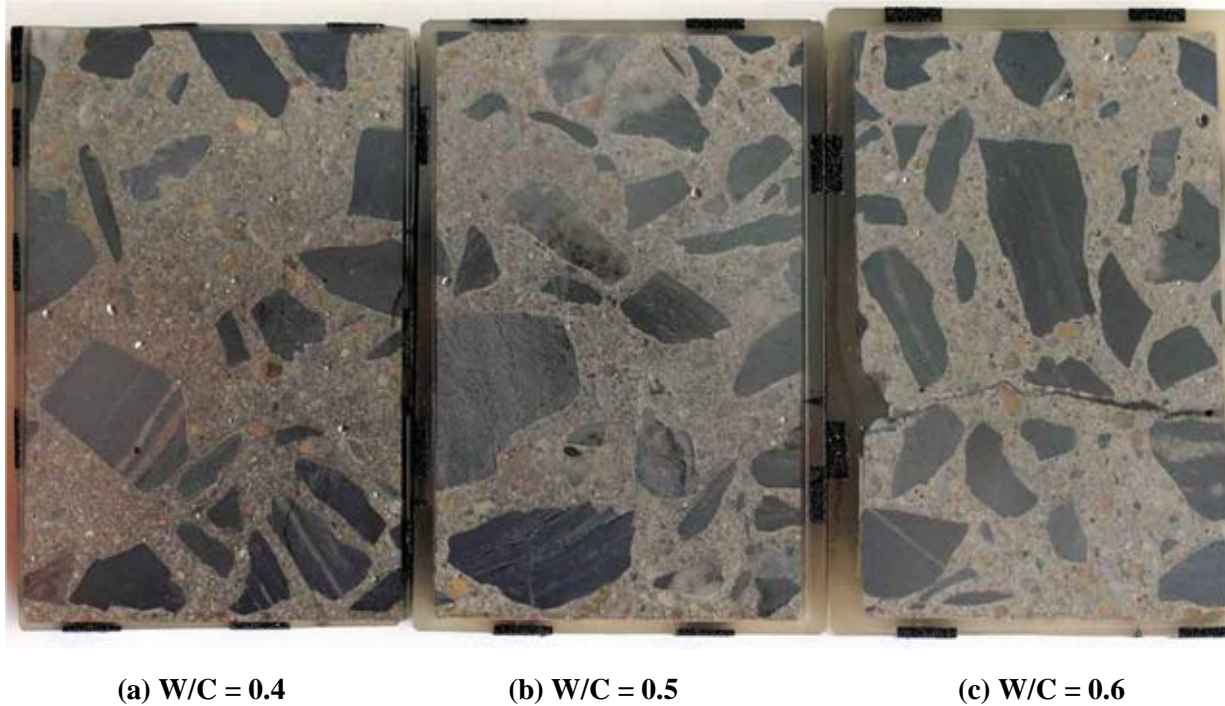
Figure 5.64 Slice specimens of cracked concrete for EPMA

a. 2D chloride diffusivity

The element distribution measurement results by EPMA test of beam no.7 in Table 4.2 are plotted in Figure 5.65. The chloride concentration distributes densely at the exposed surface and around crack plane. It indicates that chloride ions penetrated into inner concrete matrix following 2D diffusivity, one from exposed surface and another one from crack plane. Moreover, the quantification of chloride concentration also reduces from exposed surface to inner concrete; this trend is also similar from crack plane. Combine with the picture in Figure 5.65 captured by the EPMA, the results also indicate the chloride ions only penetrate in the paste part, the chloride ions do not seem to penetrate into coarse aggregate. Figure 5.66, called back from Chapter 4, shows the predicted results of chloride concentration distribution for beam no. 7 with a marked area corresponding to the experimental area conducted by EPMA.

Figure 5.65. The EPMA results of characteristic X-ray strength of beam no. 7.

Figure 5.66. The predicted results of chloride concentration distribution of beam no. 7

A comparison of color element distribution between predicted results and experimental ones (EPMA) of cracked beam no. 7 is shown in Figure 5.67. This figure shows that the change of visual color metric in the elements seem similar between predicted results and experimental ones

when try to ignore the color map of coarse aggregate. It seem that there is the less chloride concentration distributed at the crack plane where crack width was larger than 60 µm. In the literature reviews and proposed model, this area was proposed as the exposed environment. Because there were two values for the upper critical crack width of 60 µm or 80 µm, the value of 60 µm was chosen for current proposed model. Therefore, it is necessary to verify again the assumption of upper critical crack width by comparison for total chloride content in this area.

Figure 5.67. The comparison of color element distribution between predicted results and experimental results of cracked beam no. 7

    b. Chloride diffusion following only perpendicular to crack plane

Regarding Win's research (Win et al., 2004) with EPMA test, the chloride concentration depth, which is perpendicular to the crack plane, is similar to that from exposed surface. The current research results will be similar to Win's research results, if the areas corresponding to crack width is larger than 60 µm; because in this area, the environment could be considered exposed environment (Wang and Ueda, 2010). To clarify this assumption, a proposed experiment program by EPMA will be performed to determine only the chloride concentration at interval depth following direction perpendicular to crack plane. The specimen was prepared following Figure 4.19 and Figure 5.7(b). In these specimens, chloride will only penetrate into inner concrete through crack plane. The EPMA analysis will be employed to measure the chloride concentration profile which was varied from the crack plane to inner concrete.

- Beam no. 6

The element distribution measurement results by EPMA test of beam no.6 (Table 4.2) are plotted in Figure 5.68. Contrary to the experimental result of 2D chloride diffusivity, this experimental

result clearly indicates chloride ions only penetrate into inner concrete matrix via crack plane. Because the tension surface was coated by epoxy sealant, it is prevented and blocked the chloride penetration into inner concrete through tension surface. The quantification of chloride concentration is much more at crack plane and reduces from crack plane to inner concrete. The predicted results of chloride concentration distribution for beam no. 6 with a marked area corresponding to the area of experimental result conducted by EPMA is shown in Figure 5.69.
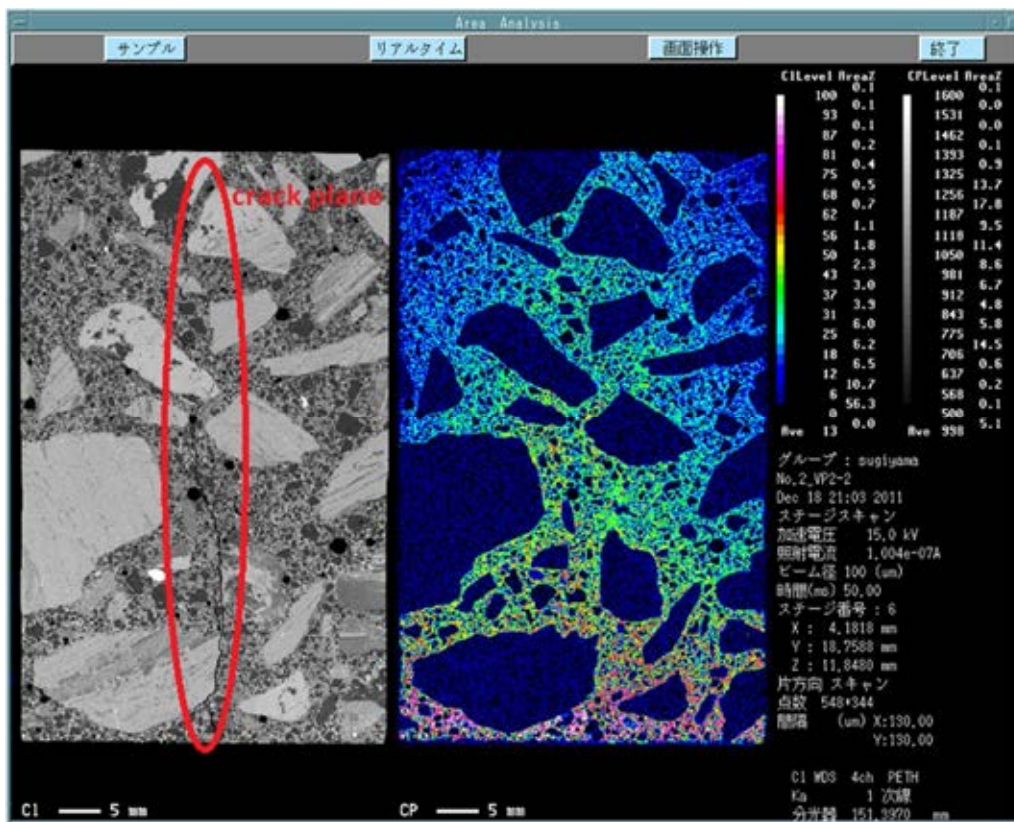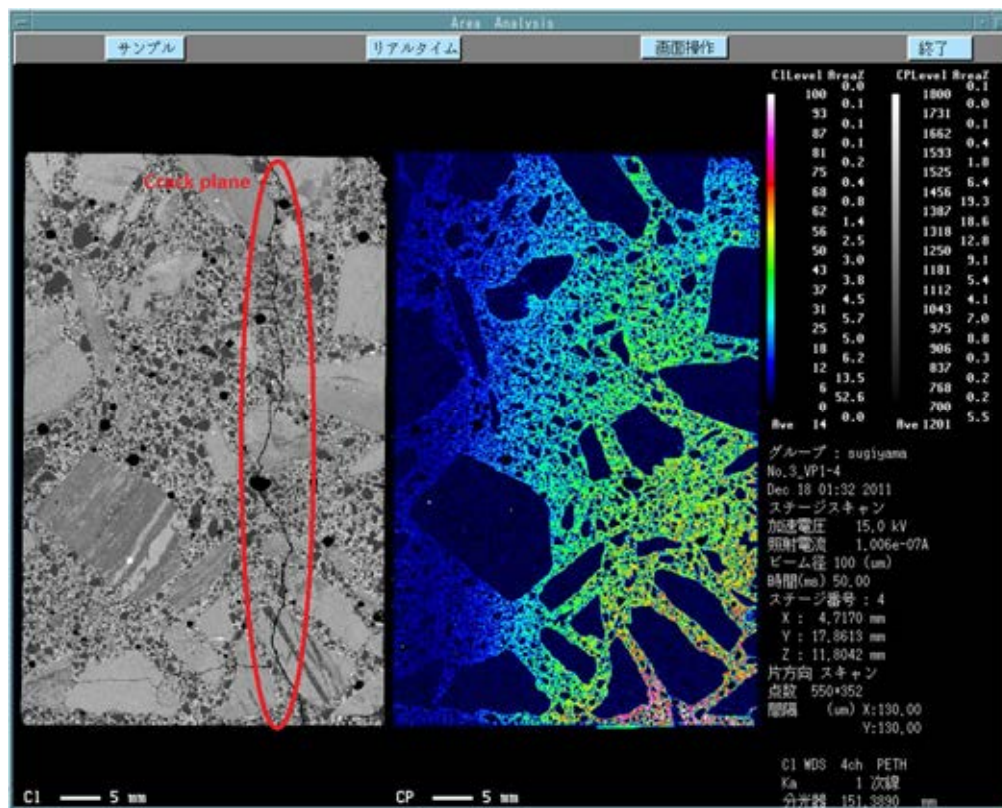

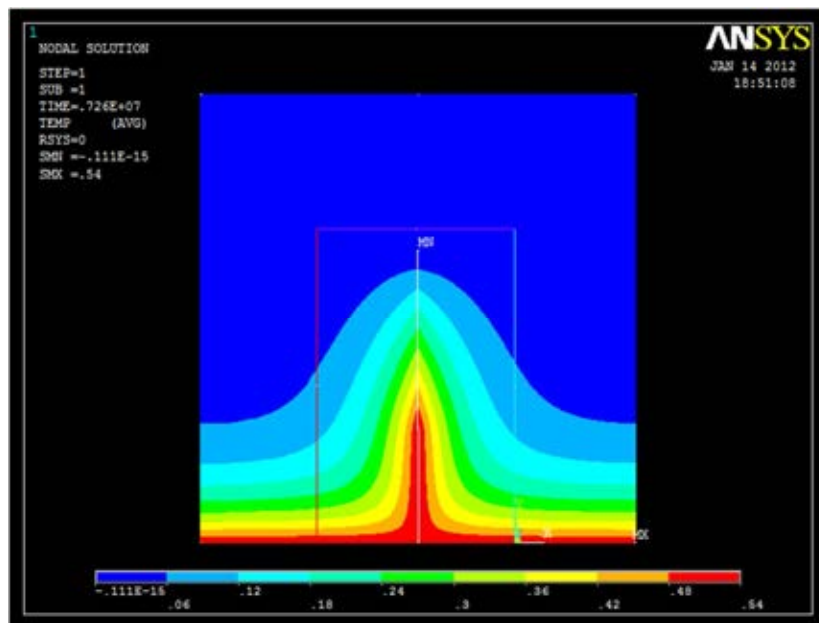**Figure 5.68. The EPMA results of characteristic X-ray strength of beam no. 6.**
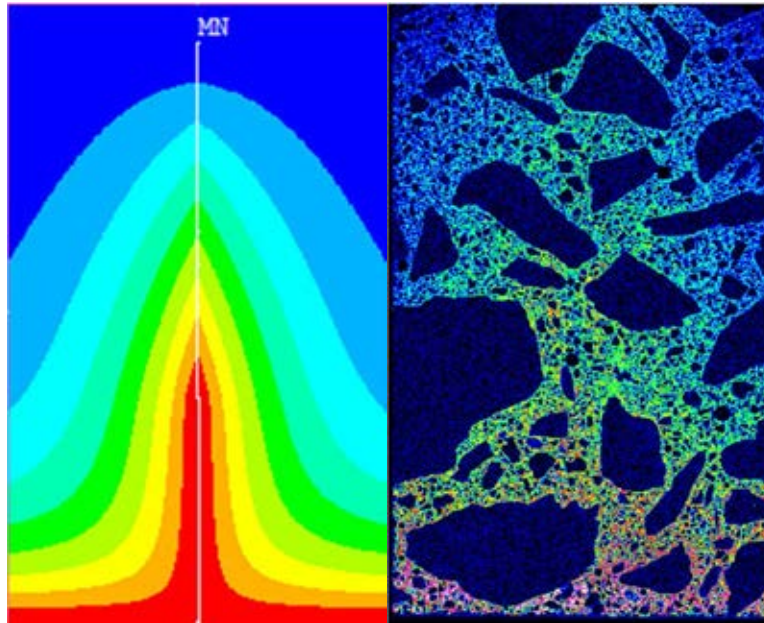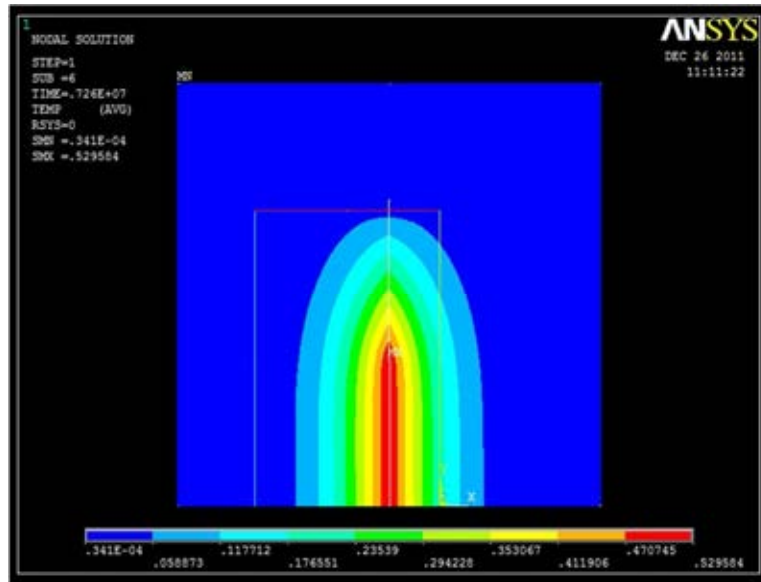
Figure 5.69. The predicted results of chloride concentration distribution of beam no. 6

A comparison of color element distribution between predicted results and experimental results (EPMA) of cracked beam no. 6 is shown in Figure 5.70. Regarding this comparison, it seems that the distribution shapes of visual color elements between predicted results and experimental results are similar, especially, when the distribution of coarse aggregate is ignored. Similar to beam no.7, It also seem that there is the less chloride concentration distributed at the crack plane where crack width was larger than 60 μm. Therefore, it is necessary to further verify the assumptions by comparison for total chloride content at this area.
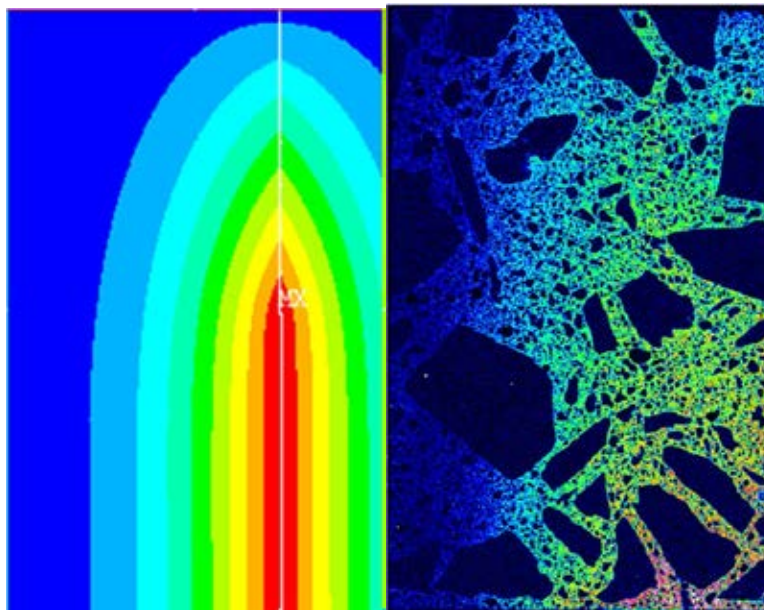
Figure 5.70. Comparison of color element distribution between predicted results and experimental results of cracked beam no. 6

- Beam no. 8:

The element distribution measurement results by EPMA test of beam no.8 (Table 4.2) are plotted in Figure 5.71. Similar to the crack beam no. 6, beam no.7 conducted with only one-dimensional chloride diffusivity perpendicular to crack plane that experimental result indicates clearly about that. In this specimen, by microscope to observe the shape of crack plane, it is clearly that the crack direction is not straight and vey tortuous. In this specimen, there is an unexpected vertical crack occurring due to the broken specimen caused by the sawing of preparation work. However, it just lost the chloride concentration in this unexpected crack and does not effect on that in the inner concrete. The predicted results of chloride concentration distribution for beam no. 8 with a marked area corresponding to the area of experimental result conducted by EPMA is shown in Figure 5.72.
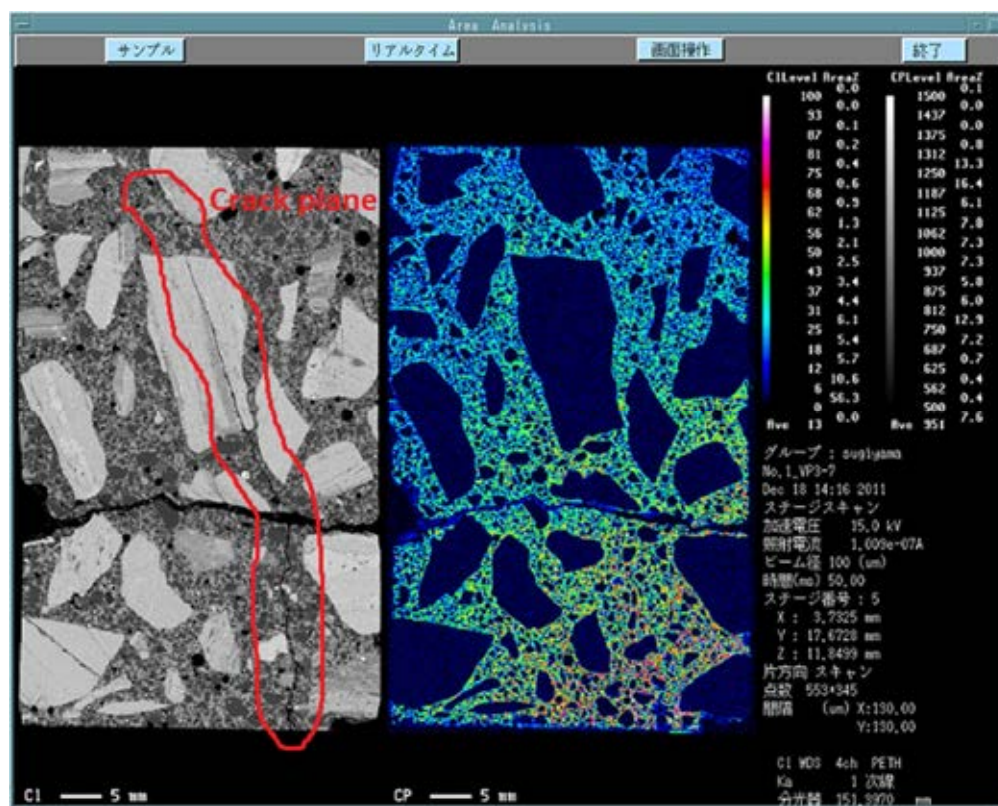
Figure 5.71. The EPMA results of characteristic X-ray strength of beam no. 8.
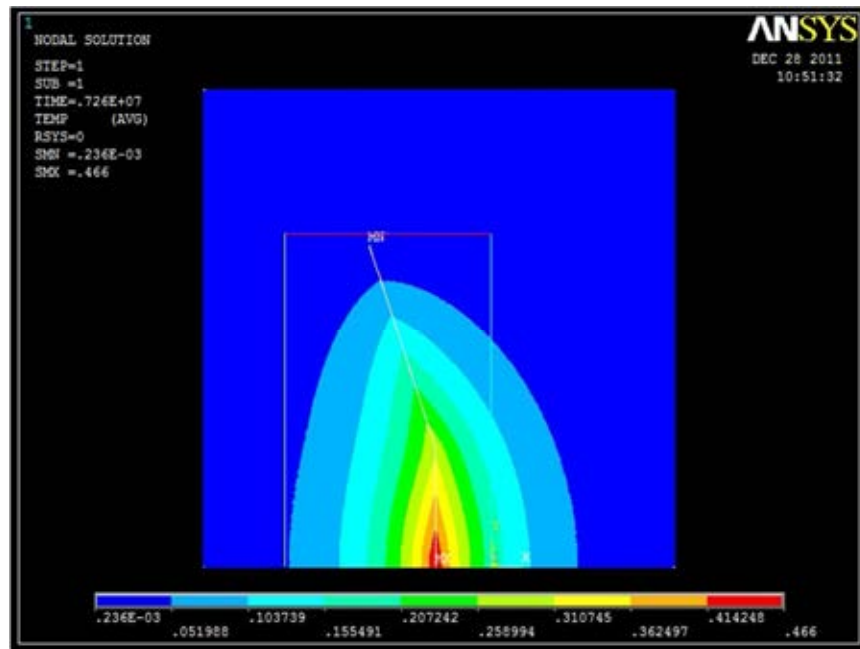
Figure 5.72. The predicted results of chloride concentration distribution of beam no. 8

A comparison of color element distribution between predicted results and experimental ones (EPMA) of cracked beam no. 8 is shown in Figure 5.73. The distribution shapes of visual color elements between predicted and experimental results are similar, even though in areas where the direction of crack plane changed. The distribution of color elements at crack plane in experimental results also fit with the predicted results.
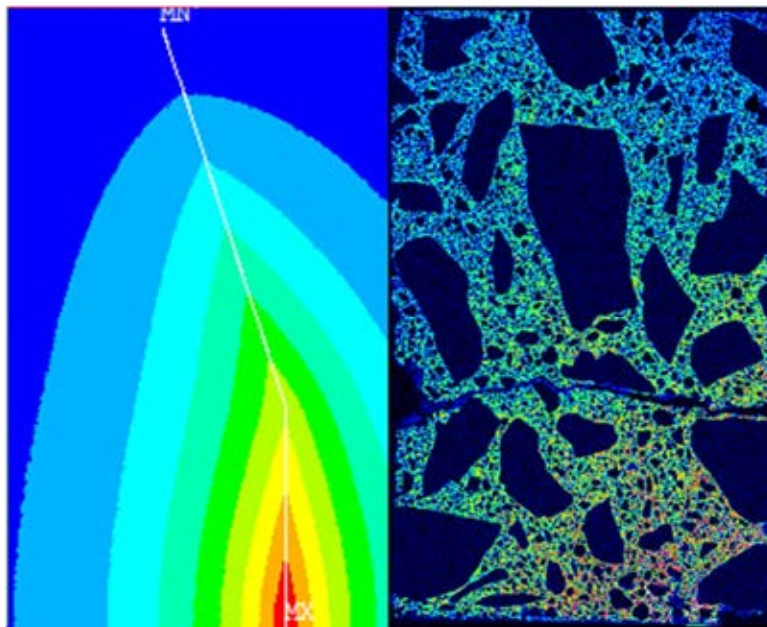
Figure 5.73. Comparison of color element distribution between predicted results and experimental results of cracked beam no. 8.

Through all EPMA image results, it is evident to recognize that the presence of coarse aggregates in matrix of cement pastes block the chloride penetration, increased the tortuosity of this matrix and decreased the chloride content locally (Delagrave, Bigas, Ollivier et al., 1997; Wall and Nilsson, 2008). However, it seems that there is more concentration of chloride ions around the edge of coarse aggregates. It can be an effect of the presence of numerous ITZ, which tends to facilitate the movement of chloride ions (Caré, 2003).

c. Verification of model by chloride profile calculated by EPMA

Mori (Mori et al., 2006) studied on the chloride penetration into cracked concrete by EPMA. In their research, the materials used was normal concrete and testing conditions were acceleration voltage of 15kV, beam current of 100 nA, pixel size of 100 μm, probe diameter of 50 μm. The relationship between total chloride concentration and X-ray intensity was conducted by Mori, Figure 5.74, and expressed as an equation below:

$$y = 65.48x + 4.78$$

(5.10)

where x is the concentration of chloride ions (mass %); y is the X-ray intensity; constant of 4.78 is the intensity of background for Mori's experiment.
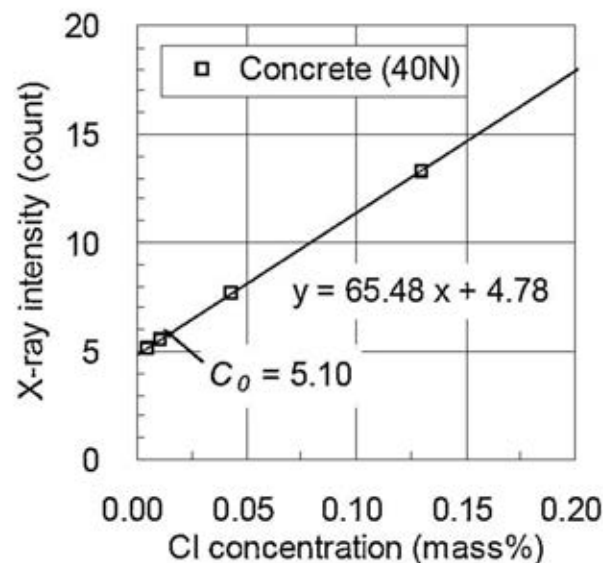
Figure 5.74. The correlation between chloride concentration and X-ray intensity for normal concrete (Mori et al., 2006).

To increase the accuracy of model, the self-conducted experiment results were added to the account of the relationship between X-ray intensity and chloride concentration proposed by Mori (Mori et al., 2006), Figure 5.74. It is plotted in Figure 5.75.
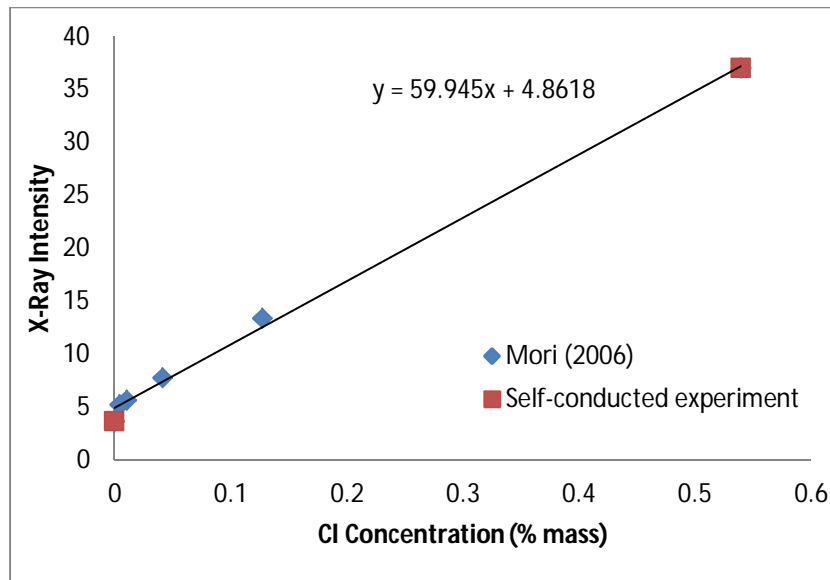
Figure 5.75. The correlation between chloride concentration and X-ray intensity for normal concrete.

However, in current research, the intensity of background found by experiment was 3.6, so the relationship between X-ray intensity and chloride concentration was rewritten as follow:

$$y = 60x + 3.6 \qquad (5.11)$$

where x is the concentration of chloride ions (mass %); y is the X-ray intensity; 3.6 is the intensity of background for only current experiment.

Generally, after the EPMA analysis, the characteristic X-ray strength of each atom is plotted as the color image map. By using the equation (5.11), the total chloride concentration will be converted from the characteristic X-ray intensity of EPMA.

To further validate the proposed model for 2D chloride diffusivity into cracked reinforced concrete, a comparison between predicted results and experimental ones of chloride content will be performed by EPMA. The chloride profile along a randomly chosen line converted from EPMA will be compare with the predicted results of chloride profile extracted from ANSY program. In each specimen, there are two lines, which are randomly chosen, presented in Figure 5.76, Figure 5.79 and Figure 5.82 for beam 6, 7, and 8, respectively. The comparisons for chloride profile of experimental results and predicted ones are shown in Figure 5.77 and Figure 5.78 (for beam 6); Figure 5.80 and Figure 5.81 (for beam 7); Figure 5.83 and Figure 5.84 (for beam 8).

Figure 5.76. The locations of line 1 and 2 for extracting chloride profile of beam no. 6

Figure 5.77. Comparison of the chloride profile (Line 1) between predicted and experimental results of cracked beam no. 6.
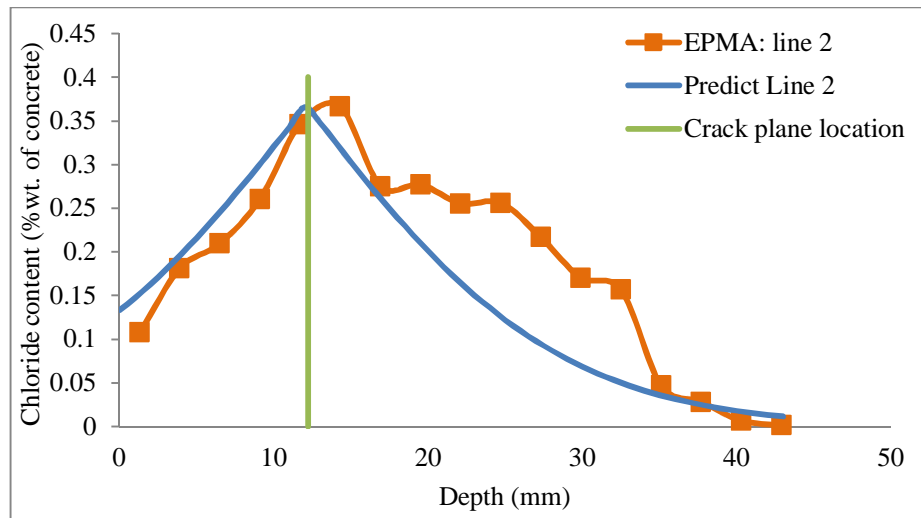
Figure 5.78. Comparison of the chloride profile (Line 2) between predicted and experimental results of cracked beam no. 6.
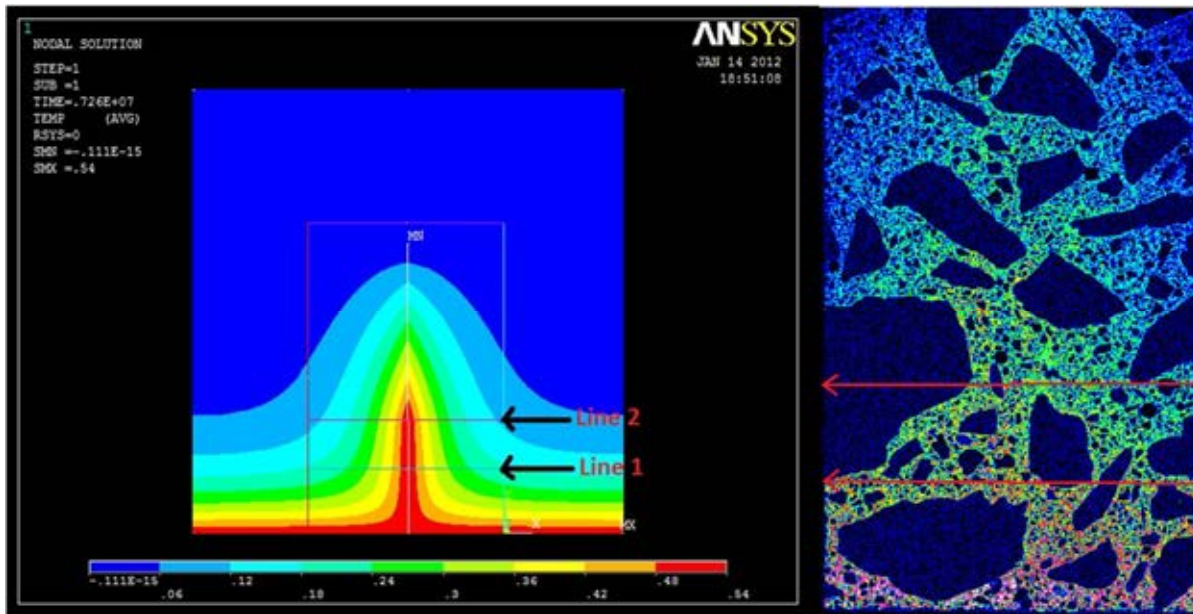
Figure 5.79. The locations of line 1 and 2 for extracting chloride profile of beam no. 7
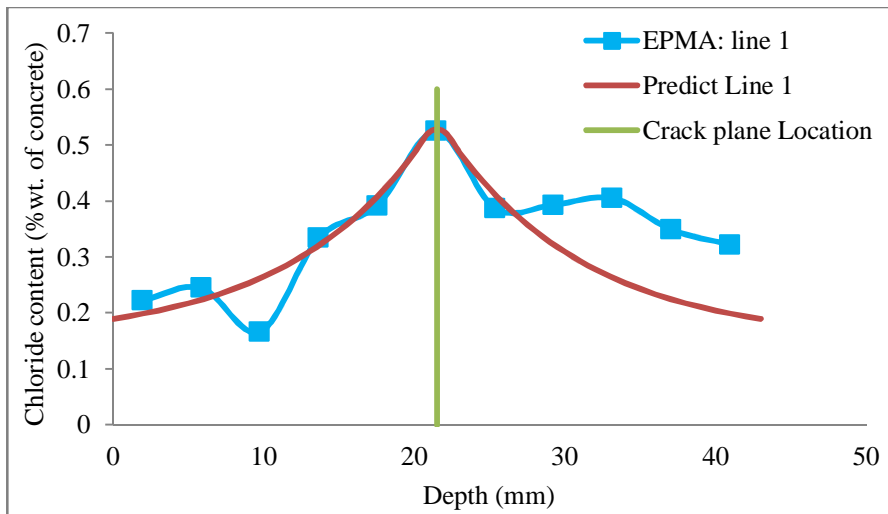
Figure 5.80. Comparison of the chloride profile (Line 1) between predicted and experimental results of cracked beam no. 7.
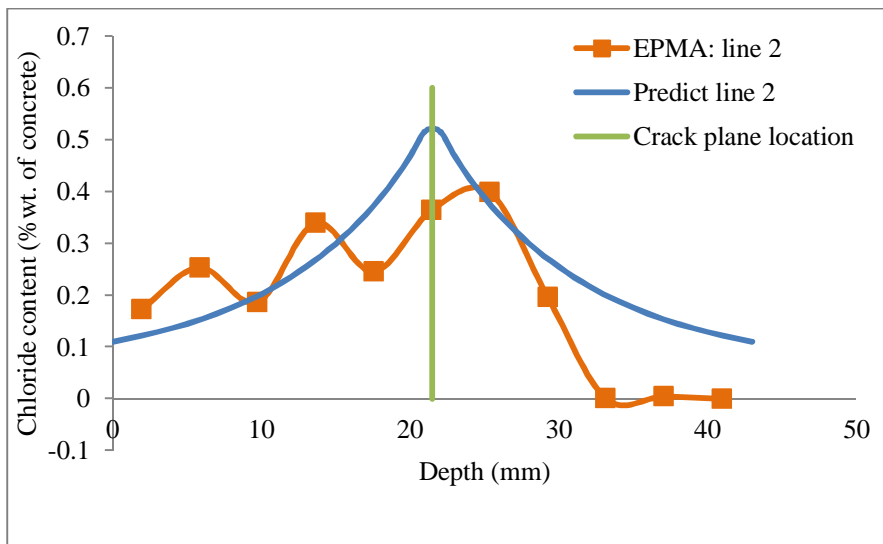
Figure 5.81. Comparison of the chloride profile (Line 2) between predicted and experimental results of cracked beam no. 7.

.
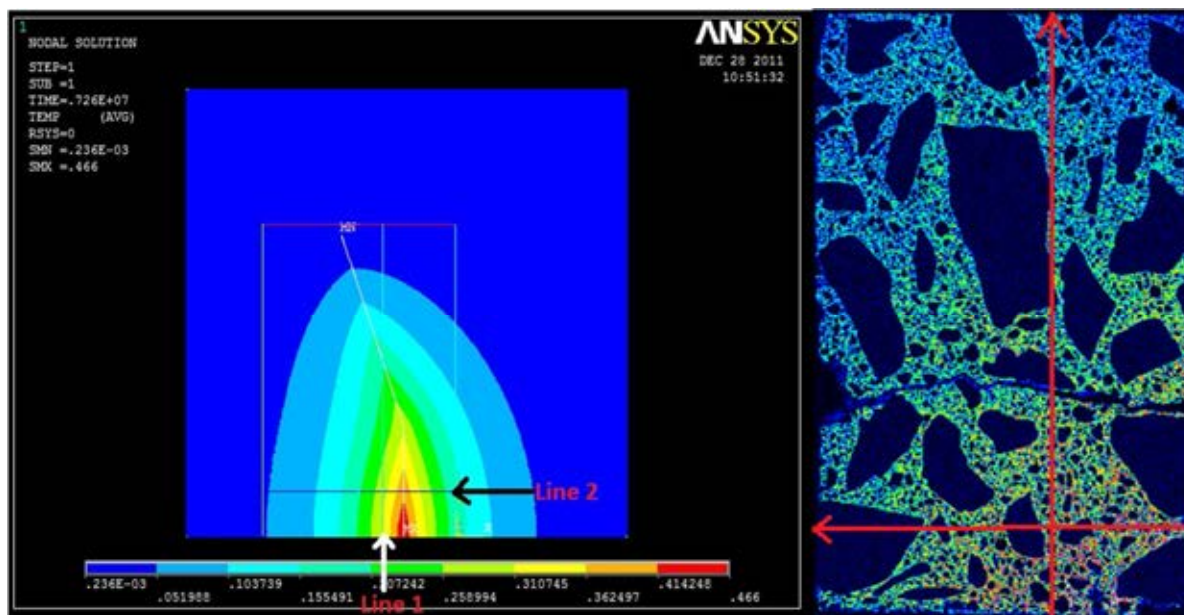
Figure 5.82. The locations of line 1 and 2 for extracting chloride profile of beam no. 8
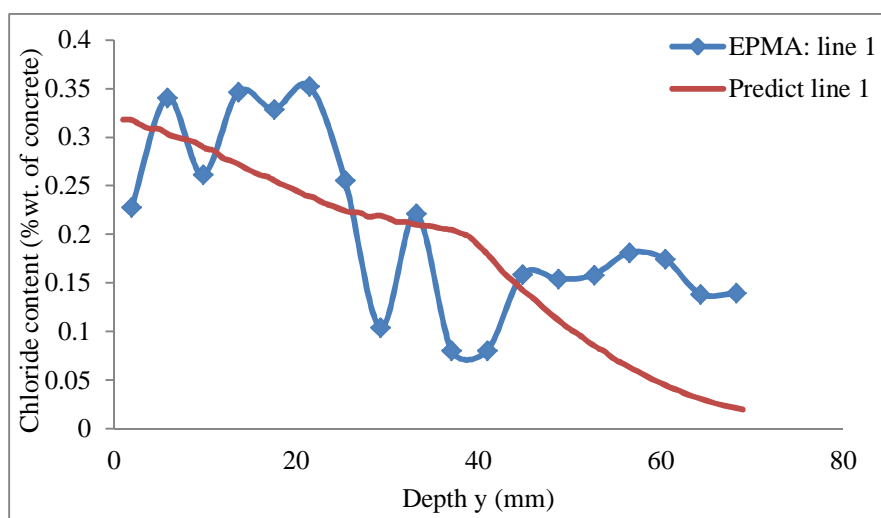
Figure 5.83. Comparison of the chloride profile (line 1) between predicted and experimental results of cracked beam no. 8.
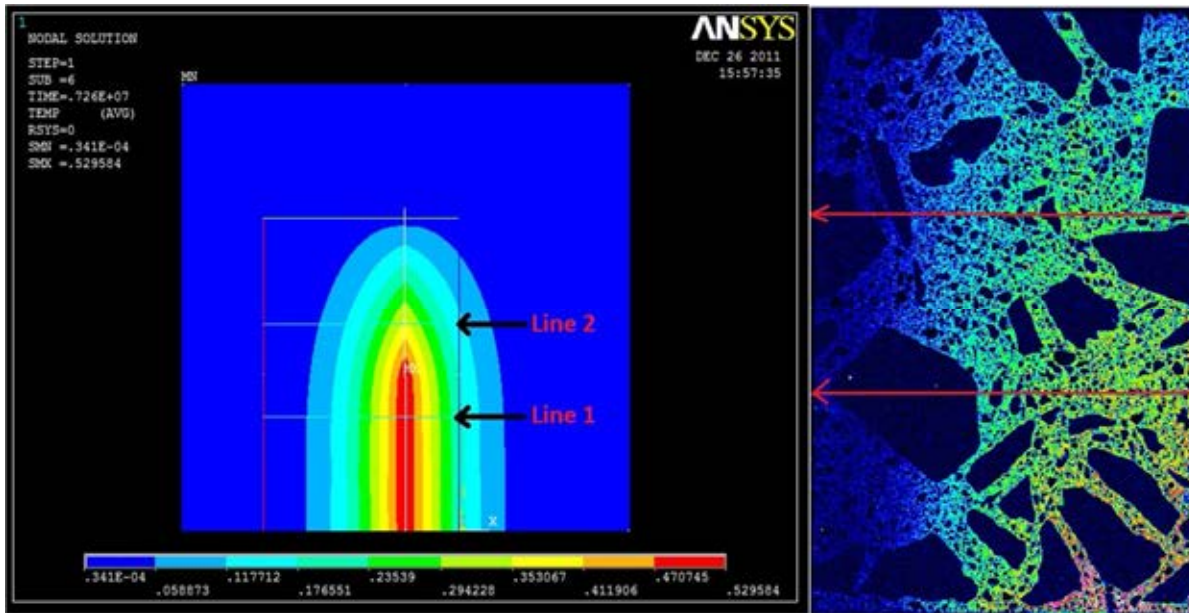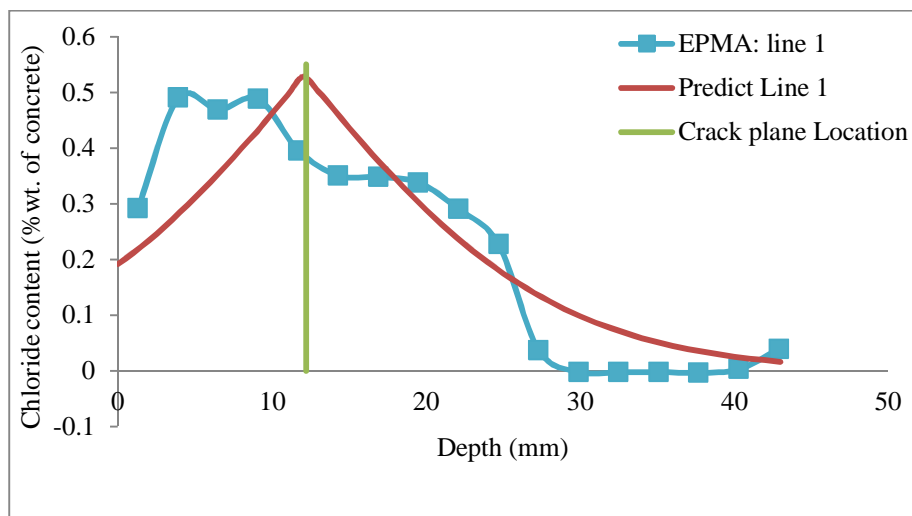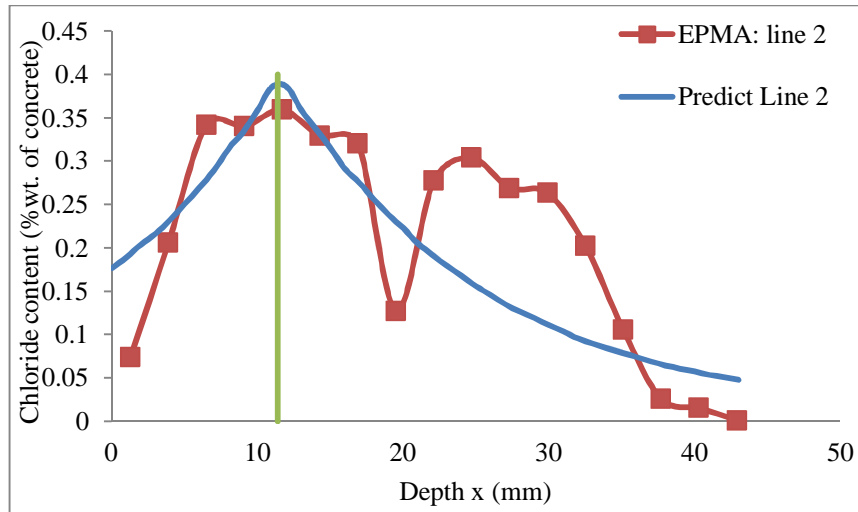
Figure 5.84. Comparison of the chloride profile (line 2) between predicted and experimental results of cracked beam no. 8.

From these figures, all most cases show the fitting between experimental results and predicted ones. The experiment results of X-ray intensity were calculated by average of X-ray intensity of points inside the area of blocks along the chosen lines. However, they showed that the average X-ray intensitys are quite lacking in convergence. The reason is the calculated width of blocks along these lines is short. In addition, it is impossible for increasing the width of these blocks to larger because the results would be changed and it would not represent for the locations of these lines. It is evident to recognize that the experimental result of chloride profile of lines decrease at the coarse aggregate where the chloride content is zero.

Comparing to the verification program conducted by the conventional chemical analysis method (part 5.3.2.1), that fit very well with predicted results, the experimental program conducted by EPMA had more deviation. This is because the influence of large aggregate on the results of chloride content extracted from EPMA analyzed results (Wall and Nilsson, 2008). The chosen dimension of blocks, used to calculate average X-ray intensity of each pore, is quite smaller than that of coarse aggregate, causing in reduction of accuracy for experimental results by EPMA. Furthermore, another reason is the adverse influence of the crack tortuosity on the chloride content results. Generally, the locations of samples conducted by chemical analysis method were far away from crack plane, the holes drilled to collect concrete powder were over 30 mm away from crack plane. That why they obtained less influence of crack tortuosity. Conversely, the EPMA was employed to survey the areas in a distance of 20 mm from crack plane, so its results obtained so much more influence from crack tortuosity.

CHAPTER VI

DISCUSIONS AND CONCLUSIONS

Regarding data analysis and findings, this final chapter will discuss about research conclusion. Based on the observations and conclusions in current research, the following implication will be presented followed up by the research limitations and recommendations for further research.

6.1 Research Conclusions

The primary purpose of entire research was to determine the effects of characteristics of natural crack (V-shaped crack) on the chloride penetration into cracked reinforced concrete. From the experimental results, the research proposed an equation for calculating chloride diffusion coefficient involved with the influence of both crack width and crack depth. In addition, two models were proposed for chloride diffusion into cracked reinforced concrete under flexural loading. Both proposed model were validated by conducted experiments. The research results suggest the following conclusions:

1. This research presented the experimental studies on the natural crack characteristics that have the influences on the chloride penetration phenomenon. With varying crack characteristics, the chloride penetration depth varied directly proportional to crack width or/and crack depth. In addition to crack width influencing on the chloride penetration investigated, an important parameter of fracture of reinforced concrete structure, crack depth, was investigated on the chloride penetration into concrete structure. The initial results of research carried out the strong influence of crack depth on the rate of chloride penetration into cracked reinforced concrete. Similar to previous research, it is also concluded that the rate of chloride penetration through a crack of concrete is independent on the concrete proportions, but it is dependent on the characteristics of the crack.

2. In addition to the influence of crack width and crack depth, the results showed that the shape and trend of the crack plane are also influential in the chloride penetration. The tortuosity and constrictivity of crack are evaluated again as the characteristics of natural crack. The experimental parameter of crack tortuosity is proposed a value of 1.24 for the width of natural crack less than 225 μm that was generated by bending moment.

3. With reinforced concrete structure, the service load may not influence on the chloride penetration directly. However, the service load had a significant role for increasing the chloride penetration by its contribution on the variation of crack width and crack depth.

4. A model for the prediction of the chloride diffusion coefficient at cracked reinforced concrete beams was proposed. In this model, the chloride diffusion coefficient at crack

not only was updated from the chloride diffusion coefficient at uncrack concrete but also was described as a function of the crack width, crack depth. To verify this model, the predicted results of proposed model for chloride diffusion coefficient are compared with the experimental results of chloride diffusion coefficient conducted by long-term testing. The results of the proposed model fitted well with the experimental results. The proposed model closely described the real characteristics of natural cracks in reinforced concrete.

5. Applying the proposed model of chloride diffusion coefficient, a model for chloride diffusion at crack location of reinforced concrete under marine environment was also proposed base on the basic of Fick's Second Law. An experiment program was prepared to verify the proposed model. The predicted results of chloride profile fitted very well with the experimental results when the immersion periods were larger than 4 weeks. Because of a limitation of this model only described the chloride diffusion mechanism, contrary to initial periods of immersion where the mechanism of capillary suction strongly effect on the chloride transport. However, the effect of capillary suction mechanism will reduce at time and replace with diffusion mechanism.

6. With another view, the chloride diffusion into cracked reinforced concrete was recognized following two-dimensional (2D) diffusivity. Therefore, another model, 2D chloride diffusion into cracked reinforced concrete, was proposed and was analyzed by ANSYS program. This model assumed the crack plane acted as the second exposed surface in addition to tension surface. Two new experiments were also conducted to describe the chloride diffusion through a crack of reinforced concrete under flexural loading. In the first experiment, the chloride profiles were obtained by conventionally chemical analysis; and the analytical results of model fitted well to that results. In the second experiment, the EPMA test was employed to plot the characteristic X-ray strength of chloride concentration distribution around a crack, as a color image map. This 2D color image map was compared with the predicted result extracted from ANSYS program. The comparison result was quite well; due to the tortuosity of crack and the distribution of coarse aggregate in the experimental results, so the accuracy of this comparison result reduced.

7. In most cases, cracks are not able to reduce the load bearing capacity or cause collapse of reinforced concrete structure because of the small crack width, less than maximum threshold crack width or crack residue upon elastic stage. However, the cracks may unprofitably effect on the durability and cause the damage of reinforced concrete structure by providing the free accesses for chloride transport from marine environment.

6.2 Limitations and Directions for Future Research

1. The current study is conducted with the time restraint. Therefore, it has some limitations as proposed expressions and application of investigation in the field.

2. The current investigation was performed in the conditions of laboratory, which is quite different from the real conditions in the field, where temperature and humidity change by time. Furthermore, the concrete beams specimens used in this research are not the full-scale concrete structures, that is why it may not reflect the real behavior of concrete structure under severe environment where is combination of loading and environment.

3. In the field, the chloride diffusion coefficient will decrease with time and the concrete used for marine environment usually mix with supplementary cementitious material. The current research conducted only OPC cement, in order to increase the accuracy of proposed models; it should continuous to investigate with other mineral additive materials such as silica fume or fly ash.

4. It is suggested that further study should be made of the prediction of crack characteristics under varying loads to evaluate their influence on the durability of concrete for the development of durability design or rehabilitation methodology.

5. The service life of concrete structures is governed by many factors; however, their interactions are not well understood. In addition to the variations in material characteristics, in quality of concrete, in environment, the loading and cracking must be included as the important factors in the model of prediction for service life of reinforced concrete.

6. The benefits of research is providing the proposed models, which can be used to predict the chloride threshold induced corrosion of the reinforced concrete structure, evaluate the durability and the service life of reinforced concrete structure.

REFERENCES

ACI-211.1 (2002). Standard Practice for Selecting Proportions for Normal, Heavyweight, and Mass Concrete. , American Concrete Institute.

ACI-224-01 (2001). Control of Cracking in Concrete Structures, The American Concrete Institute.

ACI-224.1R (1998). Causes, Evaluation and Repair of Cracks in Concrete Structures, American Concrete Institute.

Aldea, C.-M., Shah, S. P. and Karr, A. Effect of Cracking on Water and Chloride Permeability of Concrete. Journal of Materials in Civil Engineering 11(3) (1999a): 181-187.

Aldea, C.-M., Shah, S. P. and Karr, A. Permeability of cracked concrete. Materials and Structures 32 (1999b): 370-376.

ASTM-C33 (1999). Standard Specification for Concrete Aggregates, American Society for Testing and Materials.

ASTM-C114 (2000). Standard Test Methods for Chemical Analysis of Hydraulic Cement, American Society for Testing and Materials.

ASTM-C1152 (1997). Standard Test Method for Acid-Soluble Chloride in Mortar and Concrete, American Society for Testing and Materials.

Bayliss, D. A. and Deacon, D. H. Steelwork Corrosion Control.Second edition. Taylor & Francis, 2004.

Bermudez, M. A. and Alaejos, P. Models for Chloride Diffusion Coefficients of Concretes in Tidal Zone. ACI Materials Journal 107(1) (2010): 3-11.

Bertolini, L., Elsener, B., Pedeferri, P. and Polder, R. P. Corrosion of Steel in Concrete. WILEY-VCH, 2004.

Boulfiza, M., Sakai, K., Banthia, N. and Yoshida, H. Prediction of Cracking Effect on the Penetration of Chloride Ions in Reinforced Concrete, JCI Proceedings. 2000.

Boulfiza, M., Sakai, K., Banthia, N. and Yoshida, H. Prediction of Chloride Ions Ingress in Uncracked and Cracked Concrete. ACI Materials Journal 100(1) (2003): 38-48.

Broomfield, J. P. Corrosion of Steel in Concrete: Understanding, Investigation and Repair.2. Taylor & Francis, 2007.

Caré, S. Influence of aggregates on chloride diffusion coefficient into mortar. Cement and Concrete Research 33(7) (2003): 1021-1028.

Castellote, M., Alonso, C., Andrade, C., Chadbourn, G. A. and Page, C. L. Oxygen and chloride diffusion in cement pastes as a validation of chloride diffusion coefficients obtained by steady-state migration tests. Cement and Concrete Research 31(4) (2001): 621-625.

Delagrave, A., Bigas, J. P., Ollivier, J. P., Marchand, J. and Pigeon, M. Influence of the interfacial zone on the chloride diffusivity of mortars. <u>Advanced Cement Based Materials</u> 5(3-4) (1997): 86-92.

Djerbi, A., Bonnet, S., Khelidj, A. and Baroghel-bouny, V. Influence of traversing crack on chloride diffusion into concrete. <u>Cement and Concrete Research</u> 38(6) (2008a): 877-883.

Djerbi, A., Bonnet, S., Khelidj, A. and Baroghel-bouny, V. Influence of traversing crack on chloride diffusion into concrete. <u>Cement and Concrete Research</u> 38 (2008b): 7.

El-Reedy, M. A. <u>Steel-reinforced concrete structures : assessment and repair of corrosion.</u> CRC Press, 2008.

Gjørv, O. E. <u>Durability design of concrete structures in severe environments.</u>1st. Taylor & Francis, 2009.

Gowripalan, N., Sirivivatnanon, V. and Lim, C. C. Chloride diffusivity of concrete cracked in flexure <u>Cement and Concrete Research</u> 30(5) (2000): 5.

Ha, T.-H., et al. Accelerated short-term techniques to evaluate the corrosion performance of steel in fly ash blended concrete. <u>Building and Environment</u> 42(1) (2007): 78-85.

http://jp.fujitsu.com. Electron Probe X-ray MicroAnalyzer. Fujitsu Quality Laboratory. from http://jp.fujitsu.com/group/fql/en/services/analysis/method/epma/ Retrieved [2012, May 20].

Ishida, T., Iqbal, P. O. N. and Anh, H. T. L. Modeling of chloride diffusivity coupled with non-linear binding capacity in sound and cracked concrete. <u>Cement and Concrete Research</u> 39(10) (2009): 913-923.

Ismail, M., Toumi, A., Francois, R. and Gagne, R. Effect of crack opening on the local diffusion of chloride in inert materials. <u>Cement and Concrete Research</u> 34 (4) (2004): 711-716.

Ismail, M., Toumi, A., François, R. and Gagné, R. Effect of crack opening on the local diffusion of chloride in cracked mortar samples. <u>Cement and Concrete Research</u> 38(8-9) (2008): 1106-1111.

JSCE (2003). Test method for effective diffusion coefficient of chloride ion in concrete by migration. Japan, Japan Society of Civil Engineers. **JSCE-G571-2003**.

Karihaloo, B. L., Abdalla, H. M. and Xiao, Q. Z. Deterministic size effect in the strength of cracked concrete structures. <u>Cement and Concrete Research</u> 36 (2006): 17.

Kato, E., Kato, Y. and Uomoto, T. Development of Simulation Model of Chloride Ion Transportation in Cracked Concrete. <u>Journal of Advanced Concrete Technology</u> 3(1) (2005): 85-94.

Kato, Y. and Uomoto, T. Modeling of Effective Diffusion Coefficient of Substances in Concrete Considering Spatial Properties of Composite Materials. <u>Journal of Advanced Concrete Technology</u> 3(2) (2005): 241-251.

Kropp, J. and Hilsdorf, H. (1995). Performance Criteria for Concrete Durability. <u>RILEM Technical Committee 116-PCD Permeability of concrete as a criterion of its durability</u>, E & FN Spon.

Lewis, R. W., Nithiarasu, P. and Seetharamu, K. Fundamentals of the Finite Element Method for Heat and Fluid Flow. Wiley, 2004.

Li, C. Q., Zheng, J. J. and Shao, L. New Solution for Prediction of Chloride Ingress in Reinforced Concrete Flexural Members. ACI Materials Journal 100(4) (2003).

Lim, C. C., Gowripalan, N. and Sirivivatnanon, V. Microcracking and chloride permeability of concrete under uniaxial compression. Cement & Concrete Composites 22 (2000): 7.

Lindvall, A. Chloride ingress data from field and laboratory exposure - Influence of salinity and temperature. Cement and Concrete Composites 29(2) (2007): 88-93.

Luping, T. and Nilsson, L.-O. Rapid Determination of the Chloride Diffusivity in Concrete by Applying an Electric Field. ACI Materials Journal 89(1) (1993): 49-53.

Maekawa, K., Ishida, T. and Kishi, T. Multi-scale Modeling of Concrete Performance Integrated Material and Structural Mechanics. Journal of Advanced Concrete Technology 1(2) (2003).

Marsavina, L., Audenaert, K., Schutter, G. D., Faur, N. and Marsavina, D. Experimental and numerical determination of the chloride penetration in cracked concrete. Construction and Building Materials 23(1) (2009): 264-274.

Mehta, P. K. Concrete in the Marine Environment New York, USA, Taylor & Francis, 2003.

Mehta, P. K. and Monteiro, P. J. M. Concrete: Microstructure, Properties, and Materials. McGraw-Hill, 2006.

Meijers, S. J. H. Computational Modelling of Chloride Ingress in Concrete Delft Univ Pr, 2003.

Mien, T. V. Modeling of Chloride Penetration into Concrete Structures under Flexural Cyclic Load and Tidal Environment. Doctor of Philosophy, Department of Civil Engineering, Chulalongkorn University, 2008.

Mien, T. V., Stitmannaithum, B. and Nawa, T. Chloride penetration into concrete using various cement types under flexural cyclical load and tidal evironment. The IES Journal Part A: Civil & Structural Engineering 2(3) (2009a): 13.

Mien, T. V., Stitmannaithum, B. and Nawa, T. Simulation of chloride penetration into concrete structures subjected to both cyclic flexural loads and tidal effects. Computers and Concrete 6 (2009b): 15.

Mien, T. V., Stitmannaithum, B. and Nawa, T. Prediction of chloride diffusion coefficient of concrete under flexural cyclic load. Computers and Concrete 8(3) (2011).

Mohammed, T. U., Yamaji, T. and Hamada, H. Chloride Diffusion, Microstructure, and Mineralogy of Concrete after 15 Years of Exposure in Tidal Environment. ACI Materials Journal 99(3) (2002).

Mori, D., Yamada, K., Hosokawa, Y. and Yamamoto, M. Applications of Electron Probe Microanalyzer for Measurement of Cl Concentration Profile in Concrete. Journal of Advanced Concrete Technology 4 (2006): 13.

Nagesh, M. and Bhattacharjee, B. Modeling of Chloride Diffusion in Concrete and Determination of Diffusion Coefficients. ACI Materials Journal 95(2) (1998).

Nakarai, K., Ishida, T. and Maekawa, K. Multi-scale physiochemical modeling of soil–cementitious material interaction. <u>Soils and Foundations</u> 46(5) (2006): 653-663.

Nilsson, L.-O. (2005). Modelling of Chloride Ingress. <u>WP4 Report</u>. S. S. N. T. a. R. Institute. Sweden.

Northtest-NTBuild-492 (1999). Chloride Migration Coefficient from Non-steady-state Migration Experiments.

Paulsson-Tralla, J. and Silfwerbrand, J. Estimation of Chloride Ingress in Uncracked and Cracked Concrete Using Measured Surface Concentrations. <u>ACI Materials Journal</u> 90(1) (2002).

Picandet, V., Khelidj, A. and Bellegou, H. Crack effects on gas and water permeability of concretes. <u>Cement and Concrete Research</u> 39(6) (2009): 537-547.

Polder, R. B. Laboratory Testing of Five Concrete Types for Durability in A Marine Environment. in C. L. Page, P. B. Bamforth and J. W. Figg, Corrosion of Reinforcement in Concrete Construction Robinson College, Cambridge, UK.: The Royal Society of Chemistry. 1996.

Promentilla, M., Sugiyama, T., Hitomi, T. and Takeda, N. Quantification of tortuosity in hardened cement pastes using synchrotron-based X-ray computed microtomography. <u>Cement and Concrete Research</u> 39(6) (2009): 548-557.

Reinhardt, H.-W., Sosoro, M. and Zhu, X.-f. Cracked and repaired concrete subject to fluid penetration. <u>Materials and Structures</u> 31(2) (1998): 74-83.

Richardson, M. G. <u>Fundamentals of Durable Reinforced Concrete.</u> Spon Press, 2002.

Rodriguez, O. G. and Hooton, R. D. Influence of Cracks on Chloride Ingress into Concrete. <u>ACI Materials Journal</u> 100(2) (2003).

Saetta, A. V., Scotta, R. V. and Vitaliani, R. V. Analysis of Chloride Diffusion into Partially Saturated Concrete. <u>ACI Materials Journal</u> 90(5) (1993): 441-451.

Sanjuán, M. A. and Muñoz-Martialay, R. Influence of the water/cement ratio on the air permeability of concrete. <u>Journal of Materials Science</u> 31(11) (1996): 2829-2832.

Schiessl, P. and Raupach, M. Laboratory Studies and Calculations on the Influence of Crack Width on Chloride-Induced Corrosion of Steel in Concrete. <u>ACI Materials Journal</u> 94(1) (1997).

Song, H.-W., Lee, C.-H. and Ann, K. Y. Factors influencing chloride transport in concrete structures exposed to marine environments. <u>Cement and Concrete Composites</u> 30(2) (2008): 113-121.

Soutsos, M. <u>Concrete Durability: A Practical Guide to the Design of Durable Concrete Structures.</u> Thomas Telford, 2010.

Sugiyama, T., Bremner, T. W. and Tsuji, Y. Determination of chloride diffusion coefficient and gas permeability of concrete and their relationship. <u>Cement and Concrete Research</u> 26(5) (1996): 781-790.

Sugiyama, T., Kenta, S., Masahiro, K. and Kazunori, S. (2008). Quantitative Evaluation of Chloride Ingress in Fly Ash Concrete by Electron Probe Micro Analysis (EPMA). Proceedings of the International Conferernce on Durability of Concrete Structures. China. **1:** 295-301.

Sugiyama, T., Ritthichauy, W. and Tsuji, Y. Simultaneous transport of chloride and calcium ions in hydrated cement systems. Journal of Advanced Concrete Technology 1(2) (2003): 127-138.

Sugiyama, T., Ritthichauy, W. and Tsuji, Y. Experimental investigation and numerical modeling of chloride penetration and calcium dissolution in saturated concrete. Cement and Concrete Research 38(1) (2008): 49-67.

Sugiyama, T., Tsuji, Y. and Bremner, T. W. Relationship between coulomb and migration coefficient of chloride ions for concrete in a steady-state chloride migration test. Magazine of Concrete Research 53(1) (2001): 13-24.

Sun, G., Sun, W., Zhang, Y. and Liu, Z. Prediction of the Effective Diffusion Coefficient of Chloride Ion in Cement-Based Composite Materials. Journal of Materials in Civil Engineering 1(1) (2012): 410-410.

Sun, G., Zhang, Y., Sun, W., Liu, Z. and Wang, C. Multi-scale prediction of the effective chloride diffusion coefficient of concrete. Construction and Building Materials 25(10) (2011): 3820-3831.

Suryavanshi, A. K., Swamy, R. N. and Cardew, G. E. Estimation of Diffusion Coefficients for Chloride Ion Penetration into Structural Concrete. ACI Materials Journal 99(5) (2002): 441-449.

Takewaka, K., Yamaguchi, T. and Maeda, S. Simulation Model for Deterioration of Concrete Structures due to Chloride Attack. Journal of Advanced Concrete Technology 1(2) (2003): 139-146.

Trejo, D. and Pillai, R. G. Accelerated Chloride Threshold Testing: Part I-ASTM A 615 and A 706 Reinforcement. ACI Materials Journal 100(6) (2003).

Trejo, D. and Pillai, R. G. Accelerated Chloride Threshold Testing—Part II: Corrosion-Resistant Reinforcement. ACI Materials Journal 101(1) (2004).

Truc, O., Ollivier, J. P. and Carcassès, M. A new way for determining the chloride diffusion coefficient in concrete from steady state migration test. Cement and Concrete Research 30(2) (2000): 217-226.

Vu, H. Q., Stitmannaithum, B. and Takafumi, S. A Concept for 2D Model of Chloride Diffusivity into Cracked Reinforced Concrete Structures, The Twenty-Fourth KKCNN Symposium on Civil Engineering Hyogo, Japan. 2011a.

Vu, H. Q., Stitmannaithum, B. and Takafumi, S. (2011). Experimental Study for the Effect of Natural Crack Characteristics on the Chloride Penetration. Annual Concrete Conference 7 (ACC7). Rayong, Thailand, Thai Concrete Association**:** CD-ROM.

Vu, H. Q., Stitmannaithum, B. and Takafumi, S. Experimental Study on Chloride Penetration Depth of Cracked Concrete, The Twenty-Fourth KKCNN Symposium on Civil Engineering Hyogo, Japan. 2011b.

Wall, H. and Nilsson, L.-O. A study on sampling methods for chloride profiles: simulations using data from EPMA. Materials and Structures 41(7) (2008): 1275-1281.

Walraven, J. C. (2008). Design for service life: How should it be implemented in future codes. 2nd International Conference on Concrete Repair, Rehabilitation and Retrofitting. Cape Town, South Arica.

Wang, K., Jansen, D. c., Shah, S. P. and Karr, A. F. Permeability Study of Crack Concrete. Cement and Concrete Research 27(3) (1997): 381-393.

Wang, L., Soda, M. and Ueda, T. Simulation of Chloride Diffusivity for Cracked Concrete Based on RBSM and Truss Network Model. Journal of Advanced Concrete Technology 6(1) (2008): 12.

Wang, L. and Ueda, T. Nummerical determination of the chloride difusion coefficient in cracks and cracked concrete. in H. Yokota, T. Sugiyama and T. Ueda, The 2nd International Conference on Durability of Concrete Structures ICDCS2010 Sapporo, Japan: Hokkaido University Press. 2010.

Win, P. P., Watanabe, M. and Machida, A. Penetration profile of chloride ion in cracked reinforced concrete. Cement and Concrete Research 34(7) (2004): 1073-1079.

Yang, C. and Cho, S. The relationship between chloride migration rate for concrete and electrical current in steady state using the accelerated chloride migration test. Materials and Structures 37(7) (2004): 456-463.

Yang, C. C. and Cho, S. W. An electrochemical method for accelerated chloride migration test of diffusion coefficient in cement-based materials. Materials Chemistry and Physics 81(1) (2003): 116-125.

Yang, C. C. and Cho, S. W. Approximate migration coefficient of percolated interfacial transition zone by using the accelerated chloride migration test. Cement and Concrete Research 35(2) (2005): 344-350.

Yang, C. C. and Wang, L. C. The diffusion characteristic of concrete with mineral admixtures between salt ponding test and accelerated chloride migration test. Materials Chemistry and Physics 85(2-3) (2004): 266-272.
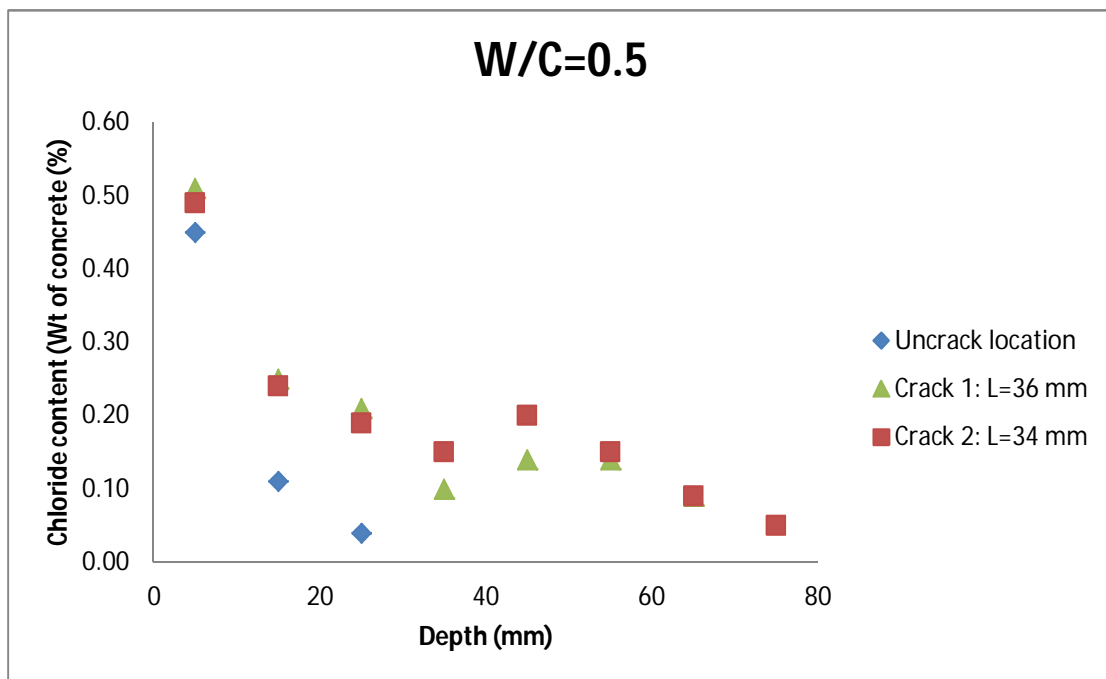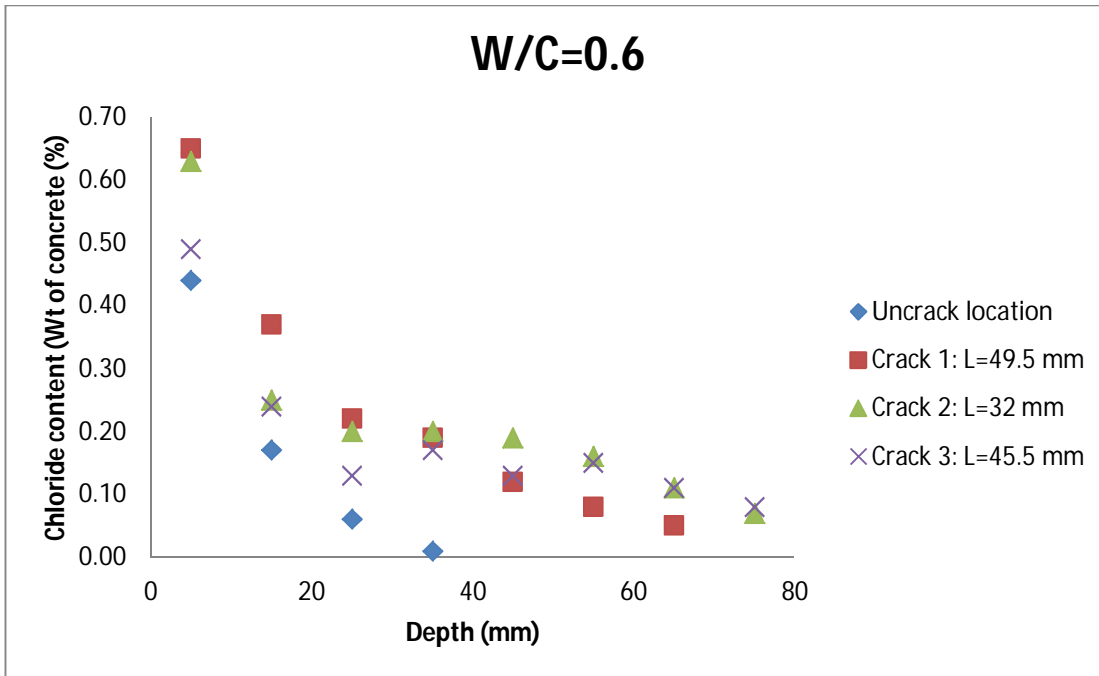
APPENDIX

A.1. The experimental results of chloride profile after 2-week immersion
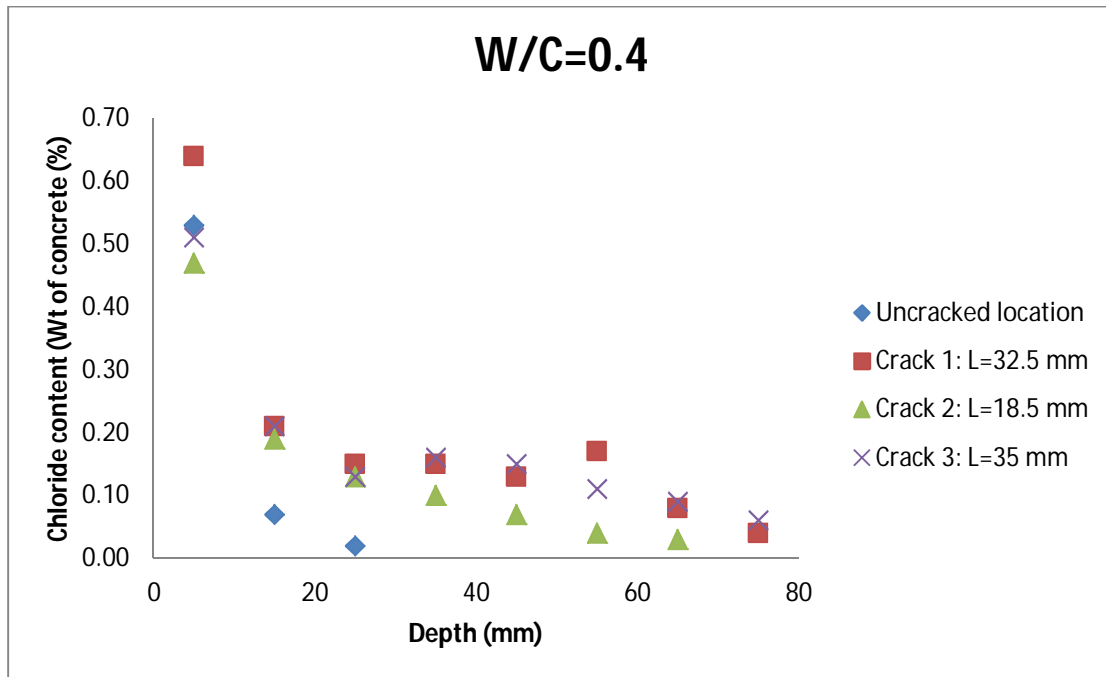
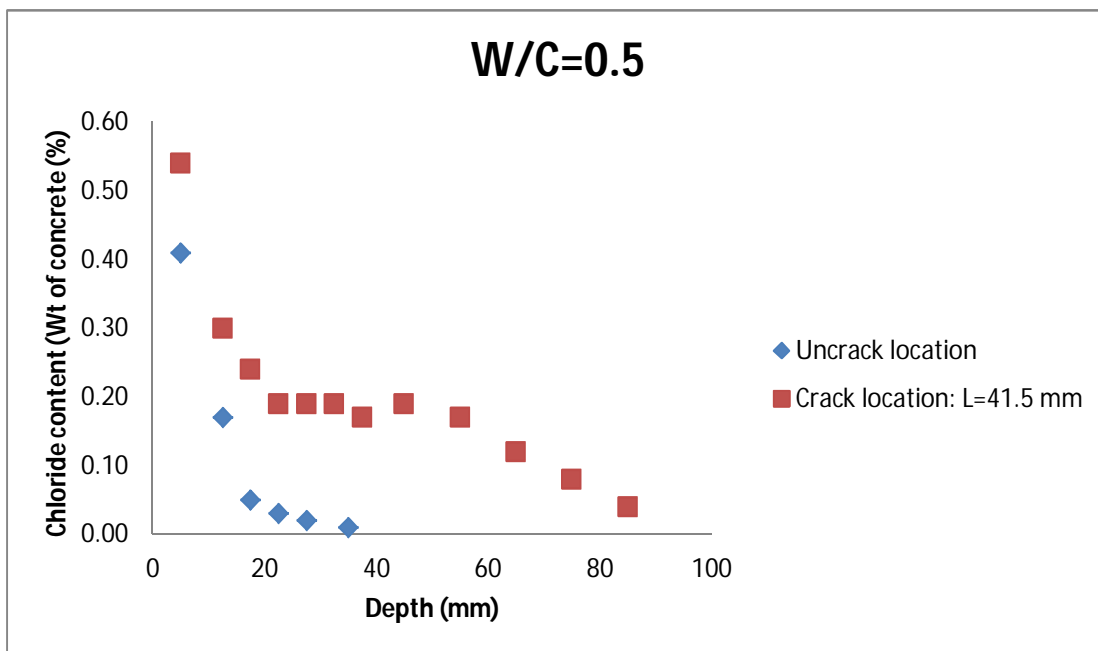The chloride profile at crack and uncrack locations for beam series 1.

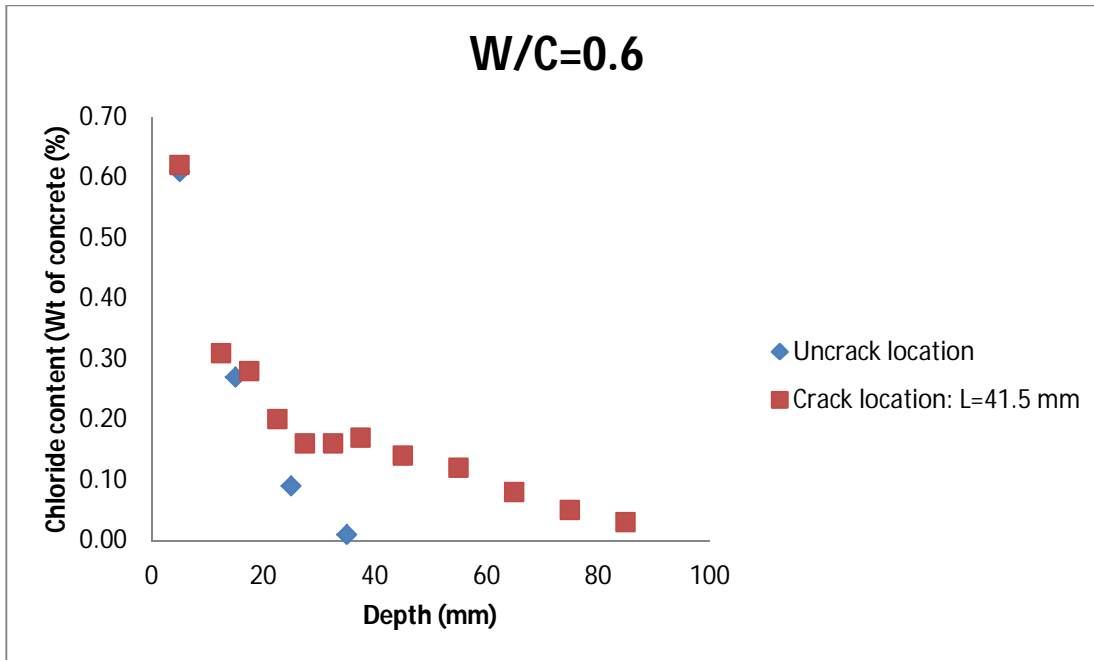The chloride profile at crack and uncrack locations for beam series 2.

The chloride profile at crack and uncrack location for beam series 3.

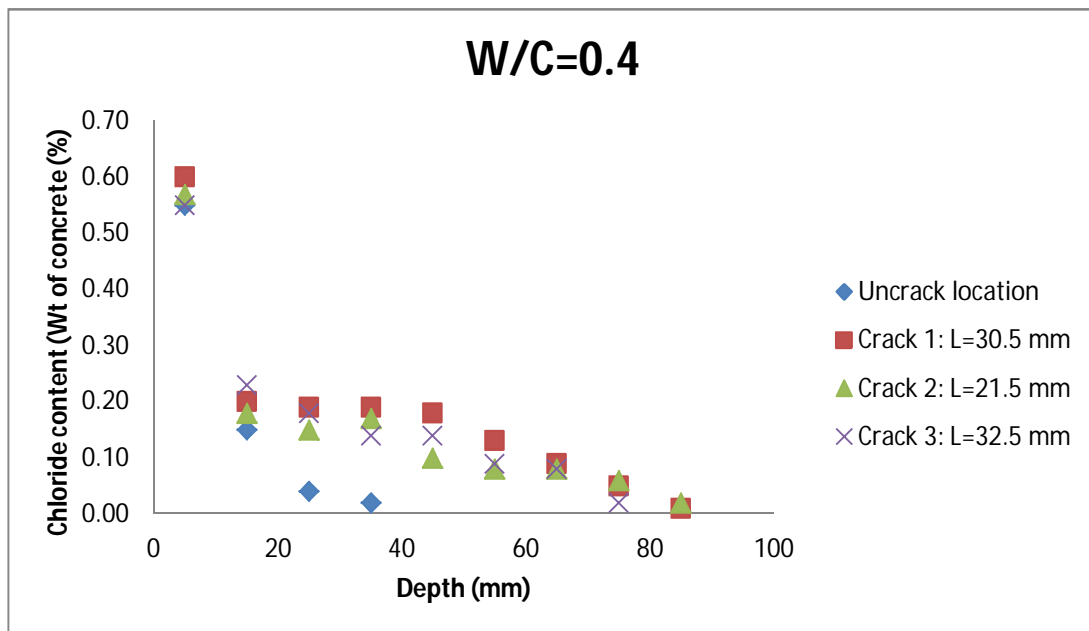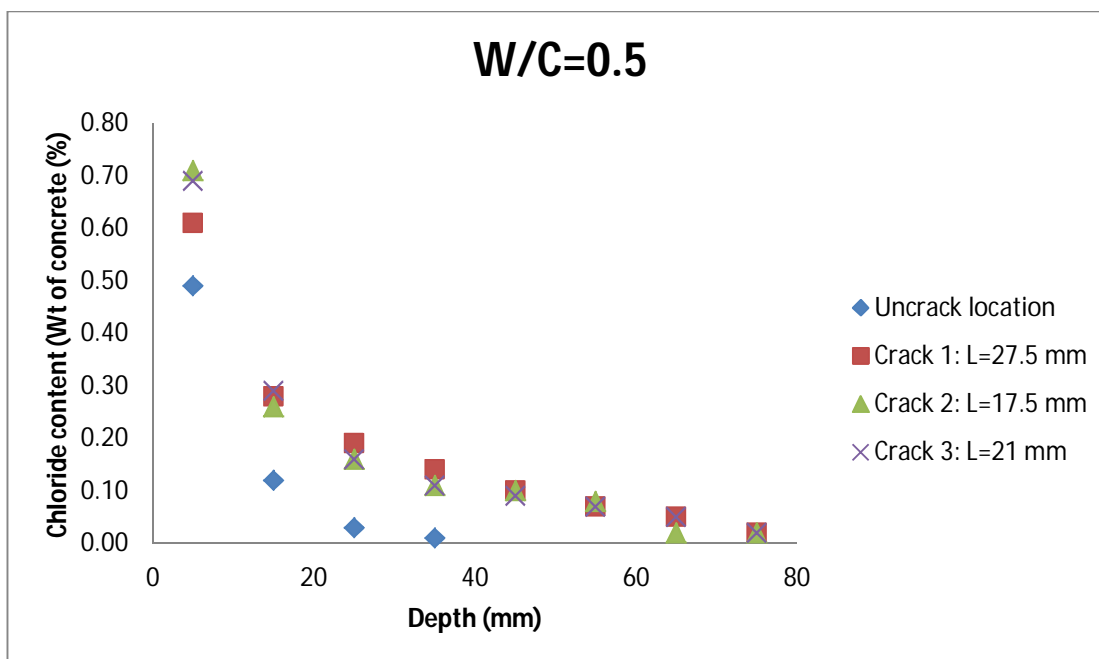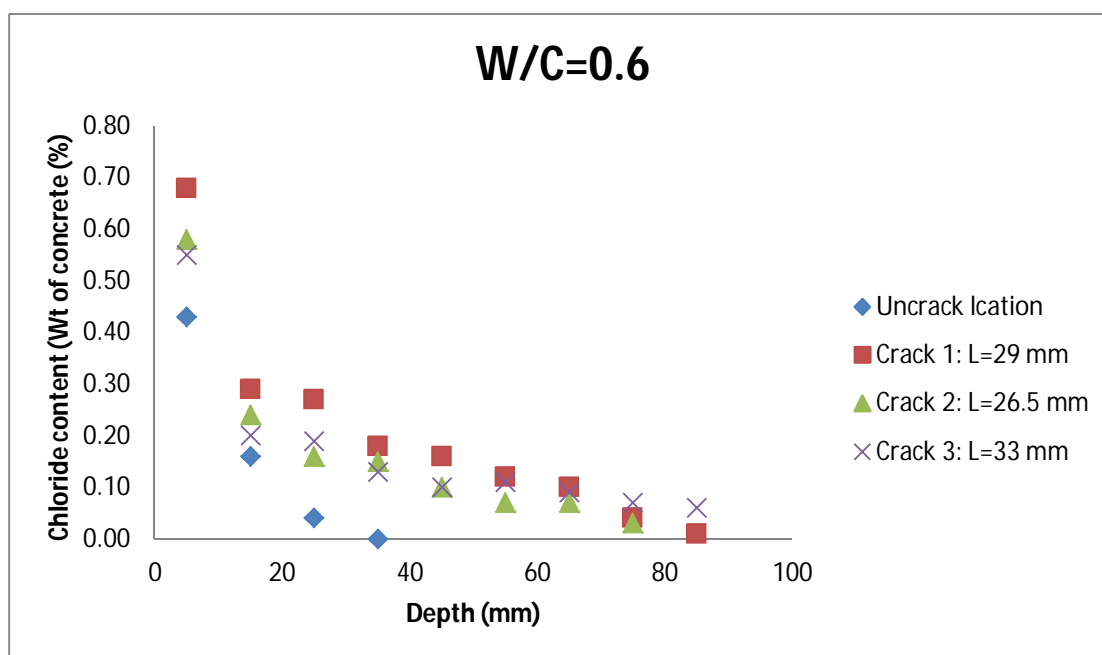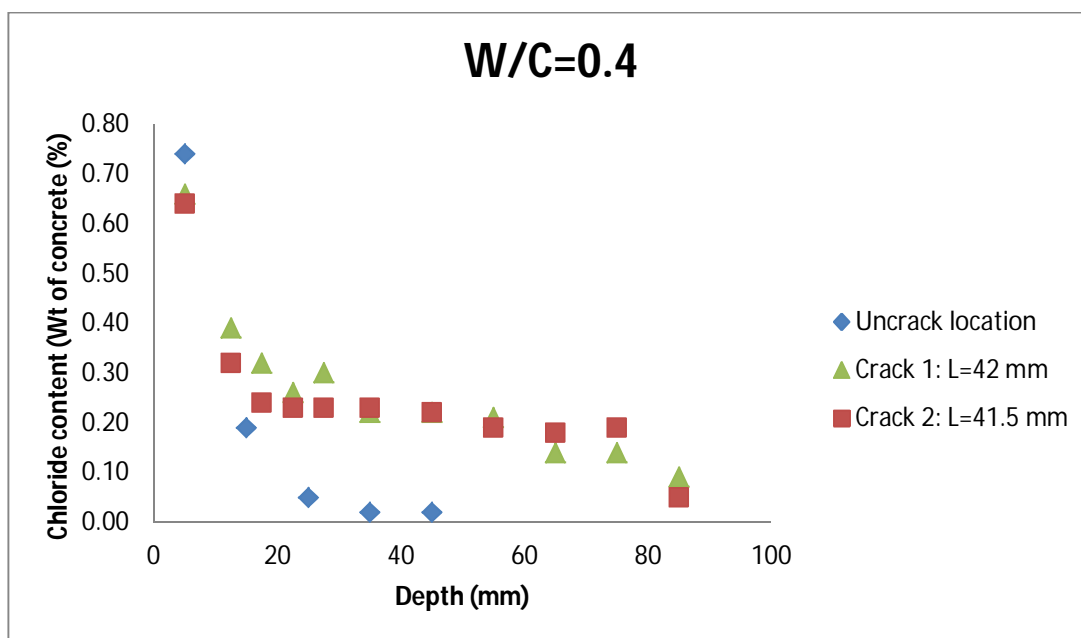**A.2. The experimental results of chloride profile after 4-week immersion**

The chloride profile at crack and uncrack locations for beam series 2.

The chloride profile at crack and uncrack location for beam series 3, W/C = 0.6.

A.3. The experimental results of chloride profile after 6-week immersion

The chloride profile at crack and uncrack locations for beam series 1.

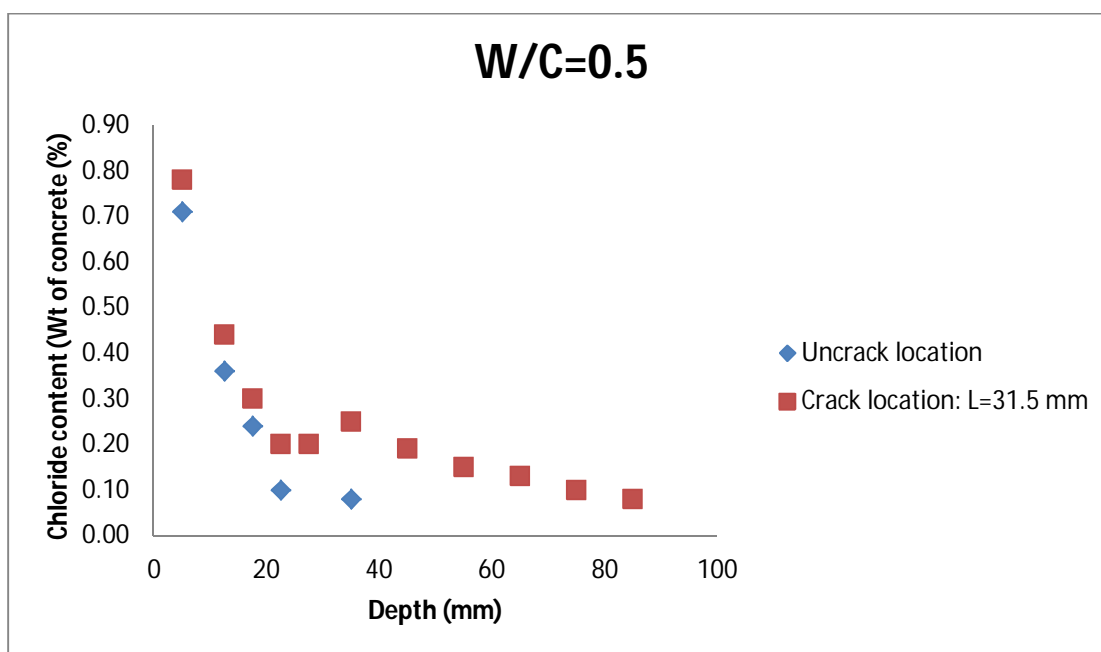**The chloride profile at crack and uncrack locations for beam series 2.**

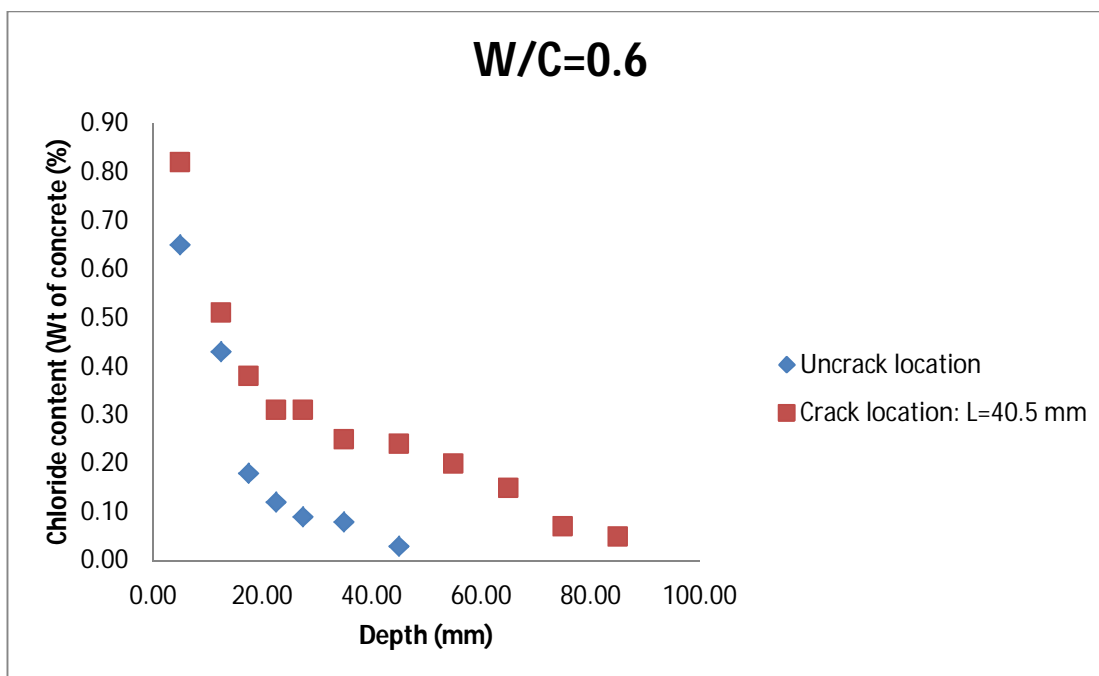**The chloride profile at crack and uncrack locations for beam series 3.**

A.4. The experimental results of chloride profile after 8-week immersion

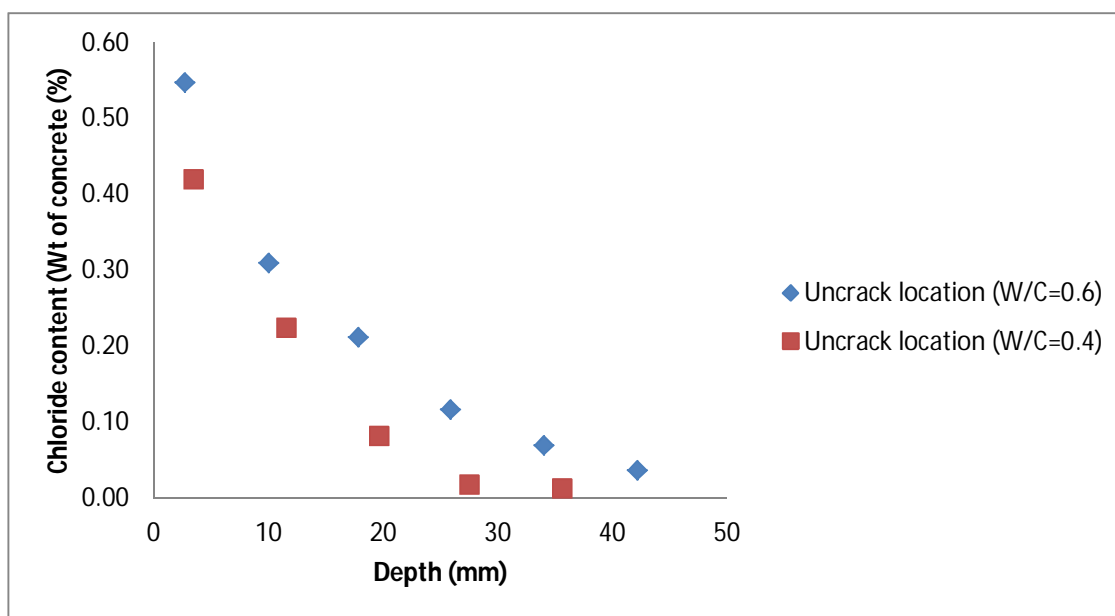**The chloride profile at crack and uncrack locations for beam series 1.**

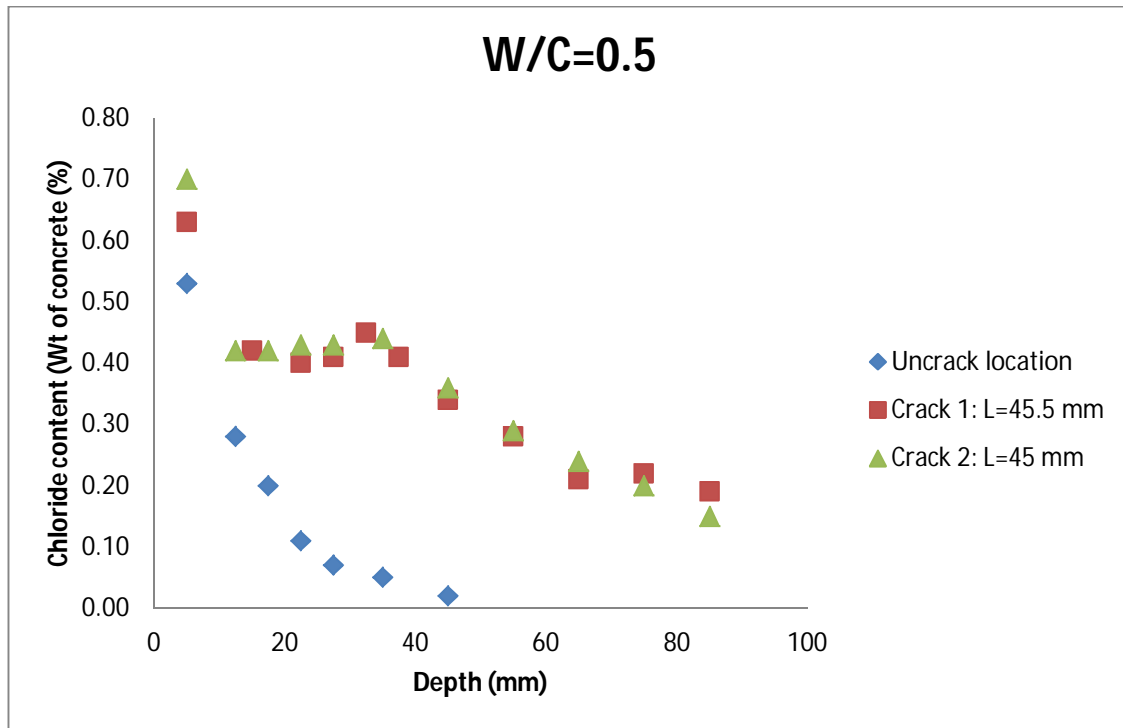**The chloride profile at crack and uncrack locations for beam series 2.**

The chloride profile at crack and uncrack locations for beam series 3.

A.5. The experimental results of chloride profile after 12-week immersion

The chloride profile uncrack location for beam series 1 and 3.

A.6. The experimental results of chloride profile after 16-week immersion

The chloride profile at crack and uncrack locations for beam series 2.

BIOGRAPHY

Hoang Quoc Vu, born in Ho Chi Minh City, Vietnam, graduated his Bachelor degree in 2003 and Master degree in 2008 at Hochiminh City University of Technology. Since 4/2003, he has been a lecture of Faculty of Engineering, HCMUT, in Vietnam. He has been granted the scholarship by AUN/SEED-Net for continuous his Ph.D. degree. He entered Chulalongkorn University on summer 2009 as a Civil Engineering major, with an emphasis in Structural Engineering. The topics related to structural engineering that he interested in are advanced concrete technology, construction materials, durability of concrete and high performance concrete.